University of Pennsylvania
ScholarlyCommons

Publicly Accessible Penn Dissertations

Fall 12-21-2011

# Optimization and Translation of MSC-Based Hyaluronic Acid Hydrogels for Cartilage Repair

Isaac E. Erickson
*University of Pennsylvania*, erickson.isaac@gmail.com

Follow this and additional works at: http://repository.upenn.edu/edissertations

 Part of the Biomaterials Commons, Biomechanics and Biotransport Commons, and the Molecular, Cellular, and Tissue Engineering Commons

Recommended Citation
Erickson, Isaac E., "Optimization and Translation of MSC-Based Hyaluronic Acid Hydrogels for Cartilage Repair" (2011). *Publicly Accessible Penn Dissertations*. 447.
http://repository.upenn.edu/edissertations/447

This paper is posted at ScholarlyCommons. http://repository.upenn.edu/edissertations/447
For more information, please contact libraryrepository@pobox.upenn.edu.

# Optimization and Translation of MSC-Based Hyaluronic Acid Hydrogels for Cartilage Repair

**Abstract**
Traumatic injury and disease disrupt the ability of cartilage to carry joint stresses and, without an innate regenerative response, often lead to degenerative changes towards the premature development of osteoarthritis. Surgical interventions have yet to restore long-term mechanical function. Towards this end, tissue engineering has been explored for the *de novo* formation of engineered cartilage as a biologic approach to cartilage repair. Research utilizing autologous chondrocytes has been promising, but clinical limitations in their yield have motivated research into the potential of mesenchymal stem cells (MSCs) as an alternative cell source. MSCs are multipotent cells that can differentiate towards a chondrocyte phenotype in a number of biomaterials, but no combination has successfully recapitulated the native mechanical function of healthy articular cartilage. The broad objective of this thesis was to establish an MSC-based tissue engineering approach worthy of clinical translation.

Hydrogels are a common class of biomaterial used for cartilage tissue engineering and our initial work demonstrated the potential of a photo-polymerizable hyaluronic acid (HA) hydrogel to promote MSC chondrogenesis and improved construct maturation by optimizing macromer and MSC seeding density. The beneficial effects of dynamic compressive loading, high MSC density, and continuous mixing (orbital shaker) resulted in equilibrium modulus values over 1 MPa, well in range of native tissue.

While compressive properties are crucial, clinical translation also demands that constructs stably integrate within a defect. We utilized a push-out testing modality to assess the *in vitro* integration of HA constructs within artificial cartilage defects. We established the necessity for *in vitro* pre-maturation of constructs before repair to achieve greater integration strength and compressive properties *in situ*. Combining high MSC density and gentle mixing resulted in integration strength over 500 kPa, nearly 10-fold greater than previous reports of integration with MSC-based constructs. Furthermore, we demonstrated the durability of this repair system by applying dynamic loading and showed its functional contribution to the distribution of compressive loads across the repair space.

Overall, the studies contained within this thesis offer the first MSC-based tissue engineering strategy that successfully recapitulates native mechanical function while also demonstrating the potential for complete functional cartilage repair.

**Degree Type**
Dissertation

**Degree Name**
Doctor of Philosophy (PhD)

**Graduate Group**
Bioengineering

This dissertation is available at ScholarlyCommons: http://repository.upenn.edu/edissertations/447

**First Advisor**
Robert L. Mauck

**Keywords**
tissue engineering, cartilage, hyaluronic acid, hydrogel, mesenchymal stem cells

**Subject Categories**
Biomaterials | Biomechanics and Biotransport | Biomedical Engineering and Bioengineering | Molecular, Cellular, and Tissue Engineering

This dissertation is available at ScholarlyCommons: http://repository.upenn.edu/edissertations/447

# OPTIMIZATION AND TRANSLATION OF MSC-BASED HYALURONIC ACID HYDROGELS FOR CARTILAGE REPAIR

**Isaac E. Erickson**

A Dissertation in Bioengineering

Presented to the Faculties of the University of Pennsylvania in

Partial Fulfillment of the Requirements for the

Degree of Doctor of Philosophy

2011

**Supervisor of Dissertation**

Dr. Robert L. Mauck
Associate Professor of Orthopaedic Surgery
Associate Professor of Bioengineering

**Graduate Group Chair**

Dr. Beth Winkelstein
Professor of Bioengineering

**Dissertation Committee**

Jason A. Burdick, Associate Professor of Bioengineering, University of Pennsylvania

Kurt D. Hankenson, Assistant Professor of Animal Biology, University of Pennsylvania

Brian J. Sennett, Associate Professor of Orthopaedic Surgery, University of Pennsylvania

Suzanne Maher, Associate Professor of Applied Biomechanics in Orthopaedic Surgery, Cornell University & Assistant Scientist, Research Division, Hospital for Special Surgery

# OPTIMIZATION AND TRANSLATION OF MSC-BASED HYALURONIC ACID HYDROGELS FOR CARTILAGE REPAIR

**COPYRIGHT**

**2011**

**Isaac Edward Erickson**

*To My Beautiful, Devoted, and Patient Wife Sara:*

**Since you still probably don't know exactly what I have been doing in the lab all these years,**

**I wrote this for you to read.**

<3 *Big Eddie Smooth*

**ACKNOWLEDGMENTS**

As my advisor, Rob has been the most influential person in my development as a scientist. Our countless discussions encompassing both scientific minutia and the bigger picture have improved my perspective and prepared me for a successful career. Rob is an amazing advisor and is ultimately responsible for any small success that I may have achieved. His tireless efforts to run a growing lab have made my time here extremely meaningful and productive. His kind and patient nature has also blessed my family as we have endured some unexpected difficulties in life.

I am also most grateful for thoughtful contributions to my thesis from the members of my committee: Drs. Jason Burdick, Kurt Hankenson, Brian Sennett, and Suzanne Maher. I recognize the sacrifice of their valuable time for the benefit of my thesis. Thanks also to George Dodge for being a friend and *ex officio* committee member.

My collaboration and friendship with Jason Burdick has been exceptionally fruitful as I've been able to expand my expertise into biomaterials and reminisce about the time when we lived near real mountains. I have also appreciated being able to 'steal' polymer synthesis related items from his lab when needed. My early training was also heavily influenced by his students Darren Brey, Cindy Chung, Jamie Ifkovits, and Joshua Katz who have grown to be good friends. More recent students Sudhir Khetan, Ross Marklein, Elena Tous, Brendan Purcell, and Iris Kim have also been extremely generous with their time for scientific discussion and to perform NMR analysis on my behalf.

Special thanks to Alice Huang for the countless time she spent training me as I joined the Mauck lab. Former members Brendon Baker and Nandan Nerurkar were also instrumental in my development as a scientist. These three have helped me to think critically about science and how it is interpreted. Newer Mauckers Lara Ionescu Silverman, Tiffany Zachry, Megan Farrell, Tristan Driscoll, Minwook Kim, Su-Jin Heo, Matt Fisher, and Jon Kluge have all added to my remarkable experience as a member of the Mauck lab.

I've also been fortunate to practice my supervisory skills on a number of undergraduate or visiting students. Specifically, Ryan Li, Swarnali Sengupta, Steven van Veen, Sydney Kestle, and Kilief Zellars have each contributed significantly to this dissertation. Sydney Kestle demonstrated her diligence and tenacity as she assisted me for over 3 years. Her contributions to this work are ubiquitous as she cheerfully completed every task put before her. In stark contrast, Kilief Zellars typically resisted tasks and training, haha, just playin. Really though, sometimes I think that someone secretly told Kilief that I was working for him. Kilief is from West Philadelphia and came to the lab a year after graduating high school. I have known him for 4 years, but it didn't take that long for him to reach brother status in my life. He has been a welcome addition to the lab and a tremendous help to me in the completion of this work.

I also thank McKay giants Dawn Elliot and Lou Soslowsky for their friendship. Surprisingly, Lou always keeps a smile despite my constantly calling him 'Boss' and even after that time he walked in while I was impersonating him at his own lab meeting. Thanks to other McKay regulars John Martin, David Beason, and J Sarver for their friendship and willing assistance. I also thank Heather Ansorge, LeAnn Dourte, Lara Ionescu Silverman, Dan Cortes, Lachlan Smith, and Mike Dishowitz for sharing offices with me despite the fact that I talk way too much. Your friendship and conversation have gone a long ways to preserve my sanity. I have to thank Anthony in the office for almost daily basketball chats, I forgive you for being a Laker fan. Barb, I love you, please don't hate me when I call you in the future to get something done over the phone for me. I should also acknowledge Scott from facilities for taking care of our space and for waking me up first thing in the morning when I would crash on my office floor.

The very first person I came into contact with when moving here was fellow University of Utah alumnus Spencer Lake who quickly became a solid labmate, neighbor, friend, and even marriage counselor. Thanks for keeping our magic alive!

My parents Jim and Debby have given me a lifetime of love and support. They have sacrificed so much in order for me to have amazing life opportunities. I thank them for their example of diligent hard work that permeated the fibers of our family and has had a profound impact on my life. Special thanks to my 'other' parents Tom and Barb for their support and patience as I've tried to provide a good life for their daughter.

The addition of our 2 year old daughter Hazel to our family has brought me so much pure unadulterated bliss that it has been difficult for me to leave the house each morning. Therefore, she is happily acknowledged for delaying my graduation.

Most importantly I must acknowledge the role of my wife Sara in this work. While her primary contribution was deciding when I should begin and end each day, without her I would not have accomplished anything. Sara has shaped me into a better person since the day we met. She is the principal source of the motivation that has kept me focused and moving forward. Her endless support allowed me to work tirelessly knowing that at the end of every day (almost) I could return home to her loving arms. The time I have spent on this thesis research was filled with joy and happiness because of her companionship and love.

As a firm believer that science and religion can coexist, I also acknowledge the role of God in preserving my life, enlightening my mind, and lifting my burdens. While this dissertation may contain no evidence of this contribution, I stand by my claim.

**ABSTRACT**

**OPTIMIZATION AND TRANSLATION OF MSC-BASED HYALURONIC ACID HYDROGELS FOR CARTILAGE REPAIR**

**Isaac E. Erickson**

**Robert L. Mauck**

Traumatic injury and disease disrupt the ability of cartilage to carry joint stresses and, without an innate regenerative response, often lead to degenerative changes towards the premature development of osteoarthritis. Surgical interventions have yet to restore long-term mechanical function. Towards this end, tissue engineering has been explored for the *de novo* formation of engineered cartilage as a biologic approach to cartilage repair. Research utilizing autologous chondrocytes has been promising, but clinical limitations in their yield have motivated research into the potential of mesenchymal stem cells (MSCs) as an alternative cell source. MSCs are multipotent cells that can differentiate towards a chondrocyte phenotype in a number of biomaterials, but no combination has successfully recapitulated the native mechanical function of healthy articular cartilage. The broad objective of this thesis was to establish an MSC-based tissue engineering approach worthy of clinical translation.

Hydrogels are a common class of biomaterial used for cartilage tissue engineering and our initial work demonstrated the potential of a photo-polymerizable hyaluronic acid

(HA) hydrogel to promote MSC chondrogenesis and improved construct maturation by optimizing macromer and MSC seeding density. The beneficial effects of dynamic compressive loading, high MSC density, and continuous mixing (orbital shaker) resulted in equilibrium modulus values over 1 MPa, well in range of native tissue.

While compressive properties are crucial, clinical translation also demands that constructs stably integrate within a defect. We utilized a push-out testing modality to assess the *in vitro* integration of HA constructs within artificial cartilage defects. We established the necessity for *in vitro* pre-maturation of constructs before repair to achieve greater integration strength and compressive properties *in situ*. Combining high MSC density and gentle mixing resulted in integration strength over 500 kPa, nearly 10-fold greater than previous reports of integration with MSC-based constructs. Furthermore, we demonstrated the durability of this repair system by applying dynamic loading and showed its functional contribution to the distribution of compressive loads across the repair space.

Overall, the studies contained within this thesis offer the first MSC-based tissue engineering strategy that successfully recapitulates native mechanical function while also demonstrating the potential for complete functional cartilage repair.

**TABLE OF CONTENTS**

## LIST OF TABLES

## LIST OF FIGURES

# CHAPTER 1: Introduction

Functional cartilage repair requires both the replacement of damaged cartilage with an equally functional material that will also integrate to adjacent host cartilage, thus forming a contiguous repair that is capable of performing the demanding mechanical functions in the joint. Tissue engineering has emerged as a promising approach to form cartilage *in vitro* that can be used for cartilage repair. Initial efforts utilizing chondrocytes and advanced culture techniques have been successful at generating cartilage-like tissue with at least one mechanical property (equilibrium modulus) that equals native cartilage. Despite these promising results, the comorbidity of autologous chondrocyte harvest can be detrimental to the health of the remaining cartilage. Furthermore, chondrocytes from an injured or diseased joint may be suboptimal for tissue engineering. As a result of these limitations, the interest in using mesenchymal stem cells (MSCs) as an alternative cell source has intensified in recent years. MSCs can proliferate *in vitro* with phenotypic stability while also maintaining their ability to differentiate towards a chondrogenic lineage when given proper chemical and environmental cues. Despite their several advantages over chondrocytes, MSCs have been routinely outclassed by chondrocytes when evaluating the mechanical maturation of tissue engineered constructs. Similarly, MSC-based constructs have reached lesser levels of functional integration *in vitro* than have chondrocyte-seeded materials. Significant work remains to optimize an approach to functional cartilage tissue engineering that would capitalize on the benefits of using MSCs. The objective of this thesis was to optimize an MSC-based approach to generate a clinically relevant engineered cartilage.

In order to provide a framework for the work described herein, Chapter 2 will provide an overview of cartilage biology and mechanics with an emphasis on its functional role in skeletal motion. Common pathologies and repair paradigms will also be described to motivate the need for improved biologic solutions. Lastly, a review of cartilage tissue engineering will discuss biomaterials, cell sources, and strategies that are commonly employed in this field.

As a first step, Chapter 3 describes an evaluation of the potential for three distinct hydrogel biomaterials for cartilage tissue engineering by evaluating mechanical properties, biochemical content, and histological appearance. Photo-polymerizable methacrylated HA (MeHA), self-assembling peptide (Puramatrix), and agarose hydrogels were each seeded with chondrocytes or MSCs with the hypothesis that construct maturation would be dependent on the interactions between each unique 3D microenvironment and the cell type encapsulated therein.

After establishing the potential for MSC chondrogenesis within MeHA, Chapter 4 reports on the optimization of MeHA macromer density to improve the maturation of constructs seeded with juvenile bovine MSCs as opposed to previous work where its formulation had been optimized for porcine auricular chondrocytes. MSCs were seeded (20 million cells/mL) in 1%, 2%, and 5% MeHA (mass/volume) and cultured for 6 weeks while analyzing the developing functional properties along with the differences in the expression of cartilage matrix associated gene expression.

Chapter 5 explores MSC seeding density as an approach to accelerate construct maturation in MeHA hydrogels of various macromer densities. While high chondrocyte seeding densities (>50 million/mL) typically result in concomitant increases in construct mechanics, encapsulating MSCs at high densities had not been shown to elicit the same response. Since the effects of MSC density had not yet been studied in MeHA, this investigation compared the effects of MSCs at 20 and 60 million/mL in 1%, 3%, and 5% MeHA. Given its positive response to seeding density, 1% MeHA was the focus of an additional study investigating the effect of dynamic culture (the gentle continuous mixing of constructs and medium) on the rate of construct maturation via increased nutrient and growth factor transport.

Continuing the pursuit of functional parity to native cartilage tissue, Chapter 6 reports on the use of a bioreactor for the application of continuous dynamic compressive loading. Dynamic loading is effective at accelerating the functional development of chondrocyte seeded constructs and MSC seeded agarose (given an initial 3 week period of pre-maturation). MSCs photo-encapsulated within 1% MeHA (50 million/mL) were exposed to either 9 weeks of daily (3hrs) cyclic deformations (10% strain), 6 weeks of loading after 3 weeks of pre-maturation, or 3 weeks of loading followed by 6 weeks of free-swelling culture.

While the development of compressive properties in tissue engineered cartilage constructs is indisputably essential, often overlooked and understudied is the potential for

an *in vitro* generated construct to integrate within a defect. In Chapter 7, an *in vitro* defect model is used to determine the capacity of MSC-based MeHA for functional integration. Considering previous reports that integration is dependent on construct maturation, MSC-seeded MeHA (1%, 3%, and 5%) was either polymerized *in situ* or allowed 4 weeks to mature before implantation within the center of a cartilage ring. The strength of integration was determined after 4 and 8 weeks along with the compressive properties of the MeHA constructs.

The rationale for creating tissue engineered cartilage with similar mechanical properties as native tissue is to restore function where cartilage is lost or diseased. This alleviates the burden that cartilage adjacent to a defect may experience with the hope that degenerative changes can be avoided. In addition to increasing MSC density to improve integration, Chapter 8 describes the first *in vitro* analyses of integration durability and the capacity for integrated constructs to contribute to load transmission in a defect.

One caveat of this work is the use of juvenile bovine MSCs. While young patients requiring cartilage repair represent an important and ever growing cohort, the majority of patients that would benefit from tissue engineered cartilage are middle-aged or elderly. Chapter 9 explores the effects that age has on *in vitro* cartilage matrix formation by bovine MSCs in pellet and MeHA hydrogel constructs with fetal, juvenile, and aged bovine MSCs.

Chapter 10 will summarize this work while highlighting some of its implications for the progression of the field of cartilage tissue engineering. Limitations will be addressed and future studies will also be outlined that could further increase our understanding of the potential of MSC-based MeHA constructs for functional cartilage repair.

# CHAPTER 2: Background

Articular cartilage is the dense white tissue covering the bones involved in joint motion. When healthy, the unique composition and mechanical properties of cartilage lubricate and distribute the loads created by normal body movement. Tissue engineering seeks to create a biologic remedy to the debilitating effects of cartilage injury and disease, but improvements in the current technology are necessary to develop a fully functional repair paradigm.

## 2.1. Articular Cartilage

### 2.1.1. Structure and Organization

Articular cartilage is composed primarily of water, collagens, proteoglycans, and highly specialized cells called chondrocytes organized in a depth-dependent fashion (**Figure 2-1**) (Muir *et al*. 1970; Clarke 1971; Maroudas 1979). The superficial zone contains flat, elongated chondrocytes, aligned collagen fibrils, and the lowest proteoglycan content of all zones (Muir 1970; Setton *et al*. 1993). The chondrocytes in the middle zone are more spherical while the collagen fibers are larger and less oriented (Broom and Marra 1986). Deep zone cartilage has the largest concentration of proteoglycans and the least amount of water (65%) (Maroudas 1968; Maroudas 1979). The collagen fibers are largest here, and similar to the chondrocytes, are oriented vertically (Redler *et al*. 1975).

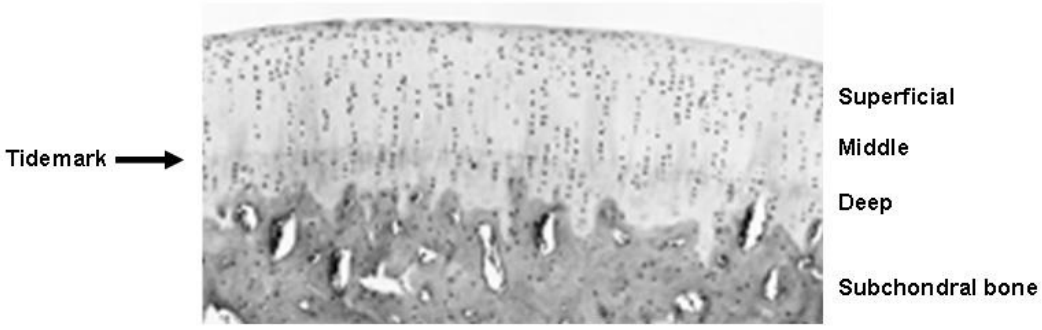


**Figure 2-1: Histological image of articular cartilage with zonal differences in the organization of chondrocytes from the superficial to deep zone (H&E staining; 40X magnification). (Wooley *et al.* 2005)**

2.1.2. Composition

Water comprises 65-80% of the wet weight of articular cartilage and is drawn to cartilage largely by $Ca^{2+}$ and $Na^{+}$ ions that neutralize the fixed negative charges on proteoglycans (Maroudas 1968; Maroudas 1979; Mankin *et al*. 1994). The large water content found within this dense cartilage matrix assists in distributing joint loads (Muir 1983). While there are many collagens found in cartilage, type II collagen comprises 90-95% of all collagens found here and 10-20% of the tissue wet weight (Muir 1980). Collagens are responsible for the tensile properties and play a role in the compressive properties as this tightly crosslinked network constrains proteoglycans (Setton *et al*. 1993). Proteoglycans or protein-polysaccharides in cartilage consist mainly of the aggregating proteoglycan—aggrecan (4-7% of cartilage wet weight) (Muir 1980; Muir 1983). Aggrecan consists of a core protein decorated with sulfated glycosaminoglycans (sGAG) keratan (~50) and dermatan (~100) sulfate (Mankin *et al*. 1994). This aggrecan molecule accumulates (~200) on the non-sulfated GAG, hyaluronate, to form massive, nearly immobile aggregates (Muir 1983). Amidst this extracellular matrix are chondrocytes, comprising ~10% of the tissue volume (Stockwell 1979). While chondrocytes are sparse, their

sensitivity to growth factors or cytokines plays a vital role in maintaining and remodeling articular cartilage through a balance of catabolism and synthesis (Nagase and Kashiwagi 2003; Karsenty 2005).

### 2.1.3. Physiological Loading

The structure and composition of cartilage are crucial to its ability to distribute near constant physiologic loading. This loading occurs at frequencies varying from 0.1-2 Hz while delivering contact stresses from 1-6 MPa, but ranging as high as 18 MPa (Lee *et al*. 1981; Kääb *et al*. 1998; Herberhold *et al*. 1999). In addition to compressive loading, joint surfaces also undergo a sliding motion at observed velocities of 20-250 mm/sec (Wang and Ateshian 1997).

### 2.1.4. Mechanical Properties

The mechanical function of articular cartilage is made possible by the interplay between aggregating proteoglycans and the constraining network of collagen molecules (Setton *et al*. 1993). This mechanical behavior can be described via biphasic theory where the proteoglycan-associated fixed charge density is responsible for interstitial fluid pressurization through osmotic and repulsive forces (Lai and Mow 1980; Mow *et al*. 1980; Mow *et al*. 1989). In biphasic theory, the resistance to fluid flow through the tissue bears the bulk of a rapidly applied stress (~95%), but as the fluid is dispelled from cartilage the remaining stress is absorbed by the solid phase of the tissue (Soltz and Ateshian 1998; Soltz and Ateshian 2000). Permeability (k) describes the ability of fluid to flow through a solid matrix and in the case of articular cartilage, extremely low values

from $10^{-15}$ to $10^{-16}$ $m^4/Ns$ have been observed. The equilibrium Young's modulus ($E_Y$) for articular cartilage of various species ranges from 0.1-1.4 MPa under a variety of testing conditions (Ateshian *et al*. 1997; Chen *et al*. 2001). The tensile modulus (5-50 MPa) is largely imparted by the collagen content and organization of articular cartilage (Roth and Mow 1980; Akizuki *et al*. 1986). Perhaps the most physiologically relevant aspect of cartilage mechanics may be the dynamic modulus (|G*|) which is primarily a measure of the initial fluid phase aspect of loading—values obtained from bovine tissue in unconfined compression range from 13-37 MPa (Park *et al*. 2004).

**Figure 2-2: Arthroscopic image of a focal cartilage defect from traumatic injury. The lack of intrinsic cartilage healing presents the need to fill defects with a suitable replacement tissue. (Ruckstuhl *et al*. 2008)**

2.1.5. Pathology

Damage to articular cartilage occurs in several forms including degenerative joint disease (accelerated by joint misalignment and obesity), traumatic injury (**Figure 2-2**), osteochondritis dissecans (loss of underlying blood supply), and the subsequent slow degradation process that often leads from one of these forms of damage to the onset of osteoarthritis (Cohen *et al*. 1998; Walter *et al*. 1998; Wang *et al*. 2006). Futhermore, the avascular nature of cartilage severely limits its self-regenerative capacity (Caplan *et al*.

1997). Approximately nine percent of Americans over thirty suffer from osteoarthritis and over 200,000 undergo total knee replacement annually.

### 2.1.6. Current Treatment

Attempts to treat cartilage damage center around both long and short term goals to relieve pain, restore function, slow/prevent disease progression, and if necessary to delay the need for total knee replacement. The treatment of cartilage injury or damage typically begins with lavage and debridement to remove tissue that may impede joint motion (Buckwalter 2002; Detterline *et al*. 2005). Microfracture is a marrow-stimulating procedure that generates a healing response through clot formation and subsequent scar formation, but does not restore full mechanical function (Steadman *et al*. 2001; Detterline *et al*. 2005). Osteochondral auto(allo)grafting is a more aggressive procedure that transfers cylindrical grafts from non-load bearing (cadaveric) regions to the defect site (Kleemann 2007). Limitations of this technique include donor-site morbidity (autografts) and poor integration due to graft incongruencies (Kleemann 2007). A cell-based repair technique involves the *in vitro* expansion of autologous chondrocytes to be delivered into a defect area covered by a periosteal flap (Micheli *et al*. 2001; Micheli *et al*. 2006). While this procedure represents the first in its class, results have not demonstrated its efficacy over that of microfracture (Knutsen *et al*. 2004). The current treatment regimes for cartilage damage still lack evidence of full functional restoration that also prevents disease progression, leaving a significant need for more advanced treatment options that can fulfill all of the objectives for cartilage repair.

## 2.2. Cartilage Tissue Engineering

Considering the need for enhanced cartilage repair strategies, many have begun developing tissue engineering solutions that typically include a scaffold biomaterial, suitable cell source, and appropriate chemical/environmental cues.

### 2.2.1. Biomaterials

Three primary classes of biomaterials for cartilage tissue engineering include sponges, meshes, and hydrogels from a variety of natural and synthetic materials. Scaffold free techniques have also been employed that generate cartilage that is biochemically similar to native cartilage without the need for a biomaterial scaffold (Masuda *et al*. 2003; Novotny *et al*. 2006; Murdoch *et al*. 2007; Mayer-Wagner *et al*. 2010). In conjunction with a suitable scaffold and cell source, chemical factors are used to drive cells towards the chondrogenic phenotype and to increase the synthesis of desired extracellular matrix proteins for the development of a cartilage-like graft material (Yaeger *et al*. 1997; Dunham and Koch 1998; Nixon *et al*. 1998; Weisser *et al*. 2001; Mauck *et al*. 2003; Zhou *et al*. 2004).

### 2.2.2. Hydrogels

While sponges and meshes have been increasingly effective at generating cartilage-like graft material both *in vitro* and *in vivo*, difficulties persist with inefficient cell infiltration and in maintaining proper phenotypes of cells spread on pore walls (Gruber *et al*. 2003). Scaffold-free methods offer a simplified approach, but as most other solutions it remains unknown if they provide sufficient mechanical strength for the demanding joint

environment. Alternatively, cells can be encapsulated directly within most hydrogels, offering a solution to problems with infiltration while helping to maintain a rounded cell phenotype typically desired of chondrocytes (Benya and Shaffer 1982). One such hydrogel, agarose, is a linear thermo-setting polysaccharide gel derived from seaweed. Agarose is effective at maintaining the phenotype of encapsulated chondrocytes and allowing for the synthesis and elaboration of a functional cartilage-like matrix (Benya and Shaffer 1982; Mauck *et al*. 2007; Byers *et al*. 2008). Another hydrogel class is the self-assembling peptide hydrogel which consists of amino acid sequences that spontaneously (in ionic solutions) form stable beta-sheets that ultimately create a nanofibrous hydrogel structure. Kisiday *et al* have utilized this hydrogel type to form cartilage-like matrix when seeded with articular chondrocytes (Kisiday *et al*. 2002; Kisiday *et al*. 2004).

HA is a large (up to 10 MDa) polysaccharide consisting of alternating units of D-glucuronic acid and N-acetyl-D-glucosamine (Bayliss *et al*. 1983; Bonnet *et al*. 1985; Stern 2003). While HA is found in all of our connective tissues, it represents only 1% of all gycosaminoglycans in articular cartilage (Mankin *et al*. 1994). In addition to retaining and regulating the flow of water, HA serves as the backbone for proteoglycan aggregation by binding aggrecan monomers via link protein (Mankin *et al*. 1994). HA performs numerous roles in modifying cellular functions during human development and more specifically during the development of diarthrodial joints. In developed cartilage, HA is an important ligand for cell-matrix interactions with pericellular matrix via the CD44 cell receptor (Knudson 1993; Embry and Knudson 2003). Furthermore, HA is

cleaved and degraded by hyaluronidases present within intracellular lysosomal compartments (HYAL 1) and on the surface of chondrocytes (HYAL 2), resulting in a 1 to 3 week half life (Stern 2003). The biologic relevance of HA in cartilage tissue makes HA-based hydrogels an interesting choice for cartilage tissue engineering research. Photo-polymerizable HA hydrogels have been developed by methacrylating HA to create macromers that can be polymerized with UV light (Smeds *et al*. 2001; Nettles *et al*. 2004; Burdick *et al*. 2005). Methacrylated HA (MeHA) hydrogels have been shown to maintain auricular chondrocyte phenotype under certain conditions when the molecular weight and macromer density of these hydrogels were varied (**Figure 2-3**) (Chung *et al*. 2006; Chung *et al*. 2006).

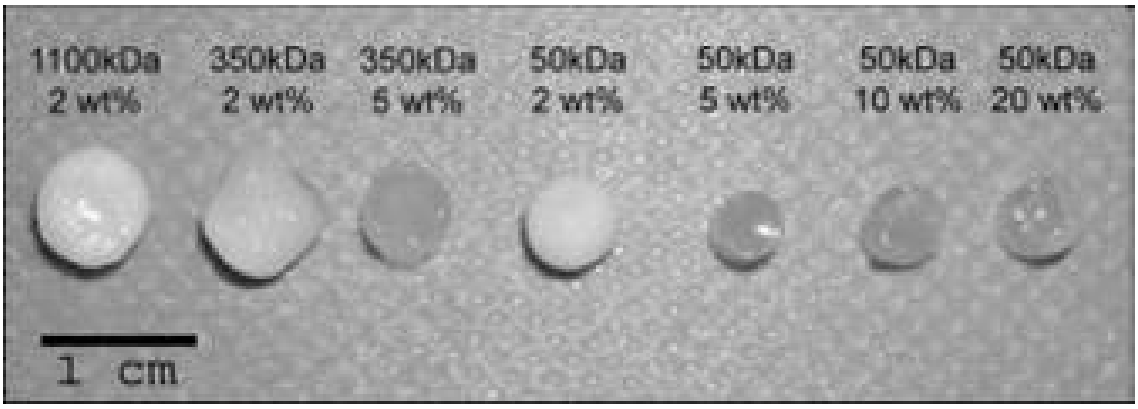


**Figure 2-3: Explanted HA constructs 12 weeks after subcutaneous implantation of HA/auricular chondrocyte constructs in nude mice. The 2 wt % constructs resemble native cartilage tissue, whereas other HA constructs remained relatively translucent, with little change in their macroscopic appearance since implantation. (Chung *et al.* 2006)**

2.2.3. Mesenchymal Stem Cells

While chondrocytes may seem the obvious choice for cartilage tissue engineering, problems associated with their use include donor-site morbidity, chondrocyte disease state, low cell number, and the de-differentiation of expanded cells (Schnabel *et al*. 2002; Stokes *et al*. 2002; Barbero *et al*. 2003; Darling and Athanasiou 2005; Diaz-Romero *et al*.

2007). Bone marrow derived MSCs have become popular for their ease of expansion and the fact that donor site morbidity is not associated with the joint space where the repair will occur. Extensive work investigating the suitability of MSCs for cartilage tissue engineering has found them capable of chondrogenesis and cartilage matrix formation, but key benchmark properties have not surpassed those found in similar chondrocyte experiments (**Figure 2-4**) (Stenderup *et al*. 2003; Song and Tuan 2004; Mauck *et al*. 2006; Sethe *et al*. 2006; Kopesky *et al*. 2007). Promoting MSC differentiation and subsequent matrix synthesis is a significantly more complex process than simply maintaining the phenotype of chondrocytes and capturing the ECM that is generated.

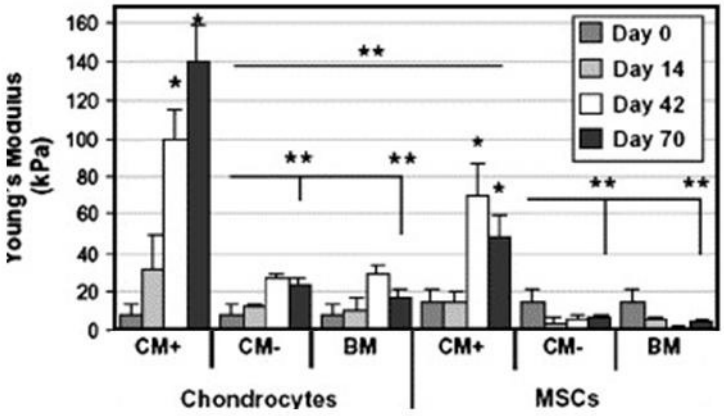


**Figure 2-4: Equilibrium compressive Young's modulus of chondrocyte- and MSC-laden agarose constructs through 10 weeks of culture in chondrogenic medium (CM; with and without TGF) or basal medium (BM). The mechanical properties in chondrocyte-laden constructs achieved a higher stiffness than MSC-laden constructs. (Mauck *et al.* 2006)**

2.2.4. Mechanical Stimulation

Mechanical stimulation provides an important environmental cue that has also been found to increase matrix synthesis and organization resulting in greater functional properties in engineered constructs (Mauck *et al*. 2003; Huang *et al*. 2010). Dynamic compressive loading increases aggrecan promoter activity in MSC-seeded Ag hydrogels

(Mauck *et al*. 2007) and the upregulation of proteoglycan synthesis has been observed in chondrocyte-seeded self-assembling peptide hydrogels (Kisiday *et al*. 2004). In chondrocyte-laden MeHA hydrogels, the expression of collagen type II and aggrecan was shown to increase after 5 days of compressive loading (**Figure 2-5**) (Chung *et al*. 2008).

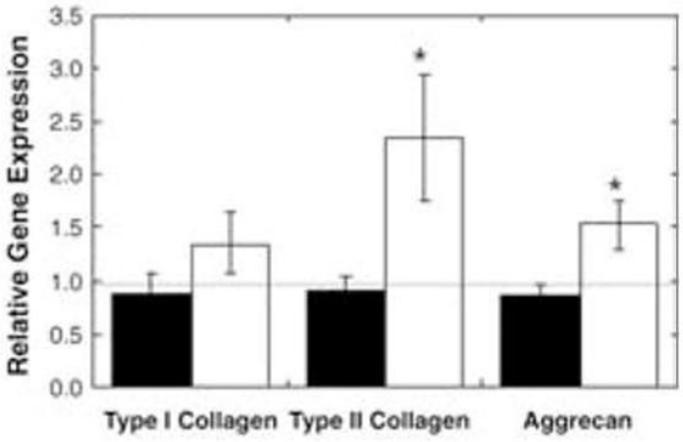


**Figure 2-5: Relative gene expression of articular chondrocyte-seeded HA hydrogels after 1 day (black) and 5 days (white) of dynamic compressive loading normalized to free-swelling controls. Significant differences ($p \leq 0.05$) between free-swelling and mechanically loaded samples are denoted by asterisks. (Chung *et al.* 2008)**

## 2.3. Functional Cartilage Repair

In order to proceed from the *in vitro* development of suitable cartilage graft materials it is important to consider what is required to promote the necessary integrative repair. Without successful integration into a cartilage defect, even an engineered tissue with the most suitable properties will be of no benefit when implanted (Ahsan and Sah 1999).

### 2.3.1. Integration

A common testing modality for integrative repair is the push-out test of integration strength, where the force required to displace a repair material from an annular cartilage construct is recorded and divided by the interface area providing the shear stress at

failure. While it is difficult to determine how large this failure stress should be to approach clinical significance, van de Breevaart Bravenboer *et al* have pushed through intact cartilage to record a failure stress of 8.8 MPa (van de Breevaart Bravenboer *et al*. 2004). This group has also achieved the greatest cartilage-cartilage integration; following 5 weeks of subcutaneous *in vivo* culture, they recorded failure stresses of 1.32 MPa for hyaluronidase and collagenase treated explants versus 0.84 MPa for untreated controls (van de Breevaart Bravenboer *et al*. 2004). Attempts at chondrocyte- or MSC-seeded hydrogel-cartilage integration using an untreated explant model have not exceeded failure stress values greater than 64 kPa (Hunter and Levenston 2004; Maher *et al*. 2009; Vinardell *et al*. 2009). However, with trypsin treatment of the explant cartilage, Obradovic *et al* seeded polyglycolic acid hydrogels with immature bovine chondrocytes and observed a failure stress of 384 kPa (Obradovic *et al*. 2001).

### 2.3.2. Durability and Load Distribution

The capacity for the repair integration interface to withstand normal loading without failure is a critical aspect of functional repair. While Fierlbeck *et al* have investigated crack propagation at the cartilage-cartilage interface in a single lap test (Fierlbeck *et al*. 2006), no attempts have been made to understand the effects of physiologic loading on the durability of *in vitro* repair. The ability for a repair construct to function by distributing loads across a defect site is also an important consideration that has yet to be studied.

## 2.4. Summary and Clinical Significance

There are over 20 million Americans suffering from cartilage injury or disease. Many of these will end up receiving one of more than 200,000 total knee replacements that are performed annually. While effective at the restoration of joint function, joint prosthetics have a limited lifetime of 10-15 years before revision procedures are often required. Therefore, there exists a great need for technologies that can repair cartilage with the objective of delaying the onset of osteoarthritis and the need for joint replacement.

Cartilage tissue engineering is an approach that would create a biologic tissue for cartilage repair. Successful generation of functional engineered cartilage could delay disease progression, simultaneously increasing patient health and activity levels. Subsequently, health care costs would also decline if engineered grafts remain durable over the long-term.

# CHAPTER 3: Differential Maturation and Structure Function Relationships in MSC and Chondrocyte Seeded Hydrogels

## 3.1. Introduction

The growing prevalence of osteoarthritis, other degenerative cartilage diseases, and traumatic injuries, motivates the goal of developing replacement cartilage tissue. To address this need, tissue engineering strategies have focused on the production of functional cartilage constructs that possess features similar to the native tissue (for review, see (Hung *et al*. 2004; Kuo *et al*. 2006)). While it is not yet clear whether an engineered construct must completely recapitulate all mechanical features of the native tissue at the time of implantation, it is clear that if permanent biologic repair is to be effected, the engineered systems must enable this eventuality. Most cartilage tissue engineering strategies combine mature chondrocytes with biocompatible and/or biodegradable 3D culture systems (for review, see (Chung and Burdick 2008)). Hydrogels, in particular, force encapsulated cells to assume a rounded shape and aid in the retention or resumption of the chondrocyte phenotype (Benya and Shaffer 1982; Hauselmann *et al*. 1994). A large number of hydrogels have been developed for these applications, ranging from simple thermoreversible gels (such as agarose) (Buschmann *et al*. 1992), to more complex bioengineered gels that present ECM relevant adhesive (i.e. RGD) (Burdick and Anseth 2002; Connelly *et al*. 2007) and/or degradation cues (e.g., MMP-cleavable elements) (Park *et al*. 2004; Lutolf and Hubbell 2005).

In many cartilage tissue engineering efforts, primary or culture expanded chondrocytes are employed. These cells, while possessing the proper phenotype, are of limited supply. Further limiting clinical use, aged and/or osteoarthritic chondrocytes produce ECM lower in collagen content compared to young chondrocytes (Tallheden *et al*. 2005; Tran-Khanh *et al*. 2005). This, coupled with *in vitro* expansion induced chondrocyte de-differentiation (Schnabel *et al*. 2002; Stokes *et al*. 2002), has initiated new efforts on the use of adult-derived mesenchymal stem cells (MSCs). MSCs can be isolated from adult bone marrow, and possess a multi-lineage differentiation capacity (Prockop 1997; Johnstone *et al*. 1998; Pittenger *et al*. 1999). In pellet cultures in defined media supplemented with TGF-β/BMP superfamily members (Majumdar *et al*. 2001), MSCs undergo chondrogenesis and deposit a proteoglycan rich ECM (Mauck *et al*. 2006). This same phenotypic conversion has been demonstrated in a number of hydrogels (Caterson *et al*. 2002; Erickson *et al*. 2002; Williams *et al*. 2003; Awad *et al*. 2004). However, while MSC chondrogenesis is apparent at the molecular/histological level, few studies have evaluated the resultant mechanical properties developed in these MSC-laden constructs or compared them directly to those achieved by chondrocytes. In one study using adipose derived adult stem cells, the mechanical properties of cell-laden agarose, alginate, and fibrous gelatin based foams were evaluated over a 4 week time course (Awad *et al*. 2004). In that study, mechanical properties increased modestly with time, though primary chondrocyte controls were not examined. More recently, we acquired bovine chondrocytes and MSCs from the same donor or groups of healthy donors and evaluated their maturation with long-term culture in agarose in a pro-chondrogenic media formulation (Mauck *et al*. 2006; Huang *et al*. 2008). Testing the equilibrium and dynamic mechanical properties of

these constructs showed that while MSC-laden constructs increased in mechanical properties, they did so to a lesser extent than chondrocyte-laden constructs.

MSC-biomaterial interactions are important for both initial viability as well as subsequent chondrogenesis. For example, human MSCs decrease in viability in hydrogels when not presented with the appropriate 3D adhesive niche (Nuttelman *et al*. 2005; Salinas *et al*. 2007). MSCs can be isolated based on their adhesion to tissue culture plastic, and thus precipitating the first step in phenotypic conversion may be necessary to maintain viability in this anchorage dependent population. Conversely, these same adhesive cues may negatively regulate chondrogenic differentiation; a recent study showed that RGD-modified alginate decreased the extent of MSC chondrogenesis as measured by ECM production (Connelly *et al*. 2007). These findings suggest that hydrogels for MSC-based cartilage tissue engineering must preserve viability while still promoting chondrogenic conversion and functional maturation.

In our previous studies showing differences in construct mechanical properties between chondrocytes and MSCs, it was not clear whether the lower properties achieved by MSCs was due to a fundamental limitation in chondrogenesis, or whether this functional maturation could be influenced by the 3D environment (i.e., hydrogel) in which the cells were placed. To further address this question, this study examined the potential of bovine MSCs to undergo chondrogenesis in 3D culture in three distinct hydrogels. We employed agarose (Mauck *et al*. 2006) as well as two hydrogels based on natural materials. The first, a commercially available self-assembling peptide gel (Puramatrix; Pu), possesses

favorable properties for the culture of numerous cell types and supports chondrocyte-mediated ECM deposition (Kisiday *et al*. 2002; Kisiday *et al*. 2005). More recently, we and others have demonstrated that equine (Kisiday *et al*. 2007) and human (Mauck *et al*. 2006) MSCs undergo chondrogenesis in this hydrogel. While not providing specific receptor mediated interactions (e.g., RGD signaling cascades are not activated), the gel does appear to promote cell adhesion and neurite extension (Holmes *et al*. 2000) and may further be susceptible to proteolytic breakdown. The second biopolymer used was a photo-crosslinked hyaluronic acid (HA) based hydrogel. This gel supports ECM deposition by articular and auricular chondrocytes, both *in vitro* and *in vivo* (Nettles *et al*. 2004; Burdick *et al*. 2005; Chung *et al*. 2006). HA expression is regulated during limb bud formation and mesenchymal cell condensation, and is a primary structural component of adult cartilage ECM (Toole 2004; Li *et al*. 2007). Chondrocytes interact with HA in the pericellular environment via CD44 receptors located on the cell surface (Knudson 1993; Knudson and Knudson 2004) and actively endocytose HA fragments (Morales and Hascall 1988). Thus, relative to the inert, non-interactive and non-degradable agarose hydrogel used in our previous studies, these two hydrogels provide an interactive and degradable, biologically relevant interface that might modulate MSC chondrogenesis and construct maturation.

To carry out this study, bovine chondrocytes and MSCs were isolated from the same group of donors and seeded in agarose, Puramatrix, and HA hydrogels. Constructs were cultured for 8 weeks with biweekly analysis of construct physical properties, MSC viability, ECM content, and mechanical properties. To further investigate the relationship

between deposited ECM and mechanical outcomes, we performed correlation analysis of the emerging structure (composition) and function (mechanical properties) of constructs formed from each cell type in each hydrogel.

## 3.2. Materials and Methods

### 3.2.1. Cell Isolation and Expansion

Bovine chondrocytes and MSCs were isolated from juvenile bovine joints within 36 hours of slaughter (Research 87, Boylston, MA). Articular chondrocytes (CH) were enzymatically isolated from carpometacarpal articular cartilage as previously described (Mauck *et al*. 2003). Chondrocytes were seeded in hydrogels immediately upon isolation. Bone marrow derived MSCs were isolated from the underlying trabecular region of the carpal bone as in (Mauck *et al*. 2006). In order to obtain a sufficient number of MSCs, cells were expanded in Dulbecco's Modified Eagle Medium (DMEM) supplemented with 10% fetal bovine serum (Gibco) and 1X penicillin-streptomycin-fungizone through passage 2 or 3. Both chondrocytes and MSCs were seeded at a density of 20 million cells/mL in agarose, methacrylated HA (MeHA), and Puramatrix self-assembling peptide hydrogels. Two complete studies were performed with cells from a minimum of 3 donor animals pooled for each experiment. Similar trends were observed in each replicate, with data from one study presented in this manuscript.

### 3.2.2. Cell Seeding in Hydrogels

To produce cell-laden agarose gels, Type VII agarose (Sigma Chemicals, St. Louis, MO) was dissolved in phosphate buffered saline (PBS) at a concentration of 4% w/v,

autoclaved, and cooled to 49°C. Agarose was combined 1:1 with a cell suspension (40 million/ml) of either chondrocytes or MSCs in DMEM to provide a seeding density of 20 million cells per ml in a 2% w/v agarose hydrogel. The cell-hydrogel suspension was cast between two glass plates separated by 2.25 mm thick spacers and gelled at 25° C for 20 minutes. Cylindrical constructs were removed from gel slabs using a sterile 5 mm diameter biopsy punch (Miltex, York, PA).

Photo-crosslinkable methacrylated hyaluronic acid (MeHA) solutions were produced as previously described (Burdick *et al*. 2005). Briefly, 65 kDa HA (Lifecore, Chaska, MN) was methacrylated by reaction with methacrylic anhydride (Sigma Chemicals, St. Louis, MO) at pH 8.0 for 24 hours, dialyzed in distilled water against a 5kDa MW cutoff, lyophilized, and stored at -20°C (Burdick *et al*. 2005; Chung *et al*. 2006; Chung *et al*. 2008). MeHA was dissolved to 2% w/v in PBS supplemented with 0.05% w/v of the photoinitiator I2959 (2-methyl-1-[4-(hydroxyethoxy)phenyl]-2-methyl-1-propanone, Ciba-Geigy, Tarrytown, NY). To produce cell-laden gels, cells were resuspended in the MeHA macromer solution (20 million cells/mL) and the suspension cast between glass plates as above. Polymerization was achieved with UV exposure through the glass plates for 10 minutes using a 365 nm Blak-Ray UV lamp (Model #UVL-56, San Gabriel, CA). Cylindrical constructs were cored from the resulting slab with a 5 mm diameter biopsy punch.

The self-assembling peptide hydrogel solution was purchased as Puramatrix ($(REDA)_4$, 1% w/v; BD Bioscience, San Jose, CA). Chondrocytes (isolated immediately) or MSCs

(after trypsinization) were washed twice in a sterile 10% w/v sucrose solution to remove residual culture medium. Cell pellets were resuspended at 40 million cells/mL in a 10% sucrose solution and mixed well with an equal volume of 1% w/v Puramatrix solution to produce a final concentration of cell-seeded 0.5% w/v Puramatrix. A sterile neoprene rubber mold with cylindrical cavities (5 mm diameter; 2.25 mm thickness) was placed on the bottom of a 100 mm culture dish. Cell/Puramatrix solution was injected into the void spaces, and sterile filter paper (pre-wet with DMEM) was placed over the mold. The filter paper served as both a source and a path for diffusion of ions from the culture medium to initiate self-assembling peptide polymerization. A glass plate was then added to sandwich the filter paper to the mold to ensure an even construct surface. Sufficient medium to cover the molds was added and constructs were allowed to polymerize for 30 minutes. The molding apparatus was then carefully disassembled and constructs removed to non-tissue culture treated 6-well plates.

3.2.3. Construct Culture and Analysis

Constructs were cultured (1mL/construct) in TGF-β3 (10ng/ml, R&D Systems, Minneapolis, MN) supplemented chemically defined chondrogenic medium consisting of high glucose DMEM with 1x PSF, 0.1 μm dexamethasone, 50 μg/mL ascorbate 2-phosphate, 40 μg/mL l-proline, 100 μg/mL sodium pyruvate, ITS+ (6.25 μg/ml insulin, 6.25 μg/ml transferrin, 6.25 ng/ml selenous acid, 1.25 mg/ml bovine serum albumin, and 5.35 μg/ml linoleic acid) in non-tissue culture treated 6-well plates. Media were changed twice weekly. Encapsulated cell viability was visualized with the Live/Dead assay (Invitrogen, Eugene, OR). Samples for Live/Dead were cross-sectioned with a sterile

scalpel and rinsed twice in sterile PBS before being incubated for 20 minutes (at 20ºC) in a PBS solution containing 2 μM Calcein AM and 4 μM Ethidium homodimer-1. Stained construct cross-sections were imaged using an inverted fluorescence microscope (Nikon T30, Nikon Instruments, Inc., Melville, NY).

### 3.2.4. Mechanical Testing

Mechanical testing in unconfined compression was carried out bi-weekly to determine equilibrium and dynamic properties as in (Mauck *et al*. 2006). On the day of testing, sample dimensions were measured with a digital caliper. Creep tests were then performed in a PBS bath between two impermeable platens with a 2 gram load applied and displacement monitored until equilibrium (~300 seconds). Subsequently, stress relaxation tests were performed by applying a single compressive deformation to 10% strain (at 0.05%/second) followed by 20 minutes of relaxation to equilibrium. The equilibrium modulus ($E_Y$) was calculated from the equilibrium stress and strain values based on the measured construct dimensions. Dynamic testing was then carried out via the application of a sinusoidal deformation of 1% applied at 1.0 Hz for ten cycles. The dynamic modulus ($|G^*|$) for each sample was calculated from the slope of the dynamic stress-strain curve as in (Park *et al*. 2003).

### 3.2.5. Biochemical Analyses

After compression testing, construct wet weights were recorded and samples were digested in papain for analysis of DNA, glycosaminoglycan (GAG), and collagen content (Mauck *et al*. 2006). DNA content (per construct) was determined using the dsDNA

Picogreen Assay (Molecular Probes, Eugene, OR) with lambda DNA as a standard. GAG content (total and percent wet weight) was determined using the 1,9-dimethylmethylene blue (DMMB) dye binding assay with chondroitin-6 sulfate as a standard (Farndale *et al*. 1986). Digested aliquots were also hydrolyzed for 16 hours in 12N hydrochloric acid at 110$^{o}$C and the orthohydroxyproline (OHP) content quantified via colorimetric reaction with chloramine T and diaminobenzaldehyde, against an OHP standard curve (Stegemann and Stalder 1967). Collagen content was extrapolated from OHP using a 1:10 ratio of OHP:collagen (Vunjak-Novakovic *et al*. 1999).

### 3.2.6. Histology

Samples from each hydrogel at each time point were fixed in 4% paraformaldehyde, infiltrated with Citrisolv, and embedded in paraffin blocks. Sections (8 μm) were mounted on glass slides and stained for proteoglycan using alcian blue (pH 1.0) and for collagen via picrosirius red as in (Mauck *et al*. 2003).

### 3.2.7. Statistical Analyses

Statistical analysis was performed using Systat (v10.2, San Jose, CA). A three-way ANOVA analysis was carried out, with cell type, time in culture, and hydrogel type as independent factors. Dependent variables were wet weight, thickness, diameter, Young's modulus, dynamic modulus, [GAG], [collagen], and DNA content. When significant effects ($p<0.05$) were observed, Fisher's LSD post hoc analysis was used to compare between groups. All values are reported as the mean ± SD. For correlation analyses,

GraphPad Prism (San Diego, CA) was used to fit data and determine goodness of fit, and t-tests were used to compare correlation slopes between conditions.

## 3.3. Results

### 3.3.1. 3D Culture: Cell Shape, Viability, and Construct Dimensions

Upon encapsulation, chondrocytes and MSCs took on a rounded shape in each hydrogel. In agarose, both cell types remained rounded throughout the culture duration, and occasional small clusters could be observed indicative of cell division (**Figure 3-1**). In the photo-crosslinked MeHA gels most cells remained rounded, while a minor fraction of both cell populations developed small protrusions. In Puramatrix gels, chondrocytes and MSCs showed both round shapes as well as pronounced filopodial projections throughout the gel, with this finding more pronounced in MSC cultures. Viability was high for each cell type in all gels, with Live/Dead staining showing no obvious differences between agarose, MeHA, and Puramatrix hydrogels on either day 14 or 42 (**Figure 3-1**).

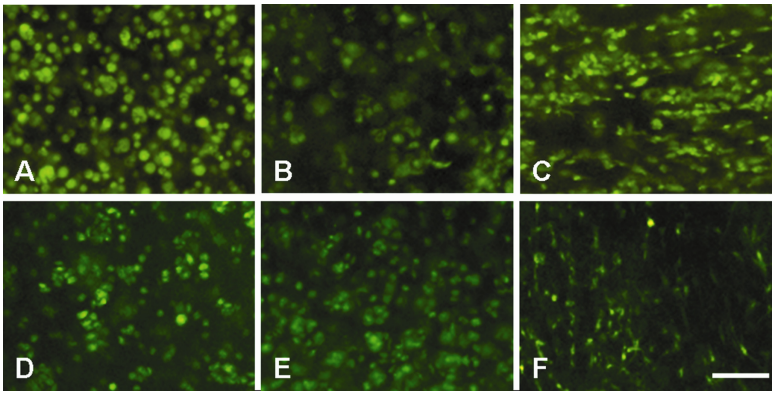


**Figure 3-1: Calcein AM staining of live cells in construct cross sections on day 42 for chondrocytes (A-C) and MSCs (D-F) in agarose (left), MeHA (middle), and Puramatrix (right) hydrogels. (40X magnification; scale bar = 50 μm)**

| | 2% Agarose | | 2% MeHA | | 0.5% Puramatrix | |
|---|---|---|---|---|---|---|
| **Chondrocytes** | **2 weeks** | **8 weeks** | **2 weeks** | **8 weeks** | **2 weeks** | **8 weeks** |
| Wet Weight (mg) | 43.7 ± 1.5* | 57.5 ± 2.7# | 46.5 ± 2.6* | 66.2 ± 4.6# | 24.2 ± 3.6* | 35.0 ± 3.0# |
| s-GAG (µg) | 553.8 ± 44.2* | 1868.1 ± 232.3# | 173.5 ± 9.6* | 647.1 ± 70.1# | 77.7 ± 33.6 | 717.1 ± 178.3# |
| Collagen (µg) | 194.6 ± 18.9* | 1200.4 ± 121.5# | 36.2 ± 10.0 | 276.3 ± 33.8# | 24.7 ± 10.3 | 530.9 ± 128.9# |
| Thickness (%change) | 3.9 ± 1.9 | 12.0 ± 1.7# | 11.4 ± 2.1* | 25.1 ± 7.7# | -26.8 ± 6.9* | -3.5 ± 9.3** |
| Diameter (%change) | -0.8 ± 0.8 | 6.2 ± 1.1# | -5.2 ± 0.1* | 3.8 ± 0.2** | -15.4 ± 0.5* | -11.2 ± 6.1# |
| **MSCs** | **2 weeks** | **8 weeks** | **2 weeks** | **8 weeks** | **2 weeks** | **8 weeks** |
| Wet Weight (mg) | 46.6 ± 0.9* | 58.5 ± 3.9# | 65.2 ± 0.6* | 87.3 ± 1.0# | 15.9 ± 0.9* | 21.0 ± 2.6# |
| s-GAG (µg) | 702.2 ± 86.1* | 1455.4 ± 181.2# | 633.2 ± 32.4* | 1602.7 ± 91.4# | 306.3 ± 21.4* | 819.2 ± 135.1# |
| Collagen (µg) | 211.1 ± 20.9* | 718.3 ± 192.4# | 204.9 ± 19.2* | 738.1 ± 170.7# | 134.1 ± 20.9* | 388.1 ± 72.5# |
| Thickness (%change) | 1.7 ± 1.2 | 13.4 ± 2.5# | 23.3 ± 3.0* | 37.1 ± 2.1# | -3.0 ± 8.8 | 2.1 ± 5.4 |
| Diameter (%change) | 0.7 ± 1.1 | 7.9 ± 4.6# | 2.3 ± 1.3 | 16.1 ± 2.1# | -42.2 ± 1.62* | -30.1 ± 3.6# |

**Table 3-1: Time dependent changes in construct dimensions and biochemical content. Mean ± SD of 3-4 samples per group at each time point. (*indicates p<0.05 versus day 0 **indicates p<0.05 from day 14, #indicates p<0.05 versus day 0 and day 14)**

While viability was similar, differences in dimensional characteristics were observed in the three cell-seeded hydrogels and summarized in **Table 3-1**. For all constructs, marked increases in wet weight were observed between day 14 and day 56 ($p<0.005$). Increased wet weight correlated with increases in s-GAG and collagen deposition within the constructs (increasing its density), as well as changes in construct diameter and thickness. Of significant note, Puramatrix hydrogels seeded with chondrocytes and MSCs decreased in volume over the initial two weeks of culture, with the most marked changes in MSC-laden construct diameters (>40% reduction for Puramatrix-MSC, $p<0.001$ vs. day 0). This decrease in diameter slowly reversed with time, but remained <30% of the starting diameter on day 56. These changes in size translated to changes in Puramatrix wet

weight, with both chondrocyte- and MSC-laden Puramatrix gels significantly lower than all other gels at day 56 ($p<0.001$). Conversely, MeHA gels increased in size with culture duration, particularly in the axial direction, increasing by ~25% and ~37% in thickness by day 56 for chondrocyte- and MSC-seeded conditions, respectively ($p<0.001$). Agarose hydrogels underwent only minor changes in dimensions throughout the culture period with either cell type.

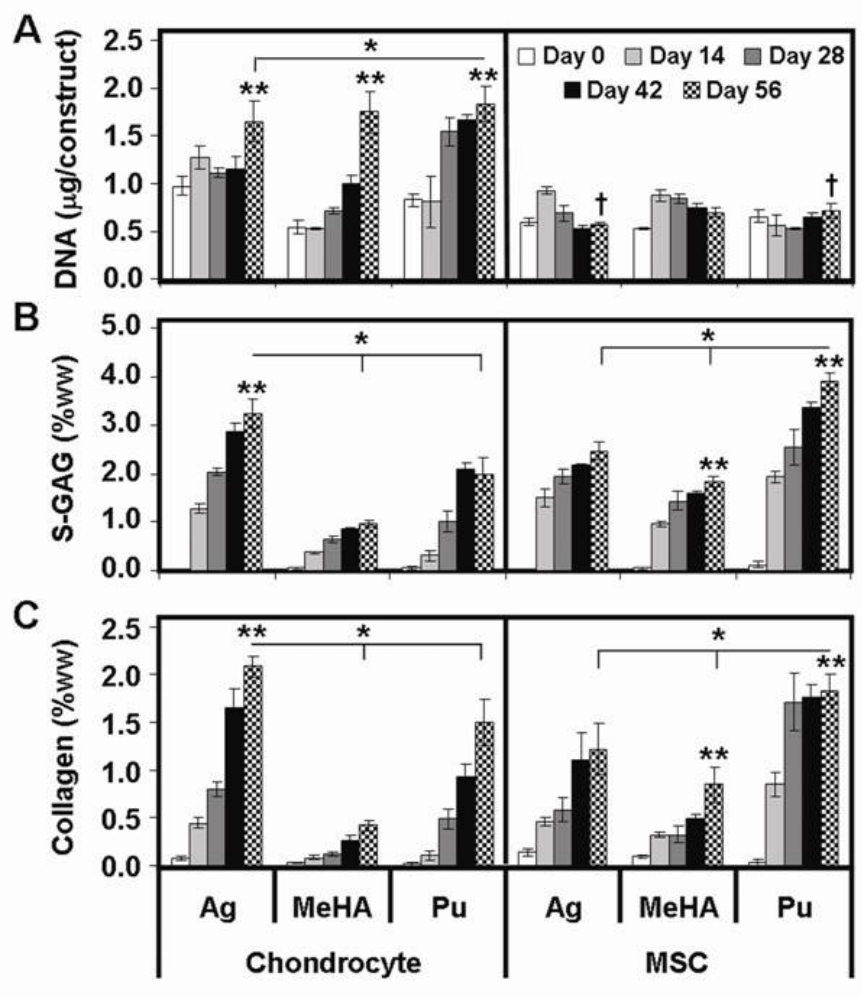


**Figure 3-2: Biochemical content of chondrocyte and MSC-seeded constructs as a function of time over an 8 week culture period. (A) DNA content, (B) GAG as a percentage of the wet weight (%ww), and (C) collagen as a percentage of the wet weight. Data represent the mean ± SD of 3-4 samples from one of two replicate studies. *indicates $p<0.05$ for day 56 comparisons between hydrogels within cell type. **indicates greater value ($p<0.05$) for comparisons on day 56 within hydrogel between cell types. †indicates no significant increase from day 0 ($p>0.05$).**

3.3.2. Biochemical Composition and Histological Analysis

Biochemical and histological analysis of constructs was carried out on a bi-weekly basis for each gel type and each cell type. In general, increasing time led to more matrix accumulation in each gel for each cell type as shown by histology and quantification of deposited ECM. For all chondrocyte-laden gels, DNA content increased 2-3 times over the 8 week culture period ($p<0.001$, **Figure 3-2A**). On day 56, there was no significant difference between the total DNA content of each hydrogel construct. In MSC-laden constructs, little change in DNA content was observed over the 8 week time course. MeHA-MSC and Puramatrix-MSC constructs contained ~20% more DNA/construct than agarose-MSC constructs on day 56. (**Figure 3-2A**; MeHA, $p=0.08$; Puramatrix, $p=0.06$, versus agarose).

Overall ANOVA results showed that sGAG deposition in each hydrogel was dependent on time in culture ($p<0.001$), hydrogel type ($p<0.001$), and cell type ($p<0.001$). For chondrocytes and MSCs, significant increases in sGAG content were observed in each gel (**Figure 3-2B**, $p<0.001$). On day 56, agarose-CH gels contained 1.5-3-fold greater sGAG per wet weight (ww) compared to MeHA-CH and Puramatrix-CH gels. Agarose-CH gels attained ~3.2%ww sGAG and were significantly greater ($p<0.001$) than both Puramatrix-CH (~2%) and MeHA-CH (~1%) gels (**Figure 3-2B**). Conversely, agarose-MSC and MeHA-MSC hydrogels contained similar amounts of GAG on a per wet weight basis, while Puramatrix-MSC gels were nearly 2 times greater. Puramatrix-MSC gels contained ~3.9% wet weight GAG, which was greater ($p<0.001$) than both agarose-MSC

(~2.5%) and MeHA-MSC (~1.8%) gels (**Figure 3-2B**). Indeed, this value was higher than the highest value achieved for chondrocyte seeded gels (agarose-CH group, $p<0.001$). Most interestingly, this was not the result of increased GAG production in Puramatrix-MSC gels, but rather was the result of the reduction in volume observed; on a per construct basis, agarose-MSC and MeHA-MSC gels contained 1500-1600 μg of GAG compared to ~800 μg for Puramatrix-MSC gels (**Table 3-1**).

Similar to GAG results, collagen content was dependent on time in culture ($p<0.001$), gel type ($p<0.001$), and cell type ($p<0.001$). Collagen content as a function of wet weight was 1.4-5 fold greater in agarose-CH than in MeHA-CH and Puramatrix-CH constructs. Agarose-CH gels contained ~2.1% ww collagen, a higher level than in Puramatrix-CH (~1.5%) and MeHA-CH (~0.4%, $p<0.02$, **Figure 3-2C**) constructs. In terms of collagen content per construct, agarose-CH contained 2-fold greater collagen than Puramatrix-CH and 4-fold greater collagen than MeHA-CH constructs ($p<0.001$; **Table 3-1**). Conversely, Puramatrix-MSC gels contained the highest collagen content (1.8%), levels greater than for agarose-MSC (1.2%, $p<0.001$), and both greater than MeHA-MSC (0.8%, $p<0.001$) constructs. For these MSC cultures, the highest collagen density observed (in the Puramatrix-MSC group) was only slightly lower than that found for the best chondrocyte-laden hydrogel group (agarose-CH, $p<0.02$). As with GAG content, the apparent improvement in collagen content in Puramatrix-MSC constructs was more a function of dimensional changes, with ~2-fold less total collagen in these constructs compared to either agarose or MeHA on a per construct basis (**Table 3-1**; $p<0.001$).

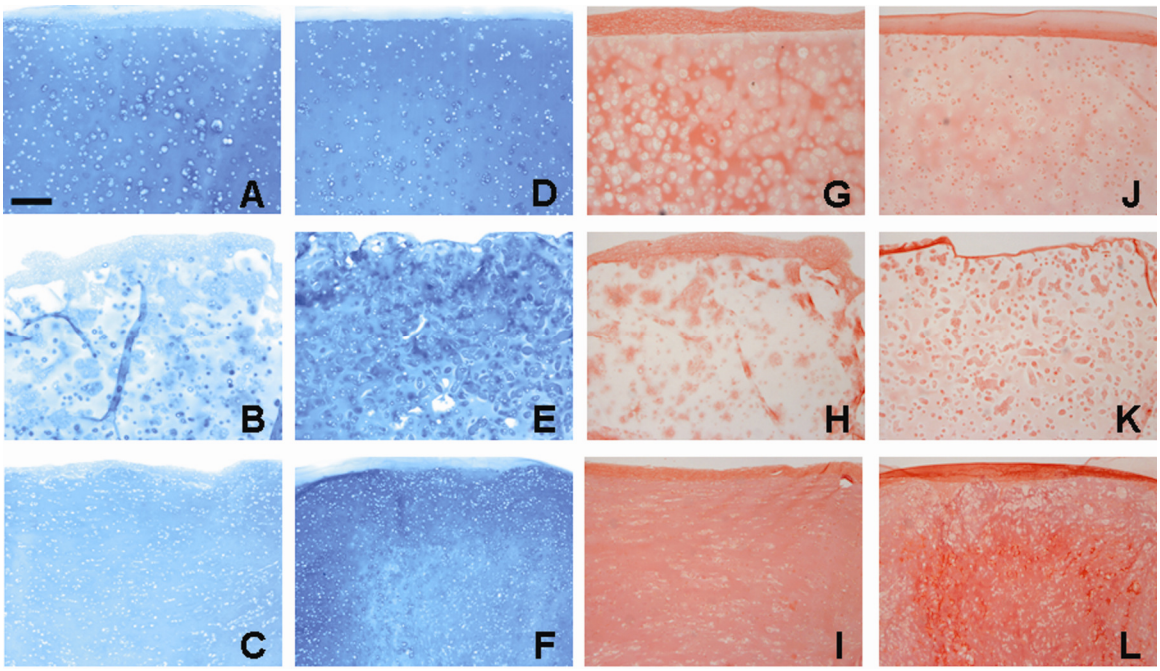


**Figure 3-3: Histological analysis of chondrocyte and MSC-seeded constructs on day 56. Alcian blue staining of proteoglycan in chondrocyte (A-C) and MSC-seeded (D-F) agarose (top), MeHA (middle), and Puramatrix (bottom) hydrogels. Picrosirius red staining of collagen in chondrocyte (G-I) and MSC-seeded (J-L) agarose (top), HA (middle), and Puramatrix (bottom) hydrogels. (100X magnification; scale bar = 200 μm)**

Histological staining of constructs produced findings consistent with gross biochemical measures. Alcian blue staining of GAG deposition in chondrocyte- and MSC-seeded constructs correlated well with biochemical measures (**Figure 3-3A-F**). Noticeably less GAG deposition was observed in MeHA-CH sections relative to all other groups. Picrosirius red staining of collagen elicited similar results; agarose-CH and Puramatrix-CH constructs stained much more intensely for collagen than MeHA-CH constructs. More collagen was observed in MeHA-MSC constructs, though staining remained less intense and less evenly distributed than in either agarose-MSC or Puramatrix-MSC constructs. (**Figure 3-3G-L**).

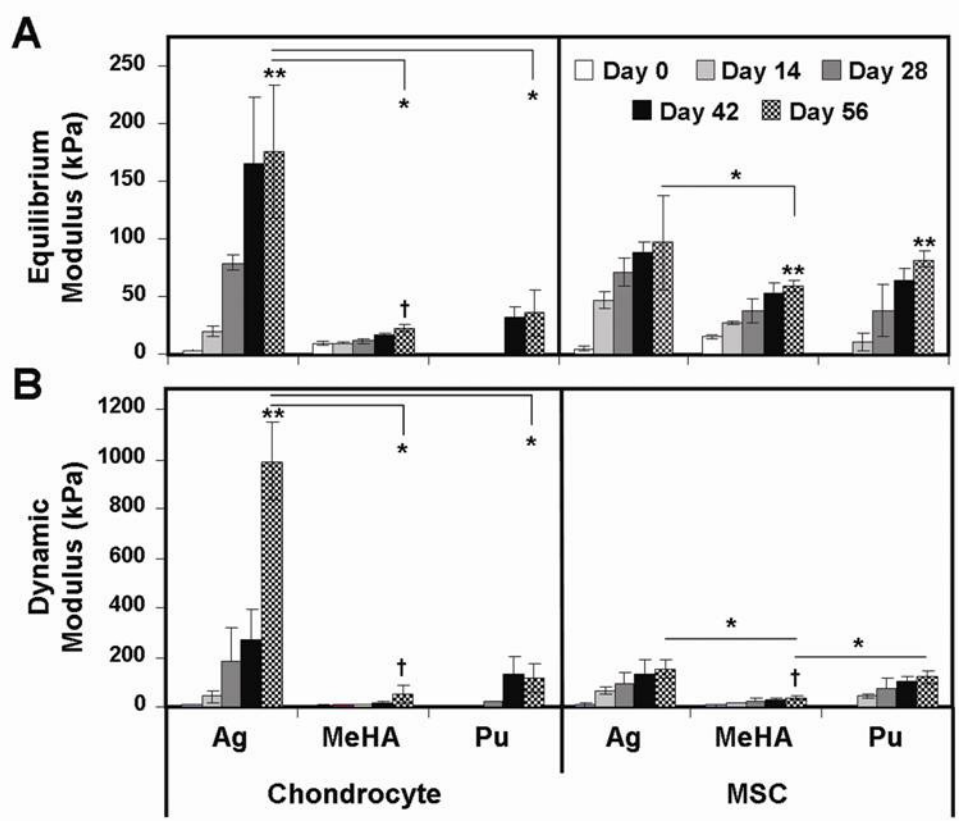


**Figure 3-4: (A) Equilibrium modulus ($E_Y$), and (B) dynamic modulus (IG*I), of agarose (Ag), MeHA, and Puramatrix (Pu) hydrogels seeded with chondrocytes or MSCs over 56 days. Data represent the mean ± SD of 3-4 samples from one of two replicate studies. *indicates $p<0.05$ for day 56 comparisons between hydrogels within cell type. ** indicates greater value ($p<0.05$) for comparisons on day 56 within hydrogel between cell types. †indicates no significance from day 0 ($p>0.05$).**

3.3.3. Mechanical Properties

The equilibrium ($E_Y$) and dynamic ($|G^*|$) compressive modulus of cell-seeded constructs were evaluated over the 8 week time course (**Figure 3-4**). Overall, time, gel type, and cell type were significant factors in both mechanical measures ($p<0.05$). The equilibrium modulus ($E_Y$) of chondrocyte-seeded constructs increased with time relative to their starting values ($p<0.001$ on day 28 for agarose-CH and $p<0.05$ on day 42 for Puramatrix-CH; for MeHA-CH, $p=0.343$ on day 56), though Puramatrix constructs were too soft for mechanical testing until day 28. On day 56, $E_Y$ of agarose-CH constructs reached ~170 kPa, a value 5-7 fold ($p<0.001$) greater than that of either MeHA-CH or Puramatrix-CH

constructs. Similar findings were noted with regards to |G*|, though the differences between groups were accentuated. On day 56, agarose-CH constructs reached a |G*| of ~1 MPa, a level 20- and 10-fold greater ($p<0.001$) than MeHA-CH and Puramatrix-CH constructs, respectively.

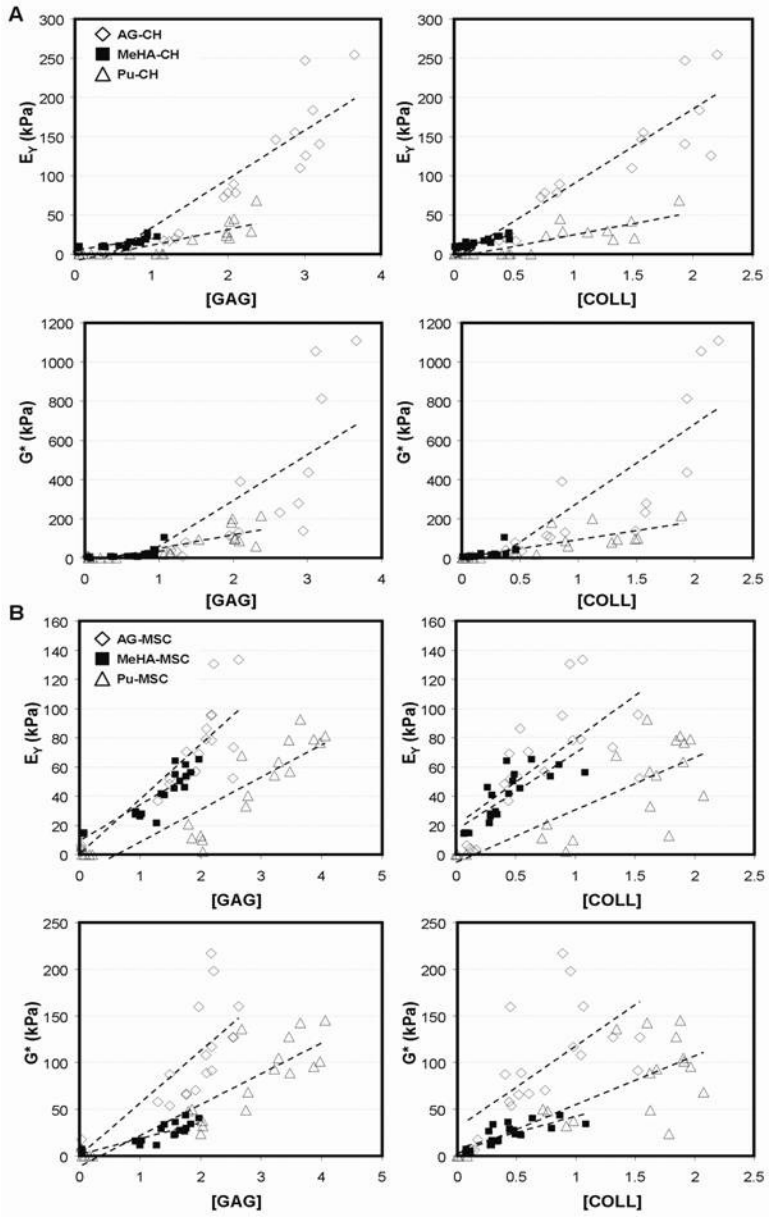


**Figure 3-5: Correlation plots relating measured mechanical properties to biochemical constituents. (A) Plots for chondrocyte seeded hydrogels. (B) Plots for MSC seeded hydrogels. Dashed line shows linear curve fit for each gel type.**

A different functional maturation process was noted for MSC-seeded constructs, with increases in equilibrium properties comparable between each hydrogel. Each hydrogel seeded with MSCs increased in $E_Y$ as a function of time in culture ($p<0.005$ vs. day 0 on day 14 for agarose-MSC, day 42 for MeHA-MSC, and day 28 for Puramatrix-MSC). The $E_Y$ of agarose-MSC constructs on day 56 was ~100 kPa, compared to ~60kPa for MeHA-MSC gels and ~80 kPa for Puramatrix-MSC gels. At this time point, $E_Y$ of MSC-seeded constructs were similar to one another, with significant difference only found between agarose-MSC and MeHA-MSC ($p<0.01$). Similarly, the $|G^*|$ of agarose-MSC constructs increased with time ($p<0.001$ vs. day 0), reaching a value of ~0.15 MPa on day 56. $|G^*|$ values for MeHA-MSC and Puramatrix-MSC increased with time as well, reaching 0.04 MPa and 0.12 MPa, respectively. At this time point, $|G^*|$ for agarose-MSC and Puramatrix-MSC gels were not different from one another ($p=0.37$), while the $|G^*|$ of the MeHA-MSC group was significantly lower than both ($p<0.05$). For both $E_Y$ and $|G^*|$, the highest values achieved for MSC-laden hydrogels on day 56 were lower than that achieved for the agarose-CH group ($p<0.001$ and $p<0.001$, respectively).

### 3.3.4. Structure-Function Correlation Analysis

To better elucidate the relationships between new matrix deposition and functional maturation, correlation analyses were performed between the level of a given biochemical constituent and the resulting construct mechanical properties. Specifically, $E_Y$ and $|G^*|$ were correlated to the concentration (as a percentage of wet weight) of s-GAG and collagen in each construct for each cell type and each hydrogel formulation. The results of these correlations are shown in **Figure 3-5**, and the slopes and correlation

coefficients are provided in **Table 3-2**. For each comparison, a significant linear fit was achieved ($p<0.005$), with R2 values ranging from 0.392 to 0.925. For chondrocyte-seeded constructs, the slope of the correlations was uniformly higher for agarose-CH gels than for either the MeHA-CH and Puramatrix-CH gels ($p<0.05$). For example, the slope of $E_Y$ vs. [GAG] for agarose-CH gels was 62.9 kPa/%ww, and was significantly higher than for MeHA (13.9 kPa/%ww) and Puramatrix (20.0 kPa/%ww) constructs. For MSC-laden constructs, modest differences were observed between gel types (all lower, $p<0.01$ compared to agarose except for MeHA $E_Y$ vs. [COLL], $p=0.08$). For the same comparison as above on MSC-laden constructs (EY vs. [GAG]), correlation slopes were 37.6, 24.7, and 22.2 kPa/%ww for agarose-MSC, MeHA-MSC, and Puramatrix-MSC, respectively. Finally, comparing the same correlations slopes across cell types allows one to draw conclusions regarding the ability of MSCs to produce functional matrix relative to a chondrocyte control. For all agarose-MSC groups except $E_Y$ vs. [COLL] ($p=.367$), correlation slopes were lower in agarose-MSC than in agarose-CH samples ($p<0.05$). For MeHA-MSC and Puramatrix-MSC constructs, the correlation slopes of $E_Y$ were generally higher than those achieved in the corresponding chondrocyte group. Conversely, the $|G^*|$ slopes in MeHA-MSC and Puramatrix-MSC were lower than their chondrocyte counterparts ($p<0.005$). In either case, for both $E_Y$ and $|G^*|$, the correlation slopes for the MSC-laden constructs remained well below that achieved in agarose-CH constructs ($p<0.05$).

| Table 2 Structure-Function Correlations | | | | | | | | | | |
|---|---|---|---|---|---|---|---|---|---|---|
| | | Chondrocytes | | | | MSCs | | | | |
| Gel | Comparison | Slope | $R^2$ | P value | Versus agarose | Slope | $R^2$ | P value | Versus agarose | Versus CH |
| Agarose | $E_Y$ vs. [GAG] | 62.9 | 0.800 | <0.0001 | | 37.6 | 0.752 | <0.0001 | | * |
| | $E_Y$ vs. [COLL] | 96.9 | 0.857 | <0.0001 | | 59.1 | 0.478 | 0.0004 | | ns |
| | G* vs. [GAG] | 233.9 | 0.490 | 0.0006 | | 56.1 | 0.658 | <0.0001 | | *** |
| | G* vs. [COLL] | 405.8 | 0.694 | <0.0001 | | 87.9 | 0.414 | 0.0011 | | * |
| MeHA | $E_Y$ vs. [GAG] | 13.9 | 0.654 | <0.0001 | *** | 24.7 | 0.925 | <0.0001 | ** | ns |
| | $E_Y$ vs. [COLL] | 34.2 | 0.800 | <0.0001 | *** | 52.8 | 0.645 | <0.0001 | ns | ** |
| | G* vs. [GAG] | 44.6 | 0.392 | 0.0021 | * | 17.0 | 0.753 | <0.0001 | *** | *** |
| | G* vs. [COLL] | 106.9 | 0.455 | 0.0008 | * | 34.6 | 0.584 | <0.0001 | *** | *** |
| Puramatrix | $E_Y$ vs. [GAG] | 20.0 | 0.696 | <0.0001 | *** | 22.2 | 0.803 | <0.0001 | ** | ns |
| | $E_Y$ vs. [COLL] | 28.9 | 0.72 | <0.0001 | *** | 35.0 | 0.630 | <0.0001 | ** | ns |
| | G* vs. [GAG] | 69.4 | 0.668 | <0.0001 | *** | 33.0 | 0.793 | <0.0001 | *** | *** |
| | G* vs. [COLL] | 95.2 | 0.642 | <0.0001 | *** | 52.2 | 0.595 | <0.0001 | ** | * |

**Table 3-2: Correlation of mechanical properties and biochemical content in chondrocyte and MSC seeded constructs. Correlation coefficients relating measured mechanical properties ($E_Y$ and IG*I) with concentration of GAG and collagen for chondrocyte and MSC seeded constructs. *indicates p<0.05, **indicates p<0.01, ***indicates p<0.001, 'ns' indicates no significant difference.**

### 3.4. Discussion

The goal of this study was to evaluate the functional formation of cartilage tissue in three distinct MSC-laden hydrogels, and to compare these findings to those produced by fully differentiated chondrocytes maintained in the same culture environment. The motivation for this study was based on our previous finding that in agarose hydrogels, MSCs underwent chondrogenesis, but formed cartilage-specific ECM of lower quantity and quality than constructs formed with donor matched fully-differentiated chondrocytes cultured under the same conditions. Given the growing body of evidence supporting biomaterial dependent stem cell differentiation, we hypothesized that cell-hydrogel interactions would modulate the rate and extent of functional chondrogenesis. Results of this study show that, surprisingly, the external hydrogel environment plays a more

significant role in chondrocyte- compared to MSC-mediated matrix deposition and functional maturation. Articular chondrocytes formed the most mechanically robust ECM in agarose hydrogels, followed by Puramatrix and then MeHA gels. Conversely, MSC-laden hydrogels showed similar results across gel types, with marked increases in mechanical properties in each gel. However, in each case, the maximum compressive properties achieved in MSC-laden constructs remained lower than that achieved by fully-differentiated chondrocytes in agarose gels. These findings are consistent with our previous observations (Mauck *et al*. 2006; Huang *et al*. 2008), and further support the notion that existing methodologies for effecting MSC chondrogenesis in 3D culture have not yet been optimized to produce cells possessing functional matrix forming capacity on par with that of a fully differentiated chondrocytes.

Several important observations were made regarding differential biomaterial effects on construct formation with either chondrocytes or MSCs. Notably, changes in construct size were pronounced in the differing hydrogels. We have previously reported only minor changes in construct diameter and thickness in agarose hydrogels seeded with chondrocytes or MSCs (Mauck *et al*. 2006). Findings in agarose in this study were consistent with that observation, and further showed pronounced increases in volume in cell-seeded MeHA gels (particularly in the axial direction), and a marked reduction in volume in Puramatrix-based constructs, particularly when seeded with MSCs. These changes in Puramatrix construct volume are consistent with recent work by Kisiday and colleagues, who reported decreases in construct diameter in bone marrow and adipose-derived MSC-seeded constructs seeded in ~0.4% $(KLDL)_3$ self-assembling peptide gels

(Kisiday *et al*. 2007). This change in construct size may limit clinical application to constructs that have been pre-matured *in vitro*, punched to size, and then implanted into defined cartilage defects. More generally, this contraction suggests that cell-mediated traction is occurring, as has similarly been reported when constructs are formed using gelatin sponges (Awad *et al*. 2004). Indeed, both chondrocytes and MSCs were elongated with numerous cell protrusions in the Puramatrix constructs. One consequence of this volume reduction in Puramatrix-based gels was to increase the effective concentration of GAG and collagen within the constructs, though the total amount per construct was lower than that produced by chondrocytes. The decreased volume resulted in Puramatrix-based constructs reaching levels of GAG and collagen concentrations (on a percentage wet weight basis) comparable to that observed for chondrocytes seeded in agarose gels. Notably, DNA content on day 56 in each MSC-seeded hydrogel was comparable, suggesting that the production levels, on a per cell basis, were lower in Puramatrix hydrogels. Regardless of this concentration effect, Puramatrix-MSC mechanical properties did not match those of agarose-CH constructs.

Another observation in this study was that articular chondrocytes in MeHA did not readily form functional matrix. This finding is consistent with our previous studies comparing auricular and articular chondrocytes in this hydrogel (Chung *et al*. 2006), wherein auricular chondrocytes produced a considerably more robust ECM than articular chondrocytes. In this previous work, constructs were cultured both *in vivo* (subcutaneously) and *in vitro* in a serum-containing medium. Here we show that *in vitro* culture in a chemically defined pro-chondrogenic media formulation does not restore

functional capacity to articular chondrocytes in this gel. This finding of lower ECM formation was not a function of cell death due to UV of photo-initiator exposure as DNA content increased similarly for chondrocytes in this gel as in the other two culture systems assayed. This suggests that the MeHA gel, in its present formulation, may not be optimized for articular-derived cells. While it is not yet clear whether matrix was made in lower quantities, or made in the same quantity and lost from the gel during culture, it is clear that these chondrocyte seeded MeHA constructs will require further modification to optimize their growth. More generally, these findings suggest that chondrocytes are more sensitive to the gel environment than MSCs (which performed much better in this MeHA formulation). This was a surprising result, given that articular chondrocytes are largely anchorage independent (as they can live well in cell aggregates (Aufderheide and Athanasiou 2007)), while MSCs require a defined extracellular niche. This finding suggests that MeHA gel properties may be optimized to improve construct maturation. For example, we have recently shown that the starting concentration of the MeHA solution (and so the starting mechanical properties of the hydrogel) alters the final mechanical properties of MSC-seeded constructs after 9 weeks of culture (see Chapter 4), and that a new hydrolytically degradable MeHA formulation promotes more rapid distribution of formed ECM components (Sahoo *et al*. 2008). By altering the biomaterial environment in these covalently crosslinked HA assemblies, an optimal environment for MSC chondrogenesis that is both permissive and pro-chondrogenic may be achieved.

To better understand how matrix deposition related to functional maturation in these constructs, we carried out a single factor correlation analysis for each hydrogel and cell

type. Similar analyses have previously been performed for chondrocytes and MSCs seeded in degradable meshes and hydrogels (Vunjak-Novakovic *et al*. 1999; Mauck *et al*. 2002; Awad *et al*. 2004). The results of this analysis show how, for a given amount of ECM deposition, mechanical outcomes vary between conditions. In agarose-CH constructs, we found a strong positive correlation between GAG and $E_Y$, and show that for MeHA and Puramatrix constructs, the correlation slopes were smaller. This indicates that not only do agarose-CH constructs make more GAG, but the functional consequence of a given amount of GAG is greater in this hydrogel. While GAG levels were generally lower in MeHA and Puramatrix gels compared to agarose, collagen concentration in Puramatrix and agarose were comparable. However, the correlation slope for this ECM component was lower for the Puramatrix samples, indicating inferior matrix assembly. For the MSC-laden cultures, a different trend was observed. For these cells, in each gel type, similar correlation slopes were achieved. This suggests that between gels, MSCs assemble functional matrix in a similar fashion, though the slopes of these correlations were lower than that found for the same comparison in agarose-CH hydrogels. This finding further supports the notion that MSCs elaborate ECM that is inferior to that produced by fully differentiated chondrocytes. While not identified in the current study, we hypothesize that there exists critical structural ECM components whose expression and deposition is not yet optimized in MSC cultures. These factors must be identified and exploited to allow MSC-based constructs to achieve properties similar to that produced by agarose-CH constructs for functional cartilage tissue engineering applications.

While robust growth was observed in MSC-seeded constructs, biochemical content and mechanical properties did not yet meet that of the native tissue. For example, while s-GAG content reached 3-4% ww for agarose-MSC and Puramatrix-MSC cultures (near physiologic levels), the highest collagen content achieved was ~2% ww, less than 20% of the native tissue. It should be noted that this low collagen content was found in both MSC and chondrocyte-based cultures, and is a persistent limitation in engineered cartilage (Huang *et al*. 2008). Moreover, we did not specifically measure type I versus type II collagen ratios, which may well have differed in the differing hydrogels, particularly those that showed considerable contraction. Furthermore, while MSC-laden cultures reached equilibrium compressive properties that were ~25% that of bovine cartilage (and ~50% that of chondrocyte cultures), the dynamic modulus of MSC-based constructs only reached ~0.2 MPa (as compared to 1 MPa for chondrocyte-based constructs). The dynamic modulus is a critical mechanical feature of the native tissue, and consequently these values must be further optimized to enable *in vivo* function. Additional quantification of other mechanical features of these constructs, such as the hydraulic permeability and tensile properties, would also be useful in understanding the key differences amongst cell types and 3D culture conditions.

### 3.5. Conclusions

The results of this study demonstrate biomaterial dependent functional cartilage tissue formation. In particular, MSC-seeded constructs increased in mechanical properties in each hydrogel, with the most robust maturation reaching 100 kPa, ¼ the value of native bovine tissue. Continuing work is focused on further optimization of gel properties (as

detailed above) and culture conditions to improve MSC-based construct maturation. Recent reports have shown that the passive mechanical properties of the material can influence MSC differentiation in 2D cultures (Engler *et al*. 2006). These changes are slightly more difficult to achieve in 3D cultures, as changing the stiffness of the 3D network often requires concomitant changes in permeability, but such studies warrant further consideration. Alternatively, we have shown that dynamic loading can improve chondrocyte-based agarose construct maturation (Mauck *et al*. 2000; Mauck *et al*. 2003), and that articular chondrocytes in MeHA gels alter matrix gene expression with mechanical loading (Chung *et al*. 2008). Similarly, dynamic loading increased construct properties of chondrocyte-seeded Puramatrix hydrogels (Kisiday *et al*. 2004). We and others have further demonstrated that mechanical loading can modulate MSC chondrogenesis in 3D hydrogel culture (Huang *et al*. 2004; Mauck *et al*. 2007; Terraciano *et al*. 2007). These and other optimization strategies offer multiple avenues for improving MSC-based engineered cartilage constructs.

**This previously published Chapter was included with kind permission from Mary Ann Liebert, Inc: Tissue Engineering Part A, "Differential Maturation and Structure Function Relationships in MSC and Chondrocyte Seeded Hydrogels", volume 15, 2009, pgs 1041-1052, Isaac E. Erickson, Alice H. Huang, Cindy Chung, Ryan T. Li, Jason A. Burdick, Robert L. Mauck.**

# CHAPTER 4: Macromer Density Influences Mesenchymal Stem Cell Chondrogenesis and Maturation in Photo-crosslinked Hyaluronic Acid Hydrogels

## 4.1. Introduction

Articular cartilage lines the surfaces of joints and functions to transmit stresses. This function is enabled by the complex interplay between the fluid within the tissue with the dense extracellular matrix (ECM); specifically the type II collagen network and the large negatively charged proteoglycans. Subsequent to trauma, or as a result of degenerative diseases, cartilage undergoes fluctuations in its mechanical and biochemical content, and thus, loses its load-bearing capacity. To address this, the last two decades have witnessed a surge in activity aimed at the formation of engineered cartilage. Much of this work employed articular chondrocytes in three-dimensional (3D) culture environments (see (Chung and Burdick 2008) for review). In 3D hydrogels in particular, chondrocytes produce cartilage ECM that is assembled into a functional network with properties that begin to approximate that of native tissue (Buschmann *et al*. 1992). Physical properties of the gel, including polymer density and crosslinking, control the localization and mechanical properties of newly formed matrix (Bryant *et al*. 1999; Ng *et al*. 2006), as well as the diffusion of large macromolecules (Albro *et al*. 2008). The potential of hydrogels is underscored by recent work showing that compressive properties can meet or exceed native tissue properties (0.5-1.0 MPa) when custom media regimens are employed (Lima *et al*. 2007; Byers *et al*. 2008).

Despite these promising findings, the clinical use of chondrocytes may have limitations. Aged chondrocytes form mechanically inferior constructs when compared to those derived from juvenile chondrocytes (Tallheden *et al*. 2005; Tran-Khanh *et al*. 2005). An alternative might be the use of mesenchymal stem cells (MSCs) (Prockop 1997; Johnstone *et al*. 1998; Pittenger *et al*. 1999), which are expandable and retain their multi-differentiation characteristics (Baksh *et al*. 2004). As with chondrocytes, a range of 3D environments have been employed for engineering cartilage with MSCs (e.g., (Erickson *et al*. 2002; Awad *et al*. 2004; Meinel *et al*. 2004; Betre *et al*. 2005; Li *et al*. 2005; Mauck *et al*. 2006)). Chapter 3 demonstrated that bovine MSCs undergo chondrogenesis in agarose (a thermoreversible hydrogel), in self-assembling peptide gels, and in photo-crosslinked hyaluronic acid (HA) hydrogels. Mechanical properties and biochemical content of these constructs increased with time in each hydogel, though tissue formation was dependent on the type of hydrogel employed.

The literature on MSC differentiation indicates that specific factors modulate the rate and/or extent of MSC chondrogenesis. The biologic interface can induce different levels of molecular level chondrogenesis and control cell shape; inclusion of RGD moieties in modified alginate gels can limit chondrogenesis above a certain threshold (Connelly *et al*. 2007), while modification of polyethylene glycol (PEG) hydrogels with a collagen mimetic peptide can enhance chondrogenesis (Lee *et al*. 2008). Direct comparisons between photo-crosslinked PEG hydrogels (simple, non-interactive) and HA hydrogels (biologic, interactions through CD44 receptors) show improved chondrogenesis in HA when all other factors are held constant (Chung and Burdick 2009). Additionally,

biophysical properties such as pore size modulate the extent to which MSCs differentiate and accumulate matrix in PEG-based semi-interpenetrating networks (Buxton *et al*. 2007). While not yet shown for chondrogenesis in 3D culture, the micromechanics of the supporting environment can also tune MSC lineage-specification in 2D culture systems (Engler *et al*. 2006).

Collectively, these findings suggest that the biological, mechanical, and biophysical properties of the microenvironment interact to control the lineage specification of MSCs, as well as tissue maturation. Our past work with crosslinked HA hydrogels suggests that macromer density (which is inversely related to pore size and directly proportional to bulk mechanical properties) can be used to tune matrix formation by auricular chondrocytes (Chung *et al*. 2006). As Chapter 3 showed that MSCs undergo chondrogenesis in HA gels, but do so to a lesser extent than in other hydrogel environments (such as agarose), the purpose of this study was to determine whether changes in HA macromer density influence ECM deposition and generation of functional cartilage-like properties by MSCs. Results indicated that increasing HA density promoted chondrogenesis and matrix formation and retention, but yielded functionally inferior constructs due to limited matrix distribution throughout the construct expanse. These data provide new insight into how early matrix deposition regulates long term construct development, and define new parameters for optimizing functional MSC-based engineered cartilage using HA hydrogels.

## 4.2. Materials and Methods

### 4.2.1. MSC Isolation and Expansion

Bone marrow was extracted from juvenile bovine tibiae (Research 87, Boylston, MA) and MSCs isolated (Mauck *et al*. 2006). MSCs were expanded in a basal medium (BM) composed of DMEM supplemented with 10% fetal bovine serum (FBS, Gibco Invitrogen, Carlsbad, CA) and 1% penicillin-streptomycin-fungizone (PSF) through 2-3 passages. Three replicate studies were performed, with MSCs from 2-3 donor animals pooled for each replicate. Each replicate showed similar trends, and data from one replicate is presented.

### 4.2.2. Fabrication of Acellular and MSC-Seeded Constructs

Photo-crosslinkable methacrylated hyaluronic acid (MeHA) macromer was synthesized (~25% degree of methacrylation) as previously described in Chapter 3 and assessed by NMR (Burdick *et al*. 2005). MeHA solutions were prepared at 1%, 2%, and 5% (mass/volume) in PBS with 0.05% w/v of the photoinitiator I2959 (2-methyl-1-[4-(hydroxyethoxy)phenyl]-2-methyl-1-propanone, Ciba-Geigy, Tarrytown, NY). For cell-laden gels, MSCs were suspended in MeHA solutions at 20 million cells/mL. Acellular and MSC-laden MeHA macromer suspensions were then cast between glass plates separated by a 2.25 mm spacer and photopolymerized with UV exposure as described in Chapter 3. As controls, agarose hydrogels (Ag; 2.25 mm thick) were formed at 20 million cells/mL (Huang *et al*. 2008). Cylindrical constructs were cored from hydrogel slabs at 4 mm (for MSC-laden gels) or 8 mm (for acellular gels).

4.2.2. Mechanical Characterization of Acellular Constructs

Acellular MeHA disks (Ø5 mm by 2.25 mm) were formed as above and tested in confined compression in a PBS bath (Mauck *et al*. 2000). Three sequential ramps of 10% strain (0.05%/second) were applied, and samples were allowed to reach equilibrium between ramps (~1200 seconds). Data from the second ramp (10-20% deformation) were extracted and fit to the Biphasic Theory of Mow and co-workers (Mow *et al*. 1980) to determine construct permeability (k) and aggregate modulus ($H_A$).

4.2.3. Macromolecular Diffusion in Acellular Constructs

Fluorescein-conjugated dextran (70 kDa and 2,000 kDa; Molecular Probes, Invitrogen) was suspended within MeHA (1%, 2%, and 5%) hydrogels at 175 µg/mL or 85 µg/mL, respectively. Gels were maintained in 2 mL of PBS at 37$^{o}$C on a rocker plate, and supernatant sampled over 72 hours. Released dextran was measured via fluorescence (485 nm/518 nm), with concentration determined from standard curves. The effective 'diffusivity' was determined by plotting concentration (normalized to final) versus the square root of time (Quinn *et al*. 2000).

4.2.4. Long-term Culture Conditions

Constructs were cultured for up to six weeks (1 mL/construct) in TGF-β3 (10 ng/mL; R&D Systems, Minneapolis, MN) supplemented, chemically defined medium. This medium consisted of high-glucose DMEM with 1× PSF, 0.1 µM dexamethasone, 50 µg/mL ascorbate 2-phosphate, 40 µg/mL L-proline, 100 µg/mL sodium pyruvate, and

ITS+ (6.25 mg/mL insulin, 6.25 mg/mL transferrin, 6.25 ng/mL selenous acid, 1.25 mg/mL bovine serum albumin, and 5.35 mg/mL linoleic acid). Media were changed twice weekly.

4.2.5. Viability and Short-term Expression Analysis

For viability assays, samples were tested at 3 and 6 weeks using the Live/Dead staining kit described in Chapter 3 (Molecular Probes, Invitrogen). Additionally, on days 0, 3, and 21, metabolic activity was quantified with the MTT assay. Briefly, samples were incubated in MTT reagent for 1 hour at 37$^{o}$C, washed in PBS, and developed color eluted with dimethyl sulfoxide (DMSO), and absorbance read at 540 nm. For gene expression, RNA was extracted from day 0, 1, 7 and 21 samples with two sequential extractions in TRIZOL-chloroform. After quantification of RNA yield and purity (Nanodrop, Thermo Scientific, Waltham, MA), reverse transcription was carried out with the Superscript First Strand Synthesis System kit (Invitrogen). cDNA amplification was carried out using SYBR Green Master Mix on a 7300 Applied Biosystems real time PCR machine with intron spanning primers. Expression of type I collagen (Col I), type II collagen (Col II) and aggrecan (AGG) were determined and normalized to GAPDH.

4.2.6. Biomechanical Analysis

Compressive equilibrium ($E_Y$) and dynamic ($|G^*|$) moduli of constructs were determined by unconfined compression between impermeable platens in a PBS bath as described in Chapter 3 (Mauck *et al*. 2000; Park *et al*. 2004). In a separate study, tensile properties were measured. MSC-seeded samples were fabricated as above, but cut from slabs into

strips (4 mm x 20 mm x 1.5 mm), and cultured in chondrogenic medium with TGF-β3 (6 mL per strip). Given the larger size of these samples and the poor findings with 5% HA in compression studies, only 1% and 2% MeHA concentrations were investigated. Samples were tested via a quasi-static extension to failure (Huang *et al*. 2008), with the ramp tensile modulus computed from the linear region of the stress-strain curve.

4.2.7. Biochemical Analysis

After testing, construct wet weights were recorded and the content of DNA, sulfated glycosaminoglycan (sGAG,) and collagen was determined as in Chapter 3. Collagen was extrapolated from orthohydroxyproline (OHP) using a 1:7.14 ratio of OHP:collagen (Neuman and Logan 1950). In one replicate, sGAG content within the culture medium was measured at each feeding.

4.2.8. Histological Analysis of MSC-seeded Constructs

Constructs were fixed in 4% paraformaldehyde, embedded in paraffin and sectioned (8 μm). Analysis was carried out on days 3, 5, 7, 10, and 14 and bi-weekly through week 6. Samples were stained for proteoglycans with alcian blue (pH 1.0) and for collagen via picrosirius red (Huang *et al*. 2008). Immunohistochemistry was used to visualize localization of collagen types I and II (Huang *et al*. 2008). Samples underwent antigen retrieval and were sequentially treated at room temperature with 300 mg/mL hyaluronidase (Type IV, Sigma, St. Louis, MO), 3% $H_2O_2$, and blocking reagent (DAB150 IHC Select, Millipore, Billerica, MA). Sections were then treated with antibodies (5 mg/mL) to type I collagen (MAB3391, Millipore) or type II collagen (11e-

116B3, Developmental Studies Hybridoma Bank, Iowa City, IA) in 3% BSA (control sections treated with 3% BSA only). Finally, biotinylated goat anti-rabbit IgG secondary antibody conjugated with streptavidin horseradish peroxidase was localized to primary antibodies, and color developed with DAB chromagen reagent (DAB150 IHC Select, Millipore). Images were acquired at magnifications of 5X or 10X.

#### 4.2.9. Statistical Analysis

Data are reported as the mean and standard deviation; sample numbers are indicated in the associated figure legends. Statistical analysis (SYSTAT 12, Systat Software, Chicago, IL) included both one-way and two-way ANOVA, with gel group (1%, 2%, 5% MeHA, and Ag) and time in culture as independent variables. When significance ($p<0.05$) was indicated by ANOVA, Tukey's *post hoc* tests were applied to enable comparisons between groups.

## 4.3. Results

#### 4.3.1. Macromer Density Influences Acellular Hydrogel Mechanics

Prior to cell-seeding studies, crosslinked MeHA hydrogels were formed at varying concentrations (1%, 2%, and 5%) and tested in confined compression. Increasing macromer concentration led to decreases in construct permeability (k), with both 2% and 5% MeHA hydrogels significantly less permeable than 1% MeHA hydrogels ($p<0.05$, **Figure 4-1**). $H_A$ showed the reverse trend, with 5% MeHA gels significantly stiffer than both 1% and 2% gels ($p<0.05$).

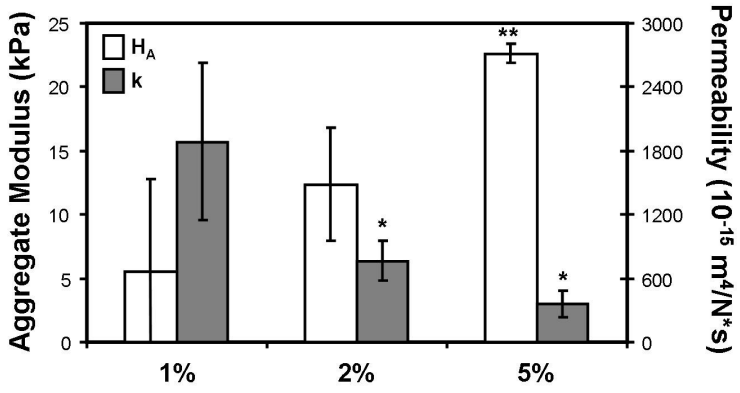


**Figure 4-1: Biphasic parameters of permeability (k) and aggregate modulus ($H_A$) for MeHA gels with increasing macromer density. ($R^2$>0.89; n=3-4/group; * indicates p<0.05 vs. 1%; ** indicates p<0.05 vs. 1% and 2%)**

4.3.2. MSC Viability and Differentiation in HA Gels with Increasing Macromer Density

After ascertaining concentration-dependent differences in hydrogel properties, MSC viability and differentiation was assessed in MeHA gels of increasing macromer concentration (1%, 2%, and 5%). Viable cells were observed uniformly in all MeHA and Ag constructs on both day 21 and day 42 (**Figure 4-2**). There appeared to be more cell clustering with higher MeHA concentrations at both time points. Little evidence of cell death was observed under any condition (data not shown). Metabolic activity showed that, relative to day 1, 1% MeHA and Ag gels increased with time ($p<0.05$), but after 21 days no significant differences were observed between groups ($p>0.05$). DNA content per construct was ~20% and ~40% higher after 42 days in 2 and 5% MeHA hydrogels compared to 1% MeHA and Ag hydrogels, respectively ($p<0.05$).

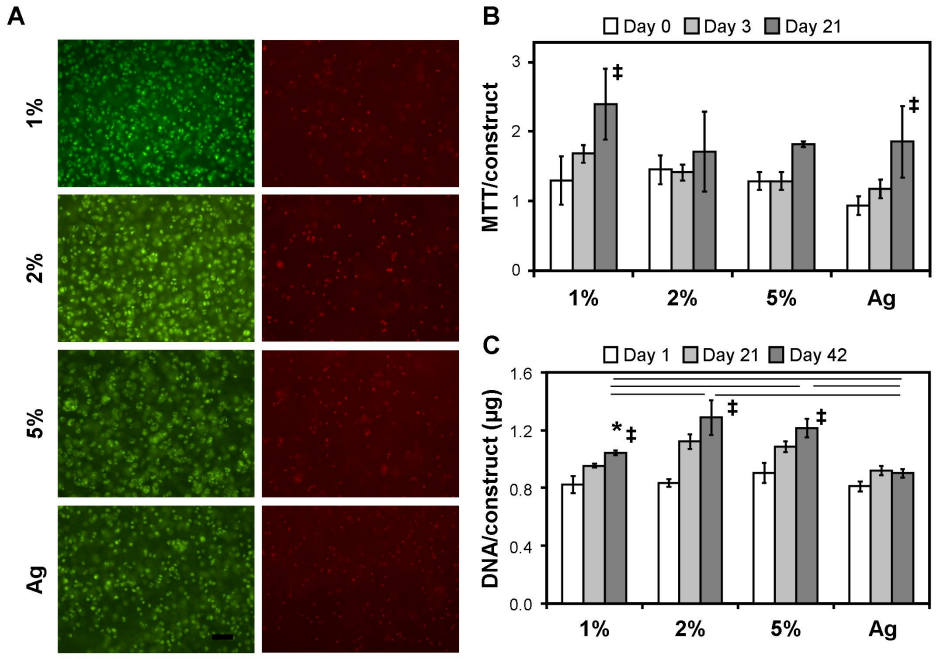


**Figure 4-2: (A) Live (green, left) and dead (red, right) MSCs in 1%, 2%, and 5% MeHA, and Ag hydrogels 21 and 42 days after encapsulation (10X magnification; 200 µm scale bar). (B) Mitochondrial activity of constructs through day 21. (C) DNA content of MSC-seeded constructs through day 42. (n=4/group/time point, ** indicates p<0.05 vs. 1% and Ag on day 42, * indicates p<0.05 vs. Ag on day 42; ‡ indicates p<0.05 vs. day 0)**

Expression analysis was performed on MSC-seeded constructs maintained in a chemically defined media supplemented with TGF-β3. Results indicated that collagen type I expression remained low throughout the 21 day period, at most increasing by a factor of two over this time course. Conversely, collagen type II expression increased dramatically in each condition, and appeared to be a function of macromer density (with levels in 5% MeHA nearly 4-fold greater than in 1% MeHA or Ag) (**Figure 4-3**). Aggrecan increased relative to starting levels in each construct by day 7, with generally higher levels of expression observed in the MeHA constructs compared to Ag constructs. For aggrecan, no clear differences were observed between MeHA gels of different concentrations. These data indicate that MSCs are viable in MeHA hydrogels over long

periods, that constructs have stable or slightly increased cell content, and that MSCs undergo chondrogenesis in each of these 3D environments.

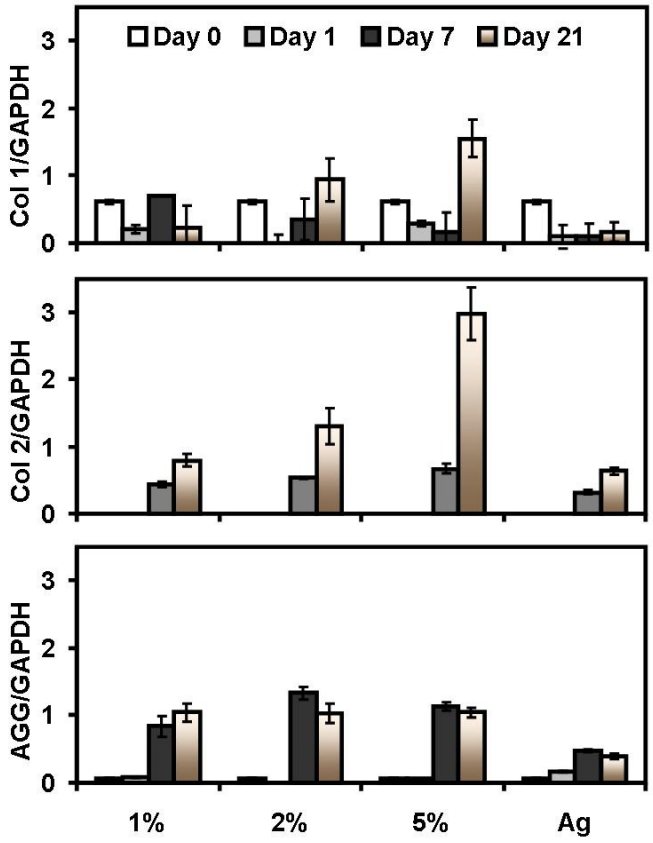


**Figure 4-3: Collagen type I (top), collagen type II (middle), and aggrecan (bottom) mRNA levels MSC-seeded MeHA (1%, 2%, and 5%) and Ag constructs through 21 days of chondrogenic culture. Note robust increases in collagen II and aggrecan, indicative of chondrogenic differentiation.**

4.3.3. Construct Dimensional Stability and Biochemical Content

Biochemical content in engineered cartilage is a function of matrix deposition and retention, as well as volumetric space. In low concentration MeHA gels, initial dimensions (diameter and thickness) decreased markedly (**Figure 4-4**). This contraction occurred in both acellular and MSC-seeded gels, suggesting that the initial contraction is a function of the gel itself, rather than cell-mediated mechanisms. Acellular and MSC-seeded 1% MeHA constructs contracted by ~10% in thickness and ~20% in diameter

over the first day. Conversely, 5% gels increased in thickness by ~5%, with no change in diameter. 2% MeHA constructs were intermediate to these extremes, while Ag constructs did not change, consistent with previous findings. With culture, construct dimensions changed as well; 1% MeHA constructs recovered towards their original geometry, while 2% and 5% MeHA constructs increased in thickness by ~30%, and in diameter by 10-20%, by day 42. Over this same time course, Ag constructs showed small increases in diameter and thickness.

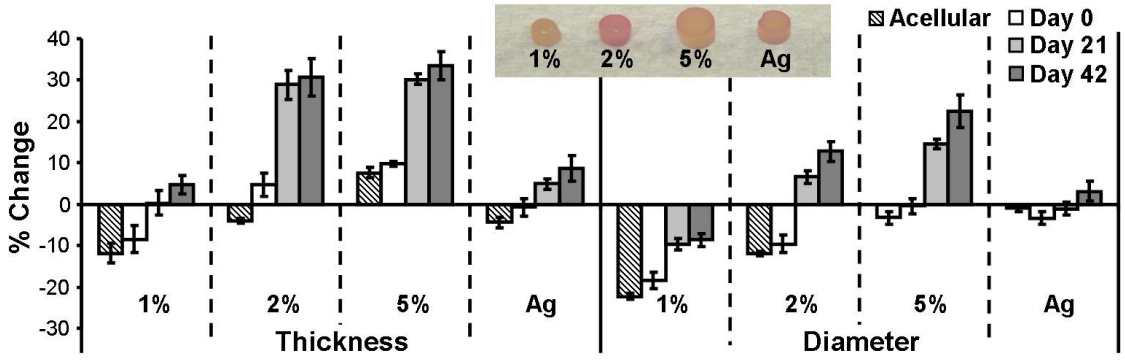


**Figure 4-4: Dimensional variation in acellular and MSC-seeded constructs with time in culture. Differences shown as the percentage of initial size (4 mm diameter and 2.25 mm thickness, n=4/group/time point). Inset image of MSC-seeded constructs after 6 weeks of in vitro culture in chondrogenic medium.**

Biochemical content of constructs was assessed through six weeks of culture. On a per wet weight (ww) basis, 1% MeHA constructs accumulated the highest s-GAG content in MeHA, reaching levels comparable to Ag constructs ($p>0.05$), while 2 and 5% MeHA constructs contained less s-GAG ($p<0.05$, **Figure 4-5A**). On Day 42, 1% MeHA and Ag constructs contained ~3% s-GAG per wet weight, while 2% and 5% MeHA constructs contained ~2% s-GAG. Conversely, in terms of total s-GAG per construct, values in 1% MeHA constructs were less than both 2% and 5% MeHA constructs ($p<0.05$; **Table 4-1**). s-GAG lost to the culture media was highest for Ag, reaching peak release rates by day 11. 5% MeHA constructs released the least amount s-GAG per day over the first 21 days,

with similar release rates from each MeHA construct observed thereafter (**Figure 4-5C**). Collagen content showed a similar trend as s-GAG, with the exception of Ag constructs, which contained higher collagen levels (1.4% ww, $p<0.05$) than each of the MeHA constructs by day 42 (1%: 0.7%ww, 2%: 0.3%ww, 5%: 0.4%ww, **Figure 4-5B**). In terms of total collagen per construct, Ag constructs contained the highest levels, while the MeHA formulations were not different from one another (**Table 4-1**).

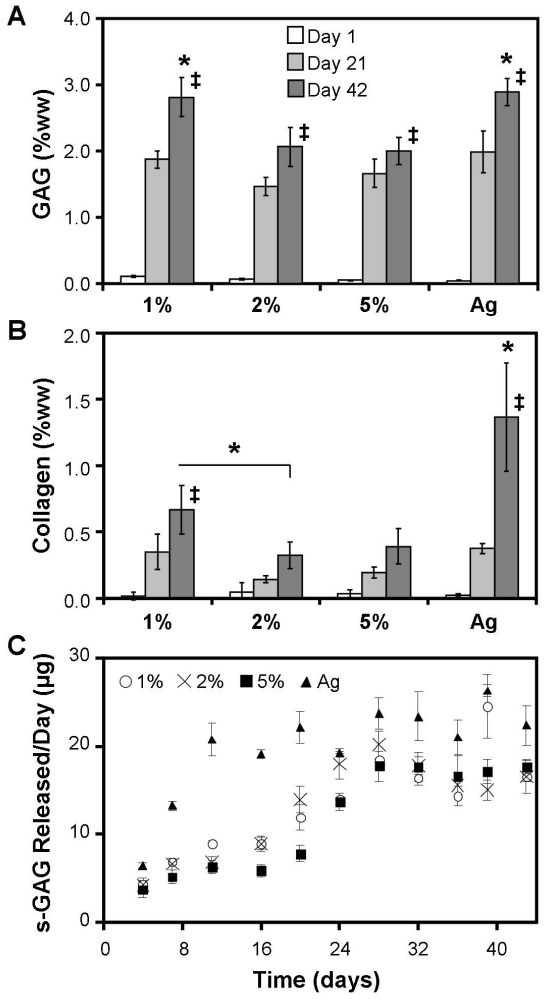


**Figure 4-5: A) s-GAG percent wet weight (% ww) in 1, 2, and 5% MeHA, and Ag constructs through 42 days of *in vitro* chondrogenic culture. (** indicates $p<0.05$ vs 2 and 5% at day 42) B) collagen content (% ww) in MeHA and Ag constructs through 42 days of culture. Increased concentration of ECM was observed in Ag and 1% MeHA hydrogels by day 42. (** indicates $p<0.05$ vs all other groups at day 42) C) s-GAG release per day per construct for MSC-seeded MeHA and Ag constructs through 42 days of culture. (n=4/group/time point, ‡ $p<0.05$ vs. day 0)**

| | | 1% MeHA | | 2% MeHA | | 5% MeHA | | 2% Agarose | |
|---|---|---|---|---|---|---|---|---|---|
| | | mean | ± SD | mean | ± SD | mean | ± SD | mean | ± SD |
| Dimensions | Thickness (mm) | 2.36 | 0.05 | 2.94 | 0.10 | 3.01 | 0.08 | 2.45 | 0.07 |
| | Diameter (mm) | 3.66 | 0.06 | 4.52 | 0.10 | 4.90 | 0.16 | 4.12 | 0.10 |
| | Wet Weight (mg) | 26.35 | 0.72 | 49.92 | 1.83 | 62.04 | 0.75 | 33.07 | 1.05 |
| Biochemistry | DNA per gel (µg) | 1.04 | 0.02 | 1.29 | 0.12 | 1.22 | 0.06 | 0.90 | 0.03 |
| | Collagen per DNA | 167.40 | 45.50 | 124.78 | 40.56 | 203.46 | 75.80 | 499.68 | 142.89 |
| | Collagen per gel (µg) | 175.17 | 49.49 | 160.66 | 52.55 | 240.18 | 80.85 | 444.79 | 132.61 |
| | Collagen %ww | 0.66 | 0.18 | 0.32 | 0.10 | 0.39 | 0.13 | 1.37 | 0.41 |
| | GAG per DNA | 707.73 | 54.25 | 800.47 | 99.27 | 1019.45 | 70.36 | 1058.92 | 73.77 |
| | GAG per gel (µg) | 739.14 | 62.73 | 1024.67 | 107.62 | 1241.54 | 132.43 | 956.25 | 88.50 |
| | GAG %ww | 2.81 | 0.30 | 2.06 | 0.30 | 2.00 | 0.20 | 2.89 | 0.21 |
| Mechanics | $E_Y$ (kPa) | 136.66 | 17.07 | 53.57 | 9.78 | 60.80 | 8.25 | 111.96 | 23.96 |
| | IG*I (MPa) | 1.05 | 0.12 | 0.21 | 0.05 | 0.16 | 0.03 | 0.83 | 0.13 |
| | Tensile Modulus (kPa) | 473.60 | 187.52 | 63.50 | 36.78 | -- | -- | 991.48 | 162.25 |

**Table 4-1: Construct dimensions, biochemical content, and mechanical properties of MSC-seeded MeHA and Ag constructs after 6 weeks of culture (mean ± standard deviation (SD); n=3-4/group).**

4.3.4. Mechanical Properties of MSC-laden Constructs

Differences in biochemical content (and concentration) of ECM resulted in widely different compressive and tensile properties. While all constructs increased in equilibrium and dynamic modulus with time ($p<0.05$), by day 42 the equilibrium modulus of 1% MeHA constructs was ~20% greater than Ag constructs ($p<0.05$, **Figure 4-6A**) and more than 100% greater than both 2% and 5% MeHA constructs ($p<0.05$). The dynamic compressive modulus data followed a similar trend, where 1% MeHA constructs were ~20% greater than Ag, and ~5-fold greater than 2% and 5% MeHA constructs ($p<0.05$, **Figure 4-6B**). On day 42, the tensile modulus of Ag constructs was ~2-fold higher than that of 1% MeHA ($p<0.05$, **Figure 4-6D**), while 1% MeHA constructs were more than 7-fold greater than 2% MeHA constructs ($p<0.05$). Failure strain did not change markedly with culture (**Figure 4-6C**).

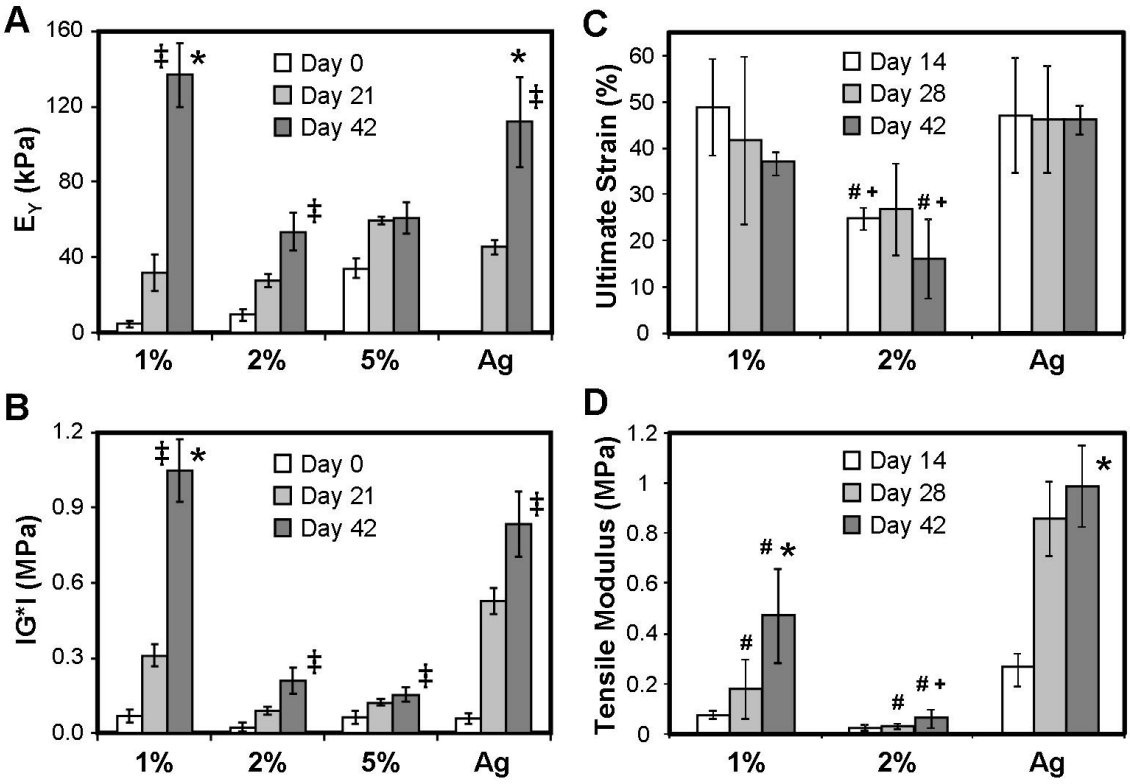


**Figure 4-6: Equilibrium compressive modulus (A) and dynamic modulus (B) of MeHA and Ag hydrogels through 6 weeks of culture (** indicates p<0.05 vs. all other groups at day 42; * indicates p<0.05 vs. 2% and 5%). Failure strain (C) and tensile modulus (D) of MSC-seeded 1 and 2% MeHA and Ag constructs at 2, 4, and 6 weeks. Biomechanical properties increase more rapidly and to a higher level in lower concentration MeHA constructs. (n=4/group/time point, ‡p<0.05 vs. day 0; * indicates p<0.05 vs. all lower groups on the terminal time point (day 42); # indicates p<0.05 vs. Ag group at same time point; + indicates p<0.05 vs. 1% MeHA group at same time point)**

4.3.5. ECM Deposition and Distribution

Histological analysis at early time points showed marked differences in matrix distribution as a function of macromer density (**Figure 4-7**). In 5% MeHA constructs, proteoglycans were sequestered into dense rings around cells by day 7. In contrast, 1% MeHA and Ag gels showed a more homogenous distribution of proteoglycans. Similarly, by day 42, proteoglycan and collagen was evenly distributed in 1% MeHA and Ag, while intense pericellular localization was evident in 5% MeHA constructs (**Figure 4-8**).

Collagen type II (**Figure 4-8**) showed increased sequestration of this ECM component in the pericellular space in higher macromer concentration MeHA constructs. Consistent with biochemical findings, histological results also show more intense collagen (bulk and type II) staining in Ag constructs compared to all MeHA constructs.

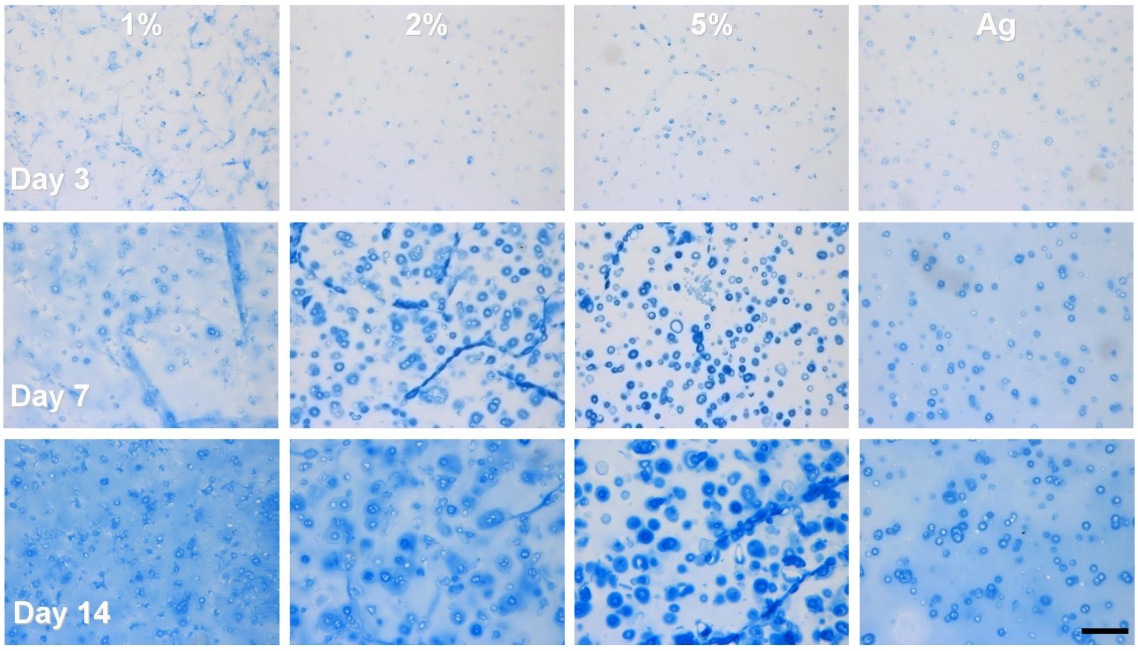


**Figure 4-7: Alcian blue stained sections of MSC-seeded 1, 2, and 5% MeHA and agarose (Ag) constructs after 3 (top), 7 (middle), and 14 days (bottom) of chondrogenic culture (10X magnification). Pericellular aggregation of proteoglycans is evident in higher % MeHA constructs in contrast to a more even distribution in 1% MeHA constructs and Ag controls. (Scale bar = 250 µm)**

4.3.6. Macromolecular Diffusion in Acellular MeHA Hydrogels

To better understand the mechanism of matrix distribution, we evaluated macromolecular diffusivity of small (70 kDa, on the order of growth factors) and large (2000 kDa, on the order of ECM aggregates) molecules in MeHA gels of varying macromer density. Release rates of 70 kDa dextran from MeHA hydrogels decreased as macromer density increased (**Figure 4-9A**). A similar finding was observed with 2000 kDa dextran (**Figure 4-9B**). Linear regression to the relative concentration plotted against the square root of

time provides a quantitative 'effective diffusivity' for comparing these responses. Linear fits captured the data well ($R^2$>0.75) for each macromer density and both dextran sizes. Macromer concentration had a significant effect on 'effective diffusivity' for both 70 and 2000 kDa dextran. For each increase in macromer concentration, a significant decrease in diffusivity was observed ($p<0.05$; **Figure 4-9C**).

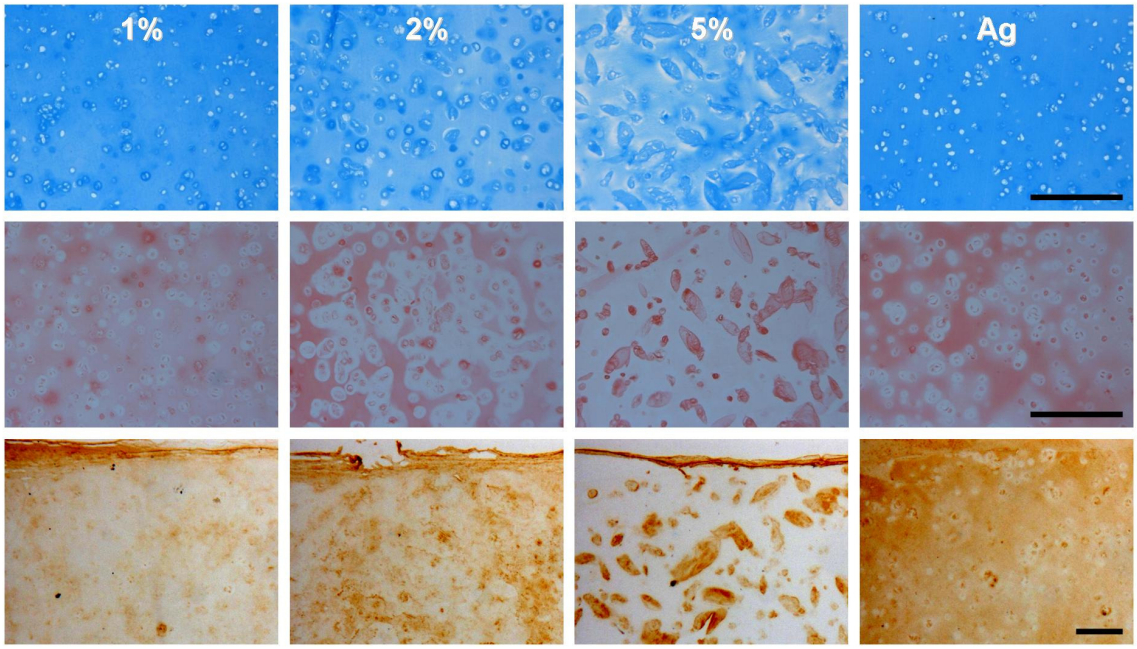


**Figure 4-8: Alcian blue (top) and picrosirius red (middle) stained sections from 1%, 2%, and 5% MeHA and agarose (Ag) constructs (10X magnification) on day 42. Collagen type II immunostaining (bottom) on day 42 (5X). Note the dependence of proteoglycan and collagen distribution on MeHA macromer concentration. (Scale bar = 250 µm)**

## 4.4. Discussion

Realization of a functional engineered cartilage construct requires that a clinically relevant cell type be situated within a 3D environment that supports cell viability as well as the production and retention of cartilage specific ECM molecules. Further, the encapsulating material must allow assembly of these molecules into a dense network with physiologic mechanical properties. In this work, we investigated the ability of MSCs to

undergo chondrogenesis in crosslinked methacrylated HA hydrogels. This hydrogel formulation has several promising attributes; it is a well defined biologic that can be photo-polymerized *in situ* to fill any sized defect (Nettles *et al*. 2004). Previous work in Chapter 3 with this gel at a 2% macromer concentration established that MSCs undergo chondrogenesis in MeHA, but also indicated that the rate and extent of functional maturation was reduced when compared to agarose. As MeHA macromer density influences ECM deposition by auricular chondrocyte seeded HA gels (Chung *et al*. 2006), this study specifically investigated how variations in this parameter influence the maturation of MSC-based constructs. Results from this study demonstrate that two competing effects occur as macromer density increases: enhanced chondrogenesis that is countermanded by biophysical impediments to distributed matrix assembly.

As previously noted for MeHA , and consistent with other hydrogels (Ng *et al*. 2005), changes in macromer density had marked effects on the mechanical properties; constructs with higher macromer densities were stiffer. Despite the increasing gel density, viability and DNA assays indicated that cells survive and divide throughout the material. Encapsulated MSCs increased expression of cartilage-specific matrix and accumulated increasing amounts of proteoglycan through 42 days. Despite the hindered diffusion observed for 70 kDa molecules, histological analysis (staining for proteoglycan deposition) showed that chondrogenesis occurred throughout the gel, and was not restricted to the periphery in higher macromer concentrations. These findings suggest that the HA gels support viability and MSC chondrogenesis at all macromer concentrations.

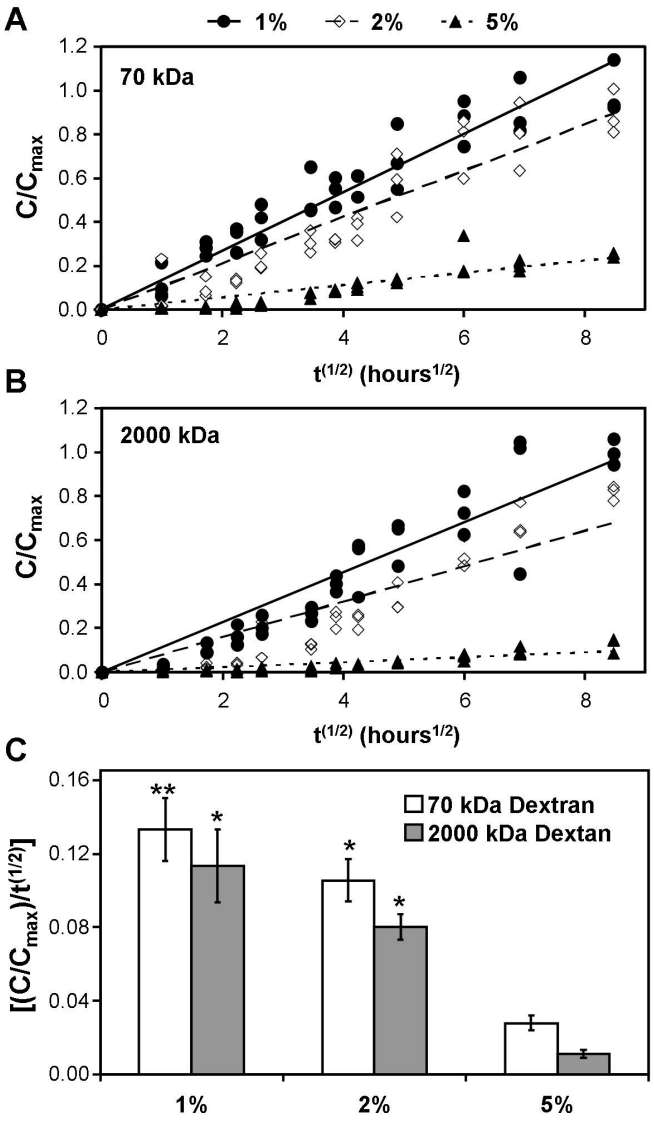


**Figure 4-9: Time course of release of 70 kDa (A) and 2000 kDa (B) fluorescein-conjugated dextran from 1%, 2%, and 5% MeHA hydrogels. Data were normalized to the maximum observed release from 1% MeHA for both dextran sizes. Effective diffusivity (C) of dextran of both sizes decreased with increasing MeHA macromer concentration. (n=3/group; ** indicates p<0.05 vs. both 2% and 5% MeHA groups; * indicates p<0.05 vs. the 5% MeHA group only)**

The enhanced chondrogenic differentiation and proteoglycan observed in higher macromer concentration MeHA constructs could arise from a number of different factors. First, we have previously shown that MeHA hydrogels enhance molecular level chondrogenesis compared to inert crosslinked networks such as PEG (Chung and Burdick

2009). HA is a component of the native cartilage ECM and so the gel presents a biologic interface with which both chondrocytes and MSCs can interact (through CD44 receptors) (Knudson and Knudson 2004). In high macromer constructs, a greater probability of receptor mediated interaction with the material exists, just as concentration dependent effects are observed when RGD is coupled to otherwise biologically inert hydrogels (Connelly *et al*. 2007). Alternatively, the higher stiffness of the material may influence differentiation. Findings in monolayer studies suggest that MSCs can interpret the microenvironmental stiffness to modulate differentiation (Engler *et al*. 2007). Here, increasing macromer density increases gel stiffness; MSCs may respond to this by increasing the degree to which they undergo chondrogenesis. Still another possibility relates to the rapid and intense accumulation of newly formed matrix in the pericellular space in higher density MeHA. While a high local proteoglycan concentration exerts negative feedback on further proteoglycan production by chondrocytes (Buschmann *et al*. 1992), this does not seem to be the case with MSCs in this system. Rather, the ECM in the pericellular space may act to concentrate locally produced factors (ECM to which the cells bind, or growth factors that themselves bind to ECM), creating a microenvironment that better supports and/or maintains chondrogenesis. Future studies will be required to elucidate the precise mechanism by which this enhanced differentiation occurs in higher density MeHA gels.

Despite the anabolic and/or pro-chondrogenic effects of increasing MeHA macromer density, these positive findings were counterbalanced by the limited diffusion of large ECM molecules away from their origin. This limitation impeded the homogenous

distribution of formed ECM, and so hampered the functional maturation. This is consistent with the findings of Buxton and colleagues, who showed that inclusion of spacers within PEG gels allowed for greater matrix distribution by human MSCs (Buxton *et al*. 2007) and by Ng and colleagues using bovine chondrocytes in an agarose system (Ng *et al*. 2005). While 5% MeHA constructs produced and retained the highest absolute amount of proteoglycan, they failed to develop increasing mechanical properties compared to lower macromer concentration constructs that produced lesser amounts of proteoglycan. This is partially due to volumetric changes observed; 1% MeHA constructs made less proteoglycan, but contracted slightly and so concentrated the formed ECM, while 5% MeHA constructs made and retained more proteoglycan, but swelled significantly. These findings suggest that new methods must be developed to take advantage of the positive features of a higher MeHA concentration, while increasing the mobility of newly formed matrix. For example, Bryant and colleagues have shown greater ECM distribution in chondrocyte-seeded PEG gels that contain degradable linkages (Bryant and Anseth 2003), and Park and co-workers have shown similar findings in MMP-cleavable hydrogels (Park *et al*. 2004). Working with a new hydrolytically degradable version of these crosslinked HA hydrogels, we have recently shown that crosslink degradation leads to more rapid dispersion of ECM in short term MSC studies (Sahoo *et al*. 2008). It is not yet clear how long the pro-chondrogenic signal provided by the HA microenvironment (be it stiffness or biologic moieties) must be present to result in long term increases in matrix production. In future studies, it will be critical to carefully tune early matrix assembly, and the positive benefits thereof, with long term requirements for matrix elaboration.

The results of this study are promising, in that they show a clear macromer density dependent development of construct mechanical properties. The equilibrium and dynamic compressive properties of MSC-seeded 1% MeHA constructs match or exceed properties achieved with Ag hydrogels seeded with the same MSC population and maintained identically. Indeed, equilibrium compressive properties and s-GAG content reach 25% and 50% of native tissue levels, respectively. However, collagen content in MeHA gels remains low, and is lower than that produced in Ag constructs. This is a significant finding, as collagen content correlates well with tensile properties in native tissue and engineered constructs. In this study, the tensile properties of 1% MeHA constructs remained significantly lower than Ag constructs. Further, it should be noted that the compressive mechanical properties (even in Ag hydrogels) remain lower than that produced by native chondrocytes in Ag hydrogels (Mauck *et al*. 2006). This is consistent with the idea that MSCs remain incompletely (or inefficiently) committed to the chondrocyte phenotype, even in MeHA.

Despite these limitations, these data provide new insight into how early matrix deposition regulates long term construct development, and define new parameters for optimizing the formation of functional MSC-based engineered cartilage using HA hydrogels. For example, in the case of higher density MeHA constructs, dynamic loading might be used to further matrix distribution. Theoretical and experimental results suggest that dynamic loading can expedite the movement of large molecules in dense hydrogels (Mauck *et al*. 2003; Albro *et al*. 2008). Such an approach may be useful in coupling the pro-

chondrogenic/matrix formation events in MeHA hydrogels, while still providing a mechanism for distribution of newly formed constituents throughout the construct, potentially improving bulk mechanical properties.

### 4.5. Conclusions

Taken together, these results provide new evidence that HA hydrogels support the functional chondrogenesis of MSCs, with mechanical properties matching or exceeding our best results to date in other hydrogel systems. With further optimization, this material holds tremendous promise in the fabrication of functional cartilage replacements to restore function to damaged or diseased native tissue.

**This previously published Chapter was included with kind permission from Elsevier: Osteoarthritis and Cartilage, "Macromer Density Influences Mesenchymal Stem Cell Chondrogenesis and Maturation in Photo-crosslinked Hyaluronic Acid Hydrogels", volume 17, 2009, pgs 1639-1648, Isaac E. Erickson, Alice H. Huang, Swarnali Sengupta, Sydney R. Kestle, Jason A. Burdick, Robert L. Mauck.**

# CHAPTER 5: High Density MSC Seeded Hyaluronic Acid Constructs Produce Engineered Cartilage with Native Properties

## 5.1. Introduction

Articular cartilage injuries and disease result in focal defects with limited intrinsic capacity for regeneration. The presence of a defect requires adjacent cartilage to bear an increased proportion of joint load (Guettler *et al*. 2004; Albro *et al*. 2008) which increases local stresses and the likelihood of continued degeneration and development of osteoarthritis (Ding *et al*. 2005; Magnussen *et al*. 2009). An ideal repair material would completely integrate to fill the defect with a cartilage-like material possessing functional load-bearing characteristics (Ateshian *et al*. 2003). However, meeting of this high benchmark for functional repair remains an elusive goal. Current regenerative strategies that deliver ex-vivo expanded autologous chondrocytes (ACI/ACT) (Brittberg *et al*. 1994) or promote endogenous healing via bone marrow stimulation (microfracture) (Steadman *et al*. 2001) may improve patient outcomes, but functional restoration of the tissue has yet to be demonstrated (Jones *et al*. 2008). Instead, a transient fibrous repair material forms lacking in native tissue properties.

An alternative approach is to engineer *de novo* cartilage *in vitro* for implantation within a cartilage defect. Indeed, recent work utilizing chondrocytes in specialized media conditions and 3D hydrogels has produced constructs that match or exceed native tissue values for equilibrium modulus and proteoglycan content (Lima *et al*. 2007; Byers *et al*. 2008; Bian *et al*. 2010; Ng *et al*. 2010). However, the clinical shortage of healthy

chondrocytes and the co-morbidity associated with their harvest (Lee *et al*. 2000) are considerable limitations. Mesenchymal stem cells (MSCs) can be obtained from patient bone marrow and expanded *in vitro* to clinically relevant numbers without losing their ability to undergo chondrogenic differentiation (Pittenger *et al*. 1999). MSCs have been combined with countless biomaterials for cartilage tissue engineering (Huang *et al*. 2010), but no such combination has yet achieved mechanical properties that approach native tissue or engineered chondrocyte-based cartilage (Mauck *et al*. 2006; Huang *et al*. 2010).

One approach for improving the functional maturation of MSC-based engineered cartilage may be to increase the starting cell density within a construct. Here, the rationale is that with more point sources for matrix production, the functional contiguity of matrix should occur at an earlier time in culture, and formed matrix should be concentrated to a greater extent. Indeed, early work using chondrocytes embedded in alginate and agarose showed that, provided a sufficient supply of nutrients, increasing seeding densities led to increasing mechanical and biochemical outcomes (Chang *et al*. 2001; Mauck *et al*. 2003). MSCs likewise depend on seeding density, where densities up to ~10 million MSCs/mL led to increased expression of cartilage matrix associated genes compared to lower cell densities (Huang *et al*. 2004). However, in work from our group and others, using both agarose and alginate hydrogels, no improvement in mechanics was observed at higher MSC densities with continual exposure to pro-chondrogenic media (Ponticiello *et al*. 2000; Kavalkovich *et al*. 2002; Huang *et al*. 2009). Indeed, in alginate gels, there appeared to be a maximum in matrix production per cell occurring in the range

of 25 million cells/mL, with both higher and lower densities leading to inferior outcomes on a per cell basis (Kavalkovich *et al*. 2002).

That same work and related studies, however, suggest that additional cues from the microenvironment can influence functional matrix elaboration, namely, the biomolecular identity of the supporting 3D network (Kavalkovich *et al*. 2002) as well as its biophysical properties (Huebsch *et al*. 2010). Our recent work (see Chapter 4) with a photo-polymerizing hyaluronic acid (HA) hydrogel (Burdick *et al*. 2005; Chung and Burdick 2009) showed that when MSCs were encapsulated (20 million/ml) in hydrogels of 1%, 2%, and 5% (w/v) macromer concentrations, the most robust constructs developed in the 1% formulation. This improved matrix functionality occurred despite the fact that MSCs had higher levels of cartilage matrix-related gene expression and matrix synthesis (per construct) in the higher macromer density constructs (Chung *et al*. 2009; Erickson *et al*. 2009). Histological analysis showed that in high density gels, discrete lacunae of poorly distributed matrix formed, while in 1% gels a well distributed and contiguous proteoglycan and collagen network was established. Overcoming these limitations in the distribution of cartilage matrix may increase the potential of higher HA macromer density hydrogels for functional development while also taking advantage of their greater initial strength and dimensional stability.

To test this hypothesis directly, the objective of this Chapter was to determine whether an increase in MSC seeding density would enhance tissue engineered cartilage properties in high macromer concentration HA hydrogels, and specifically whether this increase would

be mediated by improved matrix connectivity (**Figure 5-1**). Towards this end, HA hydrogels of 1, 3, and 5% macromer density were seeded at either 20 or 60 million MSCs/mL and cultured for 4 and 8 weeks in a chemically defined pro-chondrogenic media formulation. At each time point, construct maturation was evaluated via assessment of biomechanical, biochemical, and histological properties, along with measures of the expression of cartilage matrix associated genes. Further, under the best conditions derived above, we evaluated growth of high seeding density constructs under dynamic culture (orbital shaking) conditions to further improve functional maturation.

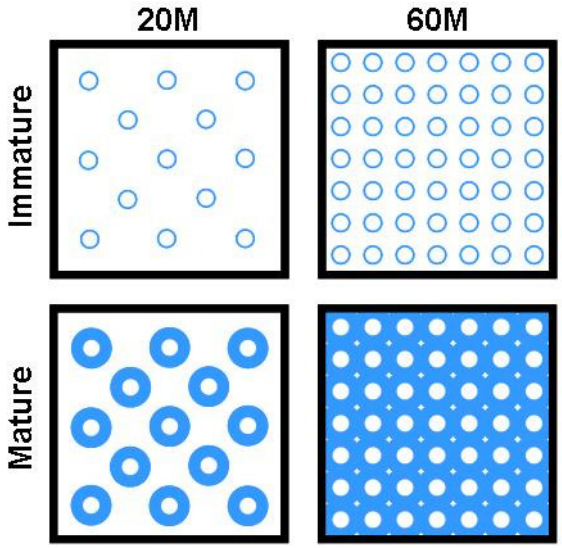


**Figure 5-1: Cartilage matrix diffusion is limited within HA hydrogels of higher macromer density (left), but increasing MSC seeding density may improve matrix connectivity (right) to enhance the functional development of tissue engineered cartilage.**

## 5.2. Methods

### 5.2.1. Hyaluronic Acid Hydrogel Synthesis

Methacrylated HA (MeHA) macromer was synthesized by reacting methacrylic anhydride (Sigma, St. Louis, MO) and 74 kDa HA (Lifecore, Chaska, MN) followed by $^{1}$H NMR characterization (25% methacrylated) as previously described (Burdick *et al.*

2005). Lyophilized MeHA was stored at -20° C before being sterilized by exposure to a biocidal UV lamp for 15 minutes. Macromer was dissolved to 1, 3, and 5% (mass/volume) in sterile PBS with 0.05% photoinitiator Irgacure-2959 (2-methyl-1-[4-(hydroxyethoxy)phenyl]-2-methyl-1-propanone; Ciba-Geigy, Tarrytown, NY).

5.2.2. MSC Isolation, Expansion, and 3D Culture

Bone marrow derived MSCs were isolated from juvenile bovine femurs as in (Mauck *et al*. 2006) and expanded through passage 3 in basal medium consisting of DMEM with 10% fetal bovine serum and 1% penicillin-streptomycin-fungizone (PSF) (Invitrogen, Carlsbad, CA). After culture expansion, MSCs were trypsinized and encapsulated at either 20 or 60 million cells/mL in 1%, 3%, and 5% (w/v) MeHA via UV polymerization (10 min) between glass plates separated by 2.25 mm as in (Erickson *et al*. 2009). Sterile 4 mm diameter biopsy punches were used to create MSC-laden hydrogel cylinders. MSCs were also encapsulated within agarose (Ag; 2% w/v; Type VII, Sigma, St. Louis, MO) hydrogels. Agarose, a well established scaffold for cartilage tissue engineering (Mauck *et al*. 2006), was included as a control. All constructs (1 ml/construct) and were cultured in a chemically defined medium consisting of high glucose DMEM with 1x PSF, 0.1 μm dexamethasone, 50 μg/mL ascorbate 2-phosphate, 40 μg/mL l-proline, 100 μg/mL sodium pyruvate, ITS+ (6.25 μg/ml insulin, 6.25 μg/ml transferrin, 6.25 ng/ml selenous acid, 1.25 mg/ml bovine serum albumin, and 5.35 μg/ml linoleic acid) that was further supplemented with TGF-β3 (10 ng/ml, R&D Systems, Minneapolis, MN). Constructs were cultured in non-tissue culture treated 6-well plates with complete medium changes occurring thrice weekly. In a second series of studies, using only the high density 1% HA

formulation, constructs were also evaluated with culture on an orbital shaker (1.2 rpm) for the duration of the study (Farrell *et al*. 2011). This 'dynamic culture' group was accompanied by a 'static culture' control group treated identically.

### 5.2.3. Mechanical and Biochemical Analysis

At defined time points (4 and 8 weeks for macromer study, 3, 6, and 9 weeks for shaking study), construct mechanical properties and biochemical content was assessed. The unconfined equilibrium compressive modulus was derived from a stress relaxation test (10% strain; 1000 sec relaxation) (Mauck *et al*. 2000). After equilibration, the dynamic modulus was determined by applying 5 sinusoidal cycles of compression at 1 Hz (1% strain amplitude) (Park *et al*. 2008). After mechanical testing each construct was weighed and digested in papain before being analyzed for DNA, sulfated glycosaminoglycan (sGAG), and collagen content (Mauck *et al*. 2006). DNA content was analyzed using the Picogreen dsDNA assay kit (Molecular Probes, Eugene, OR), sGAG using the 1,9-dimethylmethylene blue (DMMB) dye binding assay, and the orthohydroxyproline (OHP) was measured and converted to collagen as previously described (Neuman and Logan 1949; Stegemann and Stalder 1967; Farndale *et al*. 1986).

### 5.2.4. Histological Analysis

To assess the viability of encapsulated MSCs within HA and Ag hydrogels, samples were halved diametrically and stained with calcein AM and ethidium homodimer (Live/Dead kit; Invitrogen). Additional constructs were fixed in 4% paraformaldehyde, paraffin

embedded, and sectioned (8 μm). Sections were stained for collagens (picrosirius red) and proteoglycan (alcian blue) before imaging at 100 X magnification.

### 5.2.5. Gene Expression

To assess the expression of cartilage matrix associated genes, constructs were frozen in TRIZOL and mRNA isolated by phenol/chloroform extraction. After quantification of RNA yield and purity (Nanodrop, Thermo Scientific, Waltham, MA), reverse transcription with the Superscript First Strand Synthesis System kit (Invitrogen) was performed. Intron spanning primers and SYBR Green Master Mix were used to amplify cDNA on a 7300 Applied Biosystems real time PCR machine. Aggrecan (AGG) and collagen type II (COL II) gene expression levels were determined and normalized to glyceraldehyde 3-phosphate dehydrogenase (GAPDH). (Huang *et al*. 2010)

### 5.2.6. Statistical Analysis

All statistical analyses were performed using SYSTAT (v13, San Jose, CA). Three-way ANOVA was used with hydrogel formulation (1, 3, 5% MeHA, and Ag), MSC seeding density (20 or 60 M/mL), and time (0, 4, and 8 weeks) as independent variables. Two-way ANOVA was used for the analysis of the dynamic culture environment with time (3, 6, and 9 weeks) and culture condition (dynamic and static) as independent variables. Fisher's least significant difference *post hoc* test was used for each analysis of pair-wise comparisons and a threshold of $p<0.05$ was used to establish significant differences between experimental groups. The experiments were repeated at least one time in full,

with consistent results found between replicates; data from one replicate are presented here.

## 5.3. Results

### 5.3.1. Construct Formation and Mechanical Properties with Increasing Seeding Density

As expected, increasing the initial MSC seeding density from 20 million cells/mL (20M) to 60 million cells/mL (60M) resulted in a clear increase in viable cell density within the construct (**Figure 5-2A**, Day 1 images shown). Increased cell density did not appear to compromise viability at any HA concentration at later time points (not shown). While an increase in cellularity was achieved, our starting hypothesis was not borne out by experimental findings. Namely, the compressive properties of higher macromer density (i.e., 3% and 5%) HA constructs did not increase with an increase in MSC seeding density. While the modulus ($E_Y$) of 20M 3% HA constructs increased to 51 kPa by 8 weeks, tripling the seeding density to 60M did not change construct properties (56 kPa) (**Figure 5-2B**). Likewise, in 5% HA gels, $E_Y$ reached 66 kPa at 20M and 72 kPa at 60M, and were not different from one another (**Figure 5-2B**). However, and interestingly, the $E_Y$ of 1% HA constructs reached 121 kPa at 20M, and were nearly 3-fold greater (313 kPa) at 60M ($p<0.05$; **Figure 5-2B**). Consistent with our previous findings (Huang *et al.* 2009), Ag control constructs showed no change with increased seeding density, reaching 138 and 126 kPa for 20M and 60M conditions, respectively (**Figure 5-2B**). The results for dynamic modulus were similar to $E_Y$ where 3% and 5% HA constructs increased with time, but did not increase to greater levels at higher MSC seeding densities (**Figure 5-2C**). The dynamic modulus of 20M 1% HA constructs reached 1.10 MPa while their

60M counterparts reached 1.97 MPa at 8 weeks ($p<0.05$; **Figure 5-2C**). Ag controls increased with time and seeding density, reaching 0.78 MPa (20M) and 1.11 MPa (60M) after 8 weeks ($p=0.001$).

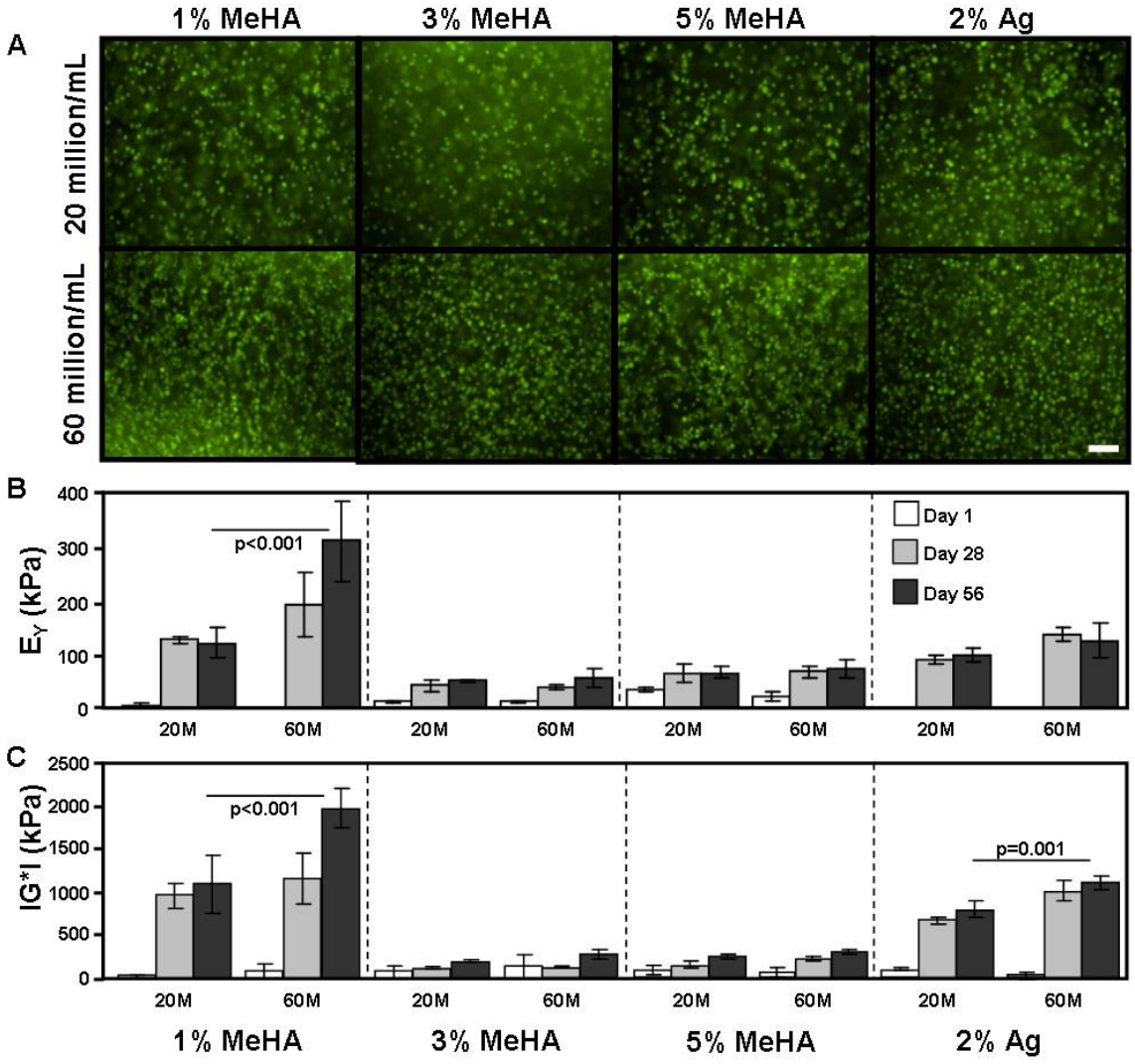


**Figure 5-2: (A) Calcein AM fluorescence 1 day after encapsulation confirmed differences in cell seeding density while demonstrating initial viability in both 20M (top) and 60M (bottom) seeding density groups (100X magnification; scale bar = 100 μm). (B) Equilibrium ($E_Y$) and (C) dynamic modulus (|G*|) of MSC-laden HA and Ag hydrogels at 20M and 60M seeding densities after 1 (white), 28 (grey), and 56 (dark grey) days of *in vitro* culture within a chemically defined chondrogenic medium with TGF-β3 (10 ng/mL). (n=4 constructs per group; bars indicate $p<0.05$)**

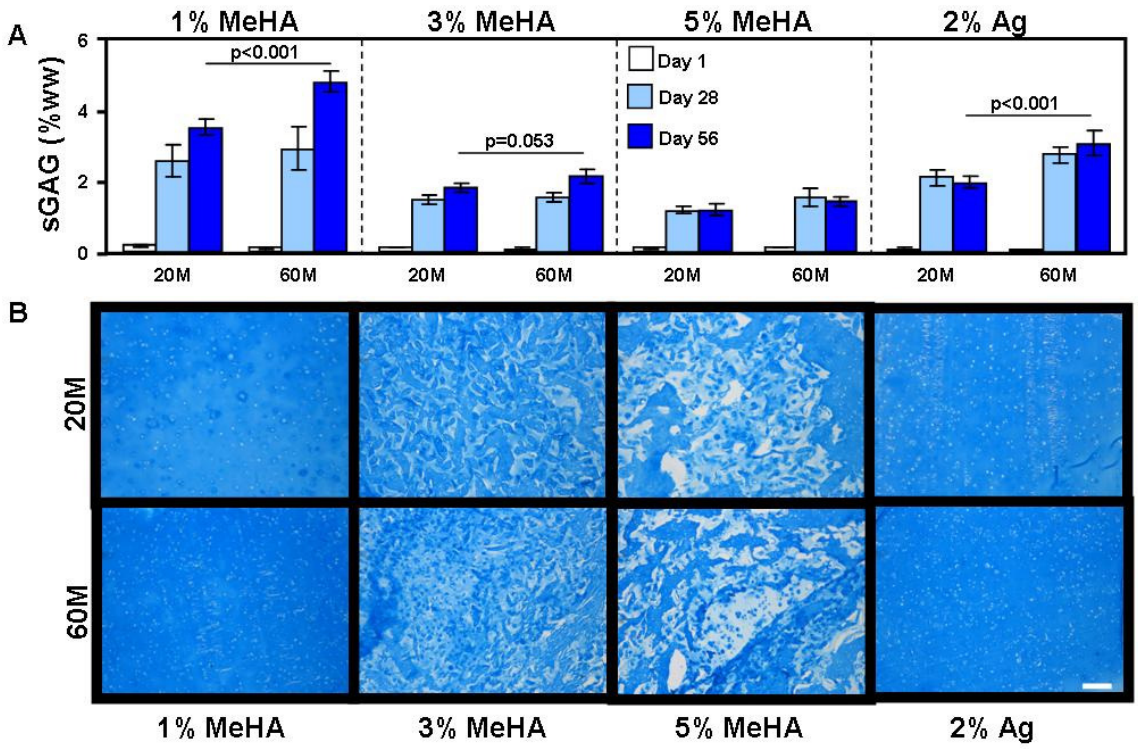


**Figure 5-3: (A) Concentration of sulfated glycosaminoglycan (sGAG) and as a percent of the construct wet weight (%ww) within MSC-laden HA and Ag hydrogels at seeding densities of 20 million MSCs/mL (20M) and 60 million (60M) MSCs/mL after 1, 28, and 56 days of *in vitro* culture within a chemically defined chondrogenic medium with TGF-β3 (10 ng/mL). (n=4 constructs per group; bars indicate p<0.05) (B) Alcian blue staining of proteoglycans in day 56 sections of MSC-laden HA and Ag constructs at 20M and 60M seeding densities. (100X magnification; scale bar = 200μm)**

5.3.2. Biochemical Content and Distribution with Increasing Seeding Density

Consistent with these observed changes in functional properties, sGAG content in 20M 1% HA constructs reached 3.5% wet weight (%ww) while 60M constructs reached 4.8%, a value similar to native bovine cartilage (**Figure 5-3A**) (see Chapter 9). 3% HA constructs reached 1.8% ww (20M) and 2.1% ww (60M) sGAG content, while the 5% HA constructs reached 1.2% ww (20M) and 1.4% ww (60M) sGAG content (**Figure 5-3A**). sGAG content in the 2% Ag constructs reached 1.9% ww (20M) and 3.0% ww (60M). Collagen content showed differing trends, where in 60M 1% HA constructs collagen reached 1.0% ww, a level significantly less than in the 20M constructs (1.8%

ww, p<0.001, **Figure 5-4A**). Similarly, 60M 3% HA reached 0.6% collagen while 20M constructs reached 0.9%. Conversely, 20M and 60M 5% HA and 2% Ag constructs were equivalent at 0.7% and 1.2% collagen, respectively (**Figure 5-4A**).

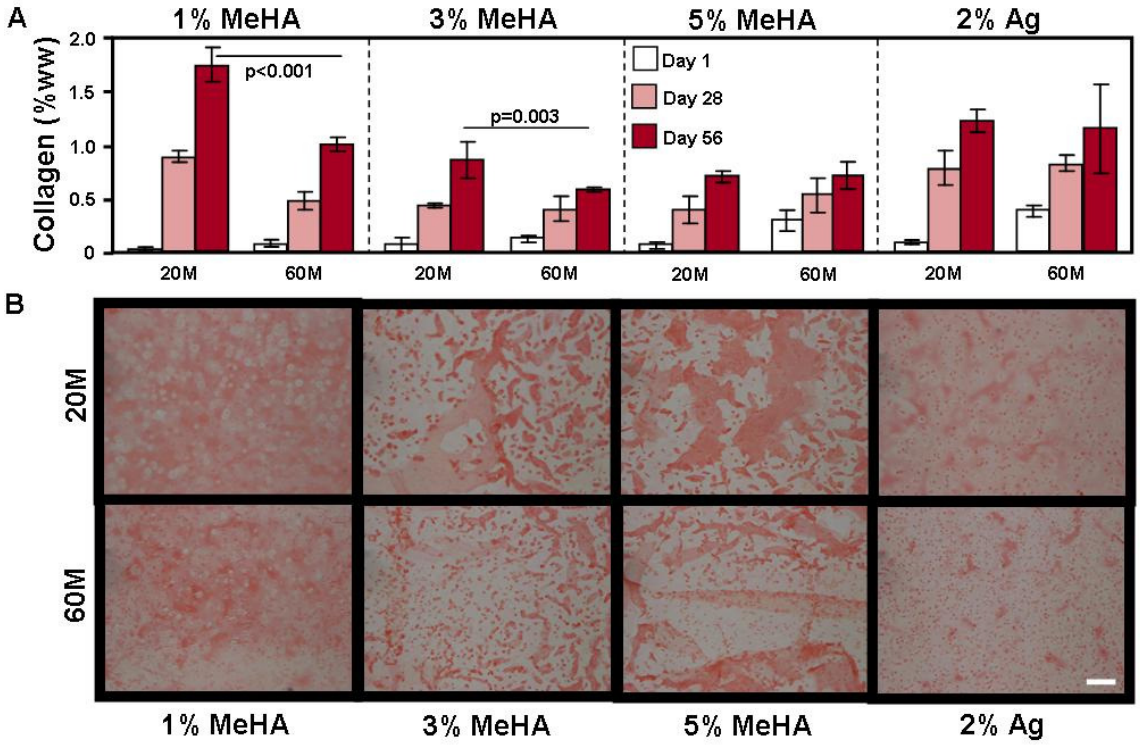


**Figure 5-4: (A) Collagen concentration as a percent of the construct wet weight (%ww) within MSC-laden HA and Ag hydrogels at seeding densities of 20 million MSCs/mL (20M) and 60 million (60M) MSCs/mL after 1, 28, and 56 days of *in vitro* culture within a chemically defined chondrogenic medium with TGF-β3 (10 ng/mL). (n=4 constructs per group; bars indicate p<0.05) (B) Picrosirius red staining of collagens in day 56 sections of MSC-laden HA and Ag constructs at 20M and 60M seeding densities. (100X magnification; 200μm scale bar)**

Consistent with biochemical measures, alcian blue staining of proteoglycans in 60M 1% HA was more intense than in the 20M group, while picrosirius red staining of collagen was more intense for 20M samples (**Figure 5-3B and Figure 5-4B**). Differences in either proteoglycan or collagen staining related to the initial MSC seeding density were not observed in 3% or 5% HA, and increasing MSC seeding density did not result in less aggregation of accumulated matrix proteins (**Figure 5-3B and Figure 5-4B**). Similar to

1% HA, the 60M 2% Ag control constructs were stained more intensely for proteoglycan than their 20M counterparts (**Figure 5-3B)**.

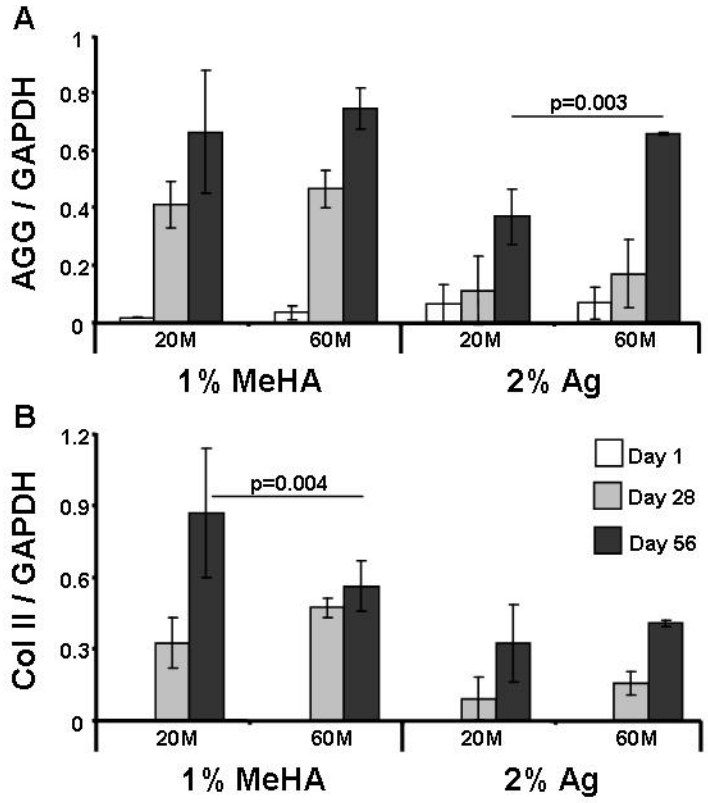


**Figure 5-5: (A) Relative expression of aggrecan (AGG) and (B) collagen type II (COL II) by MSCs in 1% HA and Ag hydrogels after 1, 28, and 56 days of chondrogenic culture. (n=2-3; bars represent p<0.05)**

5.3.3. Matrix Gene Expression with Increasing Seeding Density

Aggrecan expression (AGG) increased significantly in 1% HA and 2% Ag constructs over the duration of the study (**Figure 5-5A**). In 1% HA constructs, AGG expression (relative to GAPDH) reached 0.66 for 20M and 0.75 for 60M constructs (p=0.286), while expression in Ag was 0.37 for 20M and 0.66 for 60M (p=0.003) constructs (**Figure 5-5A**). Relative expression of collagen type II (COL II) decreased in 60M 1% HA (0.56)

compared to 20M constructs (0.87; p=0.004), while in Ag, seeding density did not alter COL II expression (0.41 vs. 0.32; p=0.427; **Figure 5-5B**).

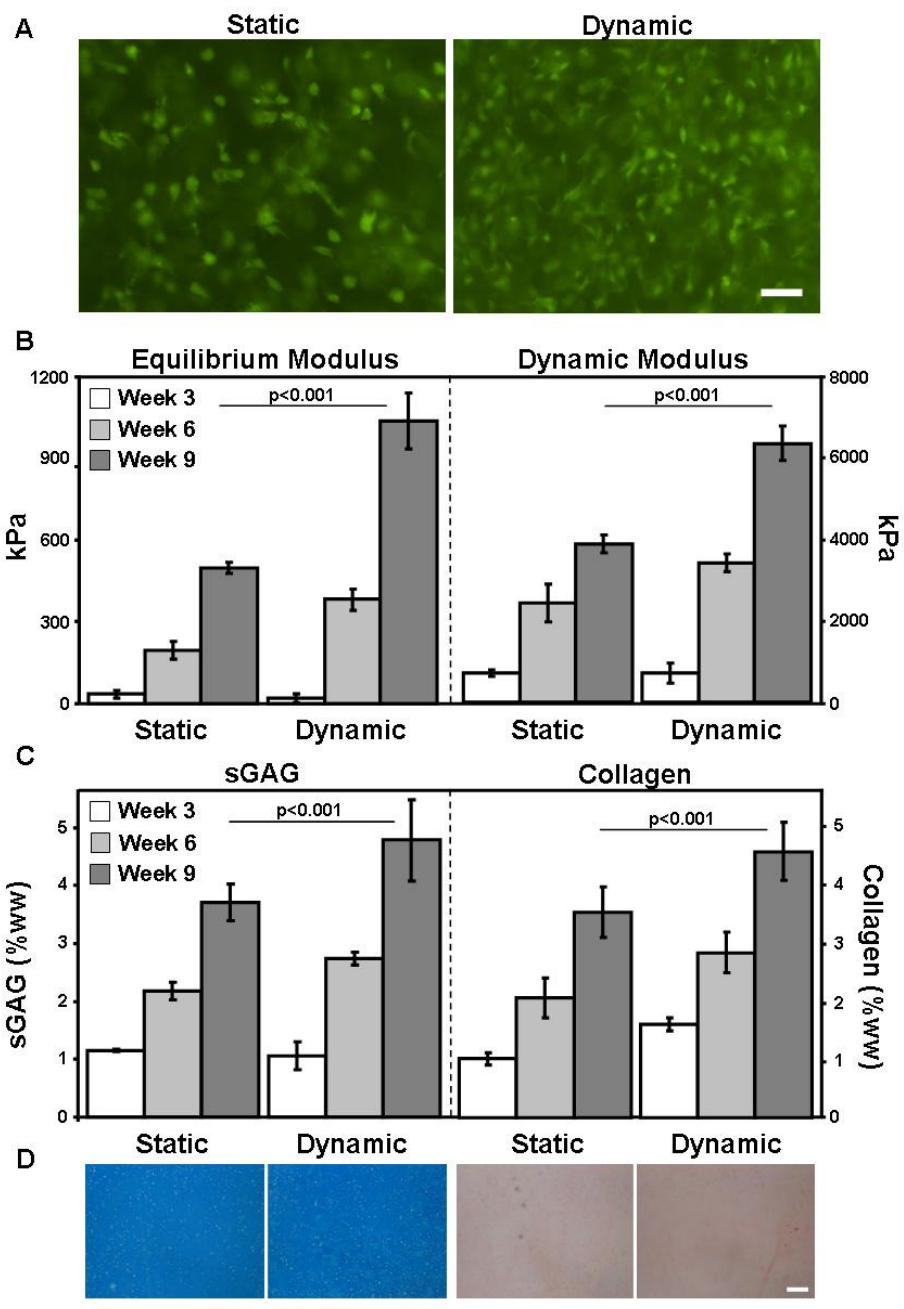


**Figure 5-6 (A) Calcein AM fluorescence 2 weeks after encapsulation showed differences in cell number and morphology between dynamic and static culture groups (200X magnification; 50 µm scale bar). (B) Equilibrium ($E_Y$) and dynamic modulus (|G*|) of static and dynamic culture groups after 3 (white), 6 (grey), and 9 (dark grey) weeks of *in vitro* culture. (C) sGAG and collagen concentration after 3, 6, and 9 weeks. (n=4-5 constructs per group; bars indicate p<0.05) (D) Proteoglycan (left) and collagen staining (right) of week 9 constructs. (100X magnification; scale bar = 200 µm)**

5.3.4. Maturation of High Density Constructs with Orbital Shaking

Gentle mixing of the culture medium had a profound effect on the maturation of high MSC density 1% HA constructs. Calcein AM fluorescence revealed an increase in cell number and in their apparent spreading (**Figure 5-6A**). Both the equilibrium and dynamic moduli of these constructs doubled with dynamic culture, reaching over 1 MPa and 6 MPa, respectively, by 9 weeks (**Figure 5-6B**). sGAG and collagen content reached 4.8% (sGAG) and 4.5% (collagen), levels 30% and 29% greater than 'static culture' controls (**Figure 5-6C**). Histological analyses confirmed these changes with more intense proteoglycan and collagen staining in the 'dynamic culture' constructs (**Figure 5-6D**).

## 5.4. Discussion

Engineered articular cartilage may be ideal for the restoration of focal defects, but only if it develops mechanical properties matching native tissue. While chondrocytes have been used to generate constructs *in vitro* with native mechanical function (Lima *et al*. 2007; Byers *et al*. 2008; Bian *et al*. 2010; Ng *et al*. 2010), the difficulty in obtaining sufficient quantities of healthy chondrocytes renders their use impractical (Lee *et al*. 2000). MSCs have also been utilized for cartilage tissue engineering, but attempts to generate constructs with native functionality have thus far been unsuccessful. The objective of this study was to determine if increasing the seeding density of MSCs in HA hydrogels would enhance construct maturation, and so close this functional divide. It was hypothesized that a greater MSC density would be particularly important in higher macromer density HA (3% and 5%) gels, where diffusivity of large macromolecules is limited. Finally, gentle mixing of long-term cultures was explored as a means of further enhancing growth

of these high density constructs by limiting the establishment of nutrient and growth factor gradients at the construct boundaries. These efforts resulted in the formation of engineered constructs that matched several key functional benchmarks of native articular cartilage.

Contrary to our original hypothesis, increased MSC density in 3% and 5% HA constructs did not improve matrix distribution, accumulation, or the development of functional properties. Chapter 4 showed that higher macromer concentrations of HA are less permissive to formed matrix distribution and the current findings indicate that even a 3-fold increase in MSC density does not enable the formation of a functionally contiguous matrix in these higher macromer concentration hydrogels. Conversely, a higher initial MSC density (60M) in low macromer concentration (1%) HA constructs did increase the functional properties, with a nearly 3-fold increase in equilibrium properties to 313 kPa (**Figure 5-2B**) after 8 weeks of culture. Interestingly, and in keeping with previous work, agarose constructs were independent of seeding density (Huang *et al.* 2009). These results highlight the fundamental differences between HA and agarose hydrogels, and establish that functional gains can be achieved with higher seeding densities, but that these changes are highly dependent on the material formulation employed.

In this work, we used a modified version of hyaluronic acid (HA) to form the stable, covalently crosslinked backbone of the hydrogel. HA is a biologically relevant molecule that plays a critical role in anchoring large proteoglycans in the cartilage extracellular matrix (Knudson 1993; Mankin *et al.* 1994). Cells can also interact directly with HA

through CD44 transmembrane receptors, and this interaction can modulate cell migration, proliferation, differentiation, and HA degradation (Embry and Knudson 2003). Interestingly, HA added to human MSCs in a 3D alginate environment increases cartilage matrix production (Kavalkovich *et al*. 2002), suggesting a direct biologic role for this molecule. Likewise, human MSCs possess abundant CD44 receptors and undergo chondrogenesis to a greater extent in these crosslinked HA networks compared to similarly crosslinked (but bioinert) poly(ethylene glycol) (PEG) gels, even after controlling for mechanical properties (Chung and Burdick 2009). Like PEG, agarose is a bioinert microenvironment that permits MSC chondrogenesis, but does not provide natural cell adhesion sites and is not degradable and so precludes cell-mediated remodeling. This may in part explain why increasing MSC density in HA constructs leads to greater functional properties than agarose constructs.

The ability for cells to remodel their microenvironment within the HA constructs is particularly relevant when considering the biochemical and biomechanical differences between the 20M and 60M 1% HA groups. The equilibrium modulus was ~3-fold greater in the 60M group, while the sGAG concentration was only ~25% greater, and the collagen concentration was actually less, ~50% of the 20M constructs. This disparity between mechanical properties and biochemical constituents indicates that other factors may be responsible for the significant increase in function we observed. Our group and others have shown that as bovine cartilage matures, collagen becomes more organized (see Chapter 9) and is better crosslinked, resulting in increases in cartilage mechanical properties (Guilak *et al*. 1997). Likewise, genome wide expression analyses showed that

MSCs differentiate towards a chondrocyte phenotype in agarose, but that hundreds of genes remain differentially expressed between the two cell types (Huang *et al*. 2010). Therefore, the observed increase in mechanics in low macromer density HA constructs may be from cell-mediated matrix remodeling or a contribution from other matrix constituents that were expressed in this natural HA microenvironment. Further analysis, on a molecular basis, is warranted to identify these key mediators of mechanical function that vary as a function of seeding density.

From our data, it appears that the ability to remodel the surrounding matrix is critical for mechanical function to be improved with increasing MSC seeding density. Along these lines, initial MSC seeding density increased chondrogenesis on a per cell basis in a gelatin foam material, but mechanical properties were not assessed (Ponticiello *et al*. 2000). Similarly, Wang and colleagues seeded umbilical cord MSCs at 5, 25, and 50 million/mL in a non-woven polyglycolic acid mesh and reported that matrix accumulation and mechanical integrity increased as a function of seeding density (Wang *et al*. 2009). Maher *et al* seeded 30 and 60 million MSCs/mL in a self-assembling peptide hydrogel to promote integration in a gap model of cartilage repair and reported that hydrogel seeded at a higher MSC density formed a more cartilage-like material and increased the integration strength of repair (Maher *et al*. 2009). Similar to HA in the present work, these studies were conducted in materials that are more permissive of matrix accumulation or remodeling, which may offer insight into why they benefit from high MSC density unlike agarose or other non-degradable materials. Current studies,

using degradable linkages (Chung and Burdick 2009) within our HA network will further optimize this important parameter.

It has also been noted that MSCs are particularly sensitive to nutrient supply (Pattappa *et al*. 2010). To address this concern, we cultured our best performing high density constructs (1% HA, 60 million cells/mL) under continual agitation conditions in chondrogenic medium. This simple modification to the culture environment resulted in profound increases in bulk mechanics and matrix accumulation. Under these conditions, equilibrium properties reached levels in excess of 1MPa, and sGAG contents of 4.8% of the wet weight. These values match or exceed native tissue levels, and represent the highest ever achieved in this HA system. While this exact technique has not reportedly been used in conjunction with any other MSC-based approach, perfusion and rotating wall bioreactors have been utilized to increase nutrient transport for chondrocyte-based systems (Sittinger *et al*. 1994; Chen *et al*. 2004). Vunjak-Novakovic *et al* observed significant increases in all biochemical and mechanical metrics when chondrocyte seeded fibrous polyglycolic acid scaffolds were cultured in a rotating wall bioreactor (Vunjak-Novakovic *et al*. 1999). Interestingly, using MSCs cultured in agarose gels in a rotating wall bioreactor, Sheehy *et al* observed an adverse effect on the growth of constructs over 3 weeks (Sheehy *et al*. 2011). Similarly in alginate, Hannouche *et al* and found that MSC chondrogenesis is delayed compared to the same MSCs in a collagen hydrogel (Hannouche *et al*. 2007) under rotational culture. These observations indicate that the level of MSC differentiation and matrix assembly, and its material environment, may differentially regulated response to dynamic culture conditions. Indeed, even in the case

of dynamic compression, MSCs do not initially respond favorably to this stimulus when encased within an agarose hydrogel, but given time to mature and synthesize pericellular matrix, a robust response follows (Huang *et al*. 2010). In the present study, using HA constructs, dynamic culture was initiated at the time constructs were formed, but the degree of mixing was likely less than would occur in a rotating bioreactor system. The precise relationship between material and fluid environments needs to be further understood to optimize this robust growth potential.

### 5.5. Conclusions

HA hydrogels formed at a macromer concentration of 1% offer a permissive microenvironment to encapsulate MSCs at a high density (60 million/mL) which generates constructs with a mean equilibrium modulus of 313 kPa at 8 weeks, approximately 50% greater than our best MSC-based results reported to date (Huang *et al*. 2009). Dynamic culture accelerated the maturation of these high MSC density 1% HA constructs, with native tissue mechanical (~1MPa) and sGAG (4.8%) levels reached within 9 weeks. The ability for HA to allow advanced construct maturation in response to both high MSC density and dynamic culture represents a significant step towards the development of functional engineered tissue for cartilage repair.

# CHAPTER 6: Dynamic Compression Promotes Cartilage-Like Functional Properties in MSC-Seeded Hyaluronic Acid Hydrogels

## 6.1 Introduction

The specialized mechanical function of articular cartilage must be recapitulated in a successful engineered cartilage repair. Chondrocytes can generate *in vitro* cartilage constructs with mechanical properties at or near native levels when cultured in specialized media formulations (Lima *et al*. 2007; Byers *et al*. 2008; Bian *et al*. 2010). While these advances in chondrocyte-based tissue engineering are highly instructive, the difficulty of obtaining sufficient numbers of healthy autologous chondrocytes represents a considerable challenge. To circumvent this limitation, many have evaluated MSCs, an autologous cell type that can be expanded *in vitro* and with a demonstrated capacity for chondrogenic differentiation. Despite their potential, MSC-based engineered cartilage has yet to achieve functional properties comparable to those produced by chondrocytes in 3D culture (Mauck *et al*. 2006; Huang *et al*. 2009; Sheehy *et al*. 2011).

Chapters 3-5 have highlighted our efforts to generate to generate cartilage-like repair constructs which began with mechanical properties that were ~20 fold less than native cartilage in Chapter 3. Optimization of macromer concentration (Chapter 4) and MSC density coupled with dynamic culture (Chapter 5) have generated constructs that reach native levels of mechanical function and sulfated glycosaminoglycan (sGAG) content. While these results are promising, additional factors may further improve the maturation and suitability of these engineered cartilage grafts for clinical use. In particular, dynamic

compressive loading has been shown to improve the maturation of both chondrocyte- and MSC-based constructs (Mauck *et al*. 2000; Huang *et al*. 2010). For MSCs in agarose, anabolic response to daily dynamic compressive loading is dependent on a preliminary 3-week pre-culture period, during which time MSCs undergo chondrogenic differentiation and establish a contiguous extracellular matrix (**Figure 6-1**) (Huang *et al*. 2010). HA, as a natural constituent of the cartilage microenvironment, provides a favorable biologic interface for MSC interaction through CD44 receptors, and can advance chondrogenesis relative to other photo-polymerizable materials (such as poly[ethylene glycol], PEG) that lack attachment sites (Chung and Burdick 2009). The objective of the present study was thus to evaluate a number of different dynamic compressive loading regimens with the goal of improving the functional properties of MSC-seeded HA constructs.

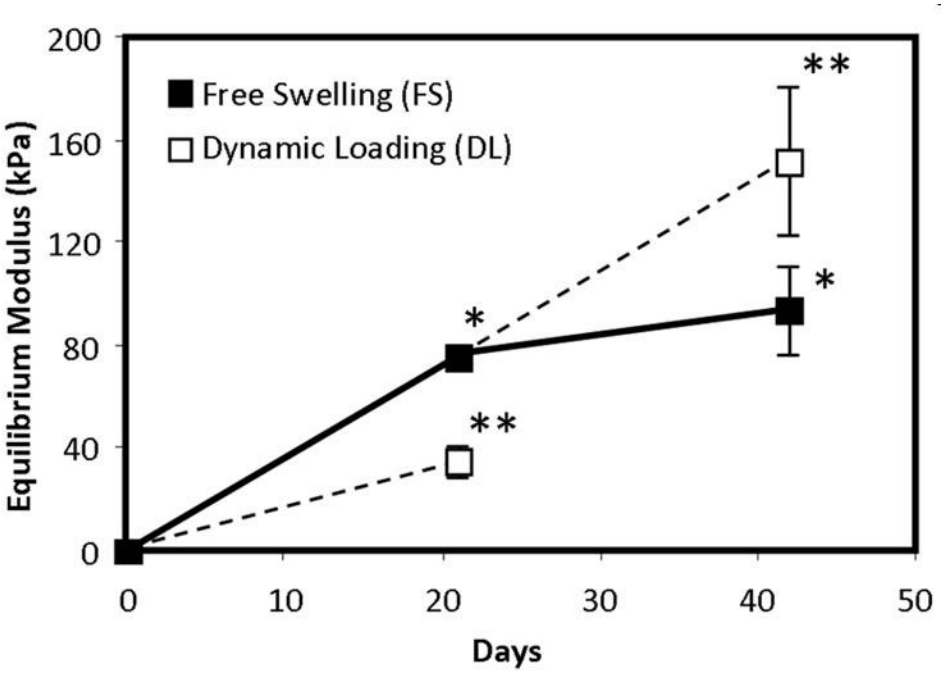


**Figure 6-1: Equilibrium compressive modulus of MSC-seeded agarose (20 million cells/mL) after dynamic loading. Loading was initiated after 3 days or 3 weeks of pre-maturation. *indicates significance from day 0, ** indicates significance between day 0 and free-swelling controls within each time point ($p<0.015$). (Huang *et al.* 2010)**

## 6.2. Methods

### 6.2.1. Construct Formation and Culture

To carry out this study, MeHA was synthesized and dissolved at 1% w/v in PBS with 0.05% w/v photoinitiator I2959 as described in Chapter 3 (Burdick *et al*. 2005). Juvenile bone-marrow derived MSCs were expanded, photo-encapsulated (50 million cells/mL) in 1% MeHA, punched to 4 mm in diameter, and cultured in chondrogenic medium with TGF-β3 for up to 9 weeks under static culture conditions.

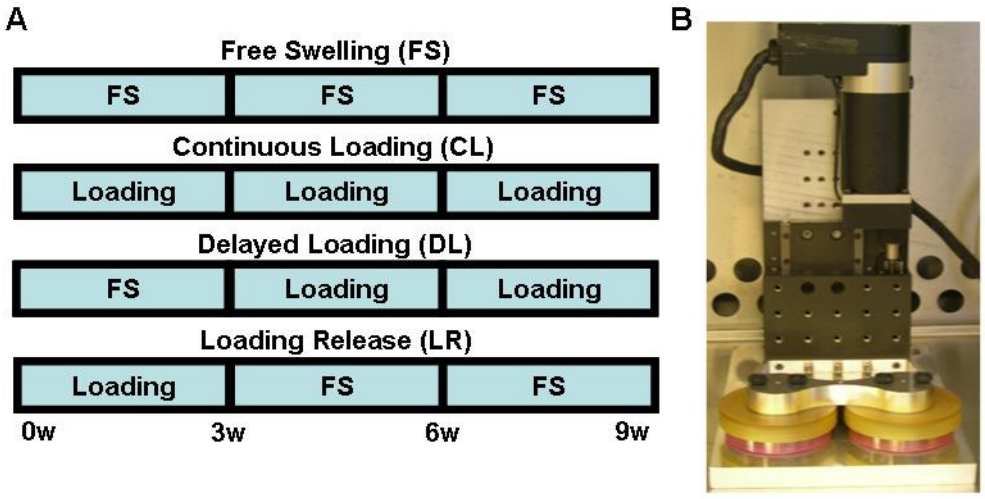


**Figure 6-2: (A) Control and loading conditions for 9 weeks of culture. CL constructs were loaded the entire 9 weeks, DL underwent 6 weeks of loading after 3 weeks of pre-culture, and the LR group was loaded the first 3 weeks followed by 6 weeks of FS culture. (B) Custom bioreactor for dynamic loading.**

### 6.2.2. Dynamic Compressive Loading

Three loading groups (**Figure 6-2A**) were exposed to dynamic unconfined compressive deformations (10%) at 1 Hz for 3 hours daily using a previously described custom bioreactor system (**Figure 6-2B**) (Mauck *et al*. 2000). The continuous loading (CL) group underwent 9 weeks of loading, initiated the day after construct formation. The delayed loading (DL) group was cultured for 3 weeks in free-swelling (FS) conditions before

loading was initiated. The loading release (LR) group was dynamically loaded for the first 3 weeks of culture, followed by return to FS conditions for an additional 6 weeks. Control constructs were maintained for the entire 9 week duration of the study in FS conditions.

### 6.2.3. Analysis Techniques

MSCs in FS and CL constructs were fluorescently labeled with the Live/Dead kit and imaged after 7 days to capture any differences in viability resulting from dynamic loading. At 3, 6, and 9 weeks, constructs from each group were tested in unconfined compression to determine the equilibrium and dynamic moduli as described in Chapter 3. After testing, constructs were papain digested and analyzed for sGAG, and collagen content. Additional samples for histology were processed and stained for proteoglycan (alcian blue) and collagen (picrosirius red) distribution.

### 6.2.4. Statistical Analysis

Two-way ANOVA was performed with time (3, 6, and 9 weeks) and loading condition (CL, DL, LR, and FS) as independent variables. Tukey's *post hoc* test was performed for each analysis of pair-wise comparisons and a threshold of $p<0.05$ was used to discern significant differences between experimental groups.

## 6.3. Results

### 6.3.1. Initial MSC Viability

Calcein AM staining in 7 day constructs revealed a greater number of viable cells in the constructs that underwent daily compressive loading (CL) than in the FS control gels (**Figure 6-3A**). More dead cells were observed in the FS constructs than in the CL constructs (**Figure 6-3B**).

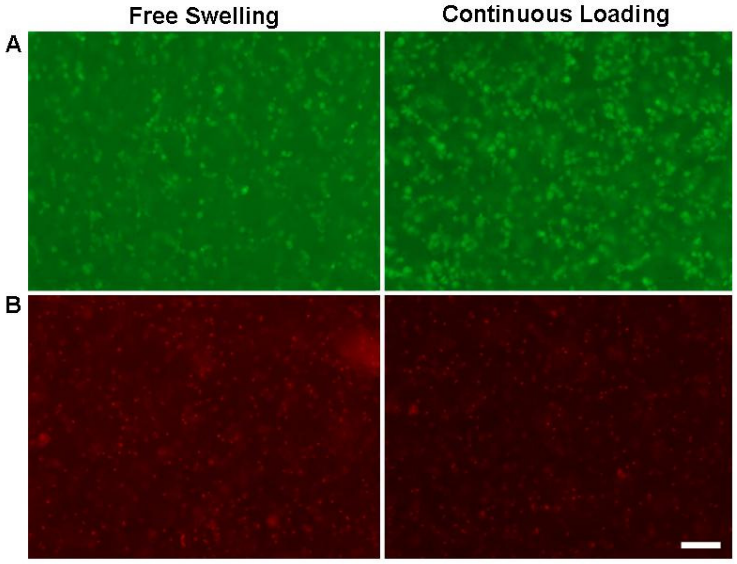


**Figure 6-3: Live/Dead fluorescent imaging after 3 weeks showed a greater number of live cells in high MSC density MeHA constructs that had undergone a daily regimen of dynamic compressive loading (right) than were found within constructs maintained in free-swelling culture conditions (left). (100X magnification; scale bar = 100 μm)**

### 6.3.2. Mechanical Properties

Over the 9 week period, dynamic loading modulated the functional growth of MSC-seeded constructs. Consistent with our previous findings with MSCs in agarose (Huang *et al*. 2010), continuous loading over the first 3 weeks decreased the equilibrium modulus ($E_Y$), though only by 20% (**Figure 6-4A**). When this loading was continued through 6 and 9 weeks, the modulus of CL constructs was greater than that of FS controls by 28%

and 70% (p=0.003), respectively (**Figure 6-4A**). Delayed loading (DL) initiated after 3 weeks of FS culture also increased construct $E_Y$ (38%) by 9 weeks. Interestingly, loading for the first 3 weeks followed by FS culture for 6 weeks (the LR group) resulted in an $E_Y$ that was comparable to the FS control group (**Figure 6-4A**).

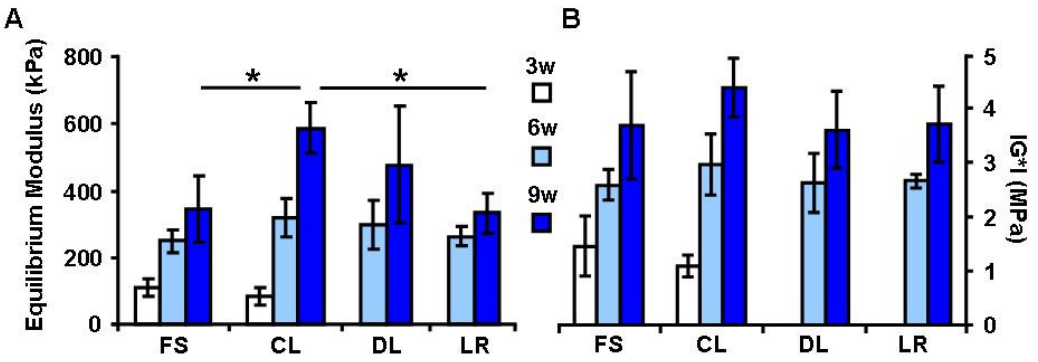


**Figure 6-4: (A) The equilibrium modulus and (B) dynamic modulus (|G*|) of MeHA constructs after 3, 6, and 9 weeks of their respective dynamic compressive loading regimens (n=4-7; *p<0.05).**

The dynamic modulus followed closely the development of the equilibrium modulus with the CL constructs reaching 4.4 MPa, about 20% greater than the FS group (3.7 MPa; **Figure 6-4B**). The DL and LR constructs reached dynamic modulus values similar to FS controls, attaining 3.6 and 3.7 MPA, respectively (**Figure 6-4B**).

### 6.3.3. Biochemical Content

sGAG concentrations correlated with increases in construct $E_Y$, with 3.7% sGAG in the CL group being ~20% greater than the other loading groups and the FS controls (**Figure 6-5A**). While collagen concentrations were not significantly different between experimental groups after 9 weeks, considerable increases in collagen were observed with time in culture where each group accumulated over 3% collagen per wet weight (**Figure 6-6A**).

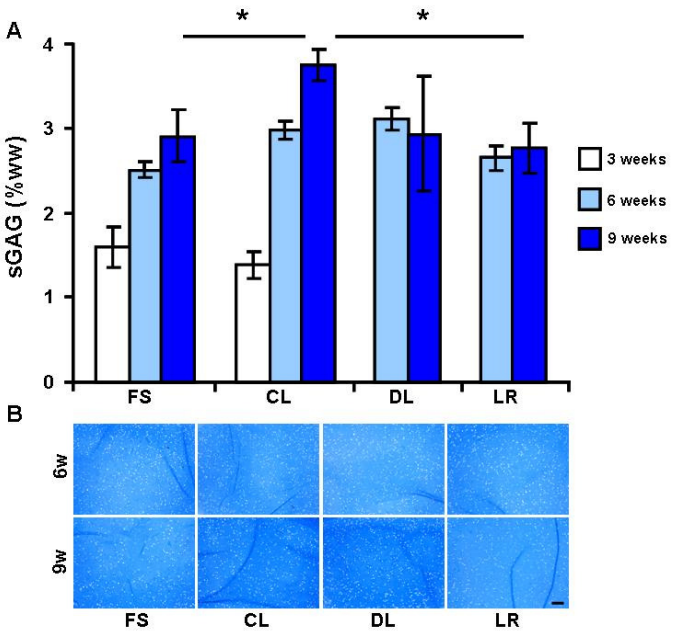


**Figure 6-5: (A) The glycosaminoglycan (GAG) concentrations (%ww) of MeHA constructs after continuous dynamic compressive loading (CL), delayed loading (DL), loading release (3 weeks loading follwed by return to FS conditions; LR), and free-swelling (no loading; FS) culture (n=4-7; *p<0.05). (B) Proteoglycan staining (alcian blue) after 6 and 9 weeks (50X magnfication; scale bar = 200 µm).**

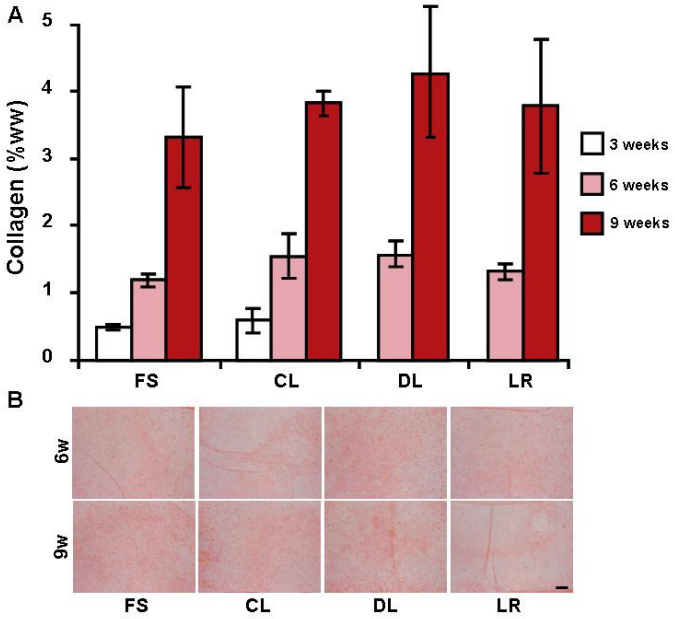


**Figure 6-6: (A) The collagen concentrations (%ww) of MeHA constructs after continuous dynamic compressive loading (CL), delayed loading (DL), loading release (3 weeks loading follwed by return to FS conditions; LR), and free-swelling (no loading; FS) culture (n=4-7; *p<0.05). (B) Collagen staining (picrosirius red) after 6 and 9 weeks (50X magnfication; scale bar = 200 µm).**

6.3.4. Histology

Proteoglycan staining was consistent with biochemical findings. Increases in intensity were evident between 6 and 9 weeks, as were increases in the dynamic loading groups (CL and DL) compared to FS controls (**Figure 6-5B**). Collagen staining appeared well distributed throughout each construct, but similar to the biochemical findings no obvious differences in staining intensity were observed between loaded and control constructs (**Figure 6-6B**).

## 6.4. Discussion

The objective of this study was to determine whether dynamic compression could be used as a tool to improve the mechanical function of our optimized MSC-based cartilage constructs formed from photo-crosslinkable HA hydrogels. After the first 3 weeks of loading we observed a slight decrease in modulus, consistent with previous findings in a MSC-seeded agarose hydrogel system (Huang *et al*. 2010). In this study, the decrease in properties was not as severe, owing perhaps to the higher seeding density and/or different material attributes of the HA system. Interestingly, when loading was continued for the next 3 weeks, the modulus tripled, more than recovering from the initial decline in properties (**Figure 6-4A**). With 3 additional weeks of loading (to 9 weeks total), constructs achieved an equilibrium modulus of 587 kPa (a level 70% higher than FS controls) along with a dynamic modulus of 4.4 MPa (20% higher than FS controls, **Figure 6-4B**). When loading was delayed 3 weeks (DL), lower mechanical properties were attained than for the CL group. These results indicate that MSCs in HA hydrogels are mechanosensitive, and that while early loading initially retarded functional

development, continued loading enhanced mechanical function over the long term. Of note, loaded samples that were returned to FS conditions after 3 weeks (the LR group) were not significantly different from FS controls, suggesting that the loading-induced enhancement of functional maturation is dependent on multiple loading events applied over the entire culture period.

Fluorescent imaging of viable cells indicated that early loading led to increased quantities of viable cells in MeHA hydrogels (**Figure 6-3A-B**). Previous reports on MSCs in agarose demonstrated that early loading negatively affects MSC chondrogenesis, but in this work the constructs were not loaded after 3 weeks. This work showed a rapid increase in functional development after the first 3 weeks that may have been amplified by the increase in cell number resulting from dynamic loading. Dynamic loading is known to increase solute transport which in turn may be responsible for the increased fraction of viable cells (Albro *et al*. 2008). The mechanical properties of CL constructs were less than FS hydrogels after 3 weeks despite the inverse relationship to cell number. If the chondrogenesis of MSCs undergoing early continuous loading was inhibited in lieu of proliferation, this may explain why the mechanics were initially less, but as the greater number of MSCs in the CL constructs did eventually differentiate, these constructs matured at a significantly more rapid pace than the FS controls.

### 6.5. Conclusions

These findings indicate that dynamic compressive loading is another approach that can be effectively used to accelerate the development of MSC-MeHA constructs to clinically

relevant functionality. Furthermore, these results offer additional insights into the profound effect that microenvironments can have on the chondrogenic response of MSCs within various biomaterials.

# CHAPTER 7: Improved Cartilage Repair via *InVitro* Pre-Maturation of MSC Seeded Hyaluronic Acid Hydrogels

## 7.1. Introduction

The role of articular cartilage is to provide a low friction joint surface that resists wear while distributing stresses in a demanding joint environment (Ateshian *et al*. 2003). Together with the limited regenerative capacity of native cartilage, these functional demands have made cartilage repair a rather intractable problem. Regenerative strategies (e.g. autologous chondrocyte implantation [ACI] or microfracture) for the repair of cartilage defects arising from disease or traumatic injury often result in fibrocartilaginous tissue that does not restore function (Meachim and Roberts 1971; Horas *et al*. 2003; Harris *et al*. 2010). Successful lateral integration is likewise a complication in both ACI and osteochondral grafting procedures (Horas *et al*. 2003; Domayer *et al*. 2008; Niemeyer *et al*. 2008; Erggelet *et al*. 2010). Failed graft integration results in changes in mechanical stress which can damage adjacent cartilage and result in the early onset of osteoarthritis (Mankin 1982; Volpin *et al*. 1990; Bullough 2004; Guettler *et al*. 2004). The clinical demand for functional, biological cartilage replacement strategies has motivated the efforts of many researchers in the fields of biomaterials and tissue engineering to create a graft material. However, the elusive goals are that the biomaterials must have sufficient mechanical stiffness and the ability to integrate with host tissue to provide clinically relevant functional outcomes.

Considerable progress has been made towards the *in vitro* tissue engineering of neocartilage with compressive properties approaching native levels. Of note, articular chondrocytes encapsulated within various biomaterials have generated constructs with native mechanical properties when exposed to specialized media and dynamic loading conditions (Lima *et al*. 2007; Byers *et al*. 2008; Bian *et al*. 2010). While these advances are significant, obtaining sufficient quantities of healthy chondrocytes from a patient to generate autologous tissue engineered cartilage remains a challenge. Towards this end, the autologous use of mesenchymal stem cells (MSCs) has become increasingly popular as MSCs are easily expanded *in vitro* while maintaining the capacity for chondrogenic differentiation (Johnstone *et al*. 1998; Pittenger *et al*. 1999). Despite their potential, one report suggests that *in vitro* repair with MSCs results in a fraction of the integration strength obtained by chondrocytes (Vinardell *et al*. 2009). To date, no reported studies of MSC-based cartilage constructs have examined the simultaneous development of compressive and integrative properties, both of which are crucial for successful cartilage repair.

While many *in vitro* studies show histological data to demonstrate 'good' orthotopic graft to host tissue integration, relatively few provide biomechanical evidence to support these claims (Emans *et al*. 2010; Oliveira *et al*. 2010; Toh *et al*. 2010). The intricacies and cost of such studies are perhaps the primary reason that more studies are not routinely conducted (Gratz *et al*. 2006). When mechanics have been assessed through *in vitro* or ectopic *in vivo* models, integration strength is reported as a function of tension or shear to failure of the cartilage repair interface. Results from these studies show that integration is

dependent on biomaterial properties (Hunter and Levenston 2004; Rice *et al*. 2008), cell type (Vinardell *et al*. 2009), construct pre-culture (Obradovic *et al*. 2001; Hunter and Levenston 2004), and growth factor supplementation (Ionescu *et al*. 2011). Cartilage age (DiMicco *et al*. 2002; Ionescu *et al*. 2011), surface degradation (Obradovic *et al*. 2001; van de Breevaart Bravenboer *et al*. 2004; Tam *et al*. 2007), and the application of tissue adhesives (Silverman *et al*. 1999; Peretti *et al*. 2003; Wang *et al*. 2007) also modulate integration strength. In general, integration occurs under conditions of active biosynthesis, can be improved by increased permissiveness of the host cartilage matrix, and by the use of tissue adhesives.

Yet to be established is whether *in situ* formed constructs or the implantation of *in vitro* matured constructs is more appropriate for cartilage repair. Two important questions emerge: first, while *in situ* gelation is the most direct and practical clinical application (Wang *et al*. 2007), it is yet to be demonstrated that *in situ* formed constructs can completely integrate and develop sufficient compressive properties to protect adjacent host cartilage. Obradovic *et al* seeded chondrocytes on polyglycolic acid (PGA) scaffolds and found that immature constructs (5 day pre-culture) integrated better than mature (5 week pre-culture) constructs (Obradovic *et al*. 2001). Conversely, an *in vitro* study by Hunter *et al* reported that construct maturation had a limited effect on the integration strength of PGA scaffolds, concluding also that *in situ* maturation is inhibited by adjacent cartilage (Hunter and Levenston 2004). Moreover, it is not clear whether the implantation of a mature construct will limit the degree to which integration occurs. The Obradovic study implanted chondrocyte-seeded PGA constructs with an equilibrium modulus of 224

kPa (confined compression) which resulted in an adhesive strength of ~250 kPa; however, this work, like the rest of the literature did not report the modulus of the repair material after *in vitro* culture within the defect model. It thus remains to be determined when implantation should take place and the subsequent maturation that can occur in the defect site.

To address some of these issues, we have optimized a photo-crosslinkable methacrylated hyaluronic acid (MeHA) hydrogel (Burdick *et al*. 2005) to maximize chondrogenesis of encapsulated MSCs (Chapters 3-4) (Chung and Burdick 2009). Our findings demonstrated that low MeHA macromer densities (1% w/v) provide a permissive environment for the formation and diffusion of cartilage matrix components and for the functional maturation of MSC-based tissue engineered cartilage. Still unknown, however, is the potential for MSC-laden MeHA to mature and integrate in a cartilage repair model. Further, the extent to which pre-culture (an initial period of construct maturation) modulates integration and compressive properties is unknown.

Thus, the objective of the present study was to determine the effects of tissue pre-maturation on the potential of MSC-laden MeHA for functional cartilage repair. Two independent factors were considered: 1) which MeHA macromer concentration (1%, 3%, or 5%) and 2) which construct maturation state (0 or 4 weeks) would result in the greatest combination of both compressive properties and integration strength. To accomplish this design, MSCs were encapsulated in MeHA and either UV polymerized within explant cartilage defects (*in situ* repair group: IS) or pre-cultured for 4 weeks (PC) before being

press-fit into a defect (**Figure 7-1**). The integration strength of repair and the simultaneous development of compressive properties were determined, as were the biochemical content, histological appearance, and the 3D space filling of repair constructs was assessed by contrast enhanced μCT.

## 7.2. Methods

### 7.2.1. MeHA Hydrogel

Methacrylated HA (MeHA) was synthesized as in Chapter 3 with NMR analysis indicating a degree of methacrylation of 25%. The MeHA macromer was then dissolved to 1, 3, and 5% (mass/volume) in sterile PBS with 0.05% photoinitiator Irgacure-2959 (2-methyl-1-[4-(hydroxyethoxy)phenyl]-2-methyl-1-propanone; Ciba-Geigy, Tarrytown, NY).

### 7.2.2. MSC Isolation and Cartilage Repair Model

Juvenile bovine MSCs were isolated and expanded through passage 3 as in Chapter 3. Cartilage was cored from the trochlear grooves of juvenile bovine femurs (3-6 months of age) using 8 mm diameter biopsy punches (Miltex, York, PA) and cultured in basal medium while MSCs were being expanded (~3 weeks). Three days before beginning the experiment, cartilage was trimmed to ~3 mm in thickness and concentric 4 mm diameter cores were removed from each cartilage sample using biopsy punches with a custom device to create cartilage defects. A schematic of the *in vitro* repair model and the design of the experiment is shown in **Figure 7-1**.

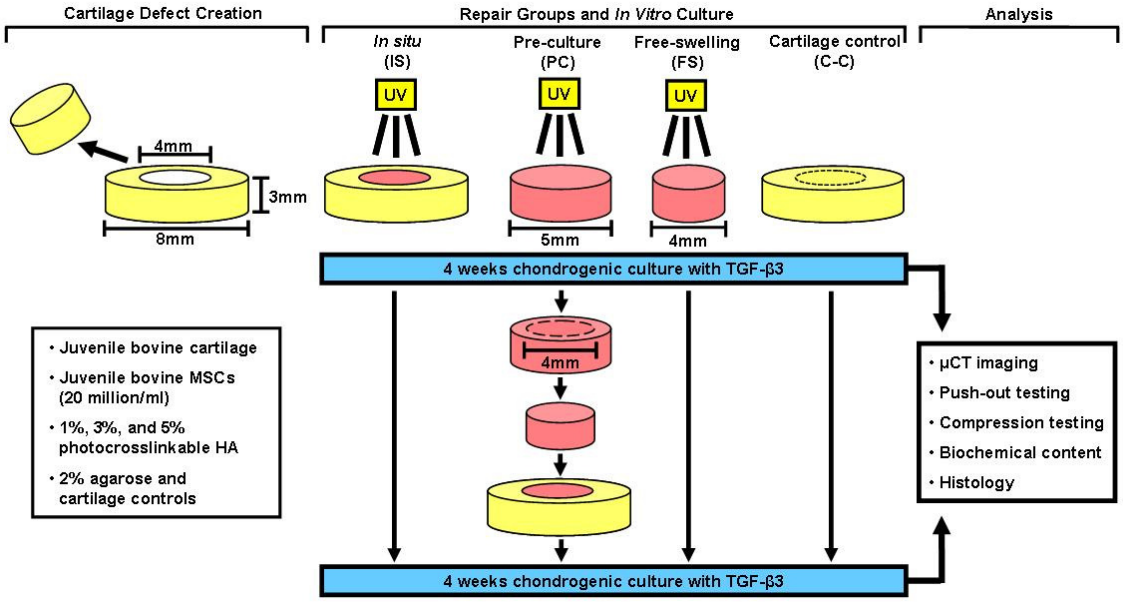


**Figure 7-1: Schematic illustrating the experimental design, creation of *in vitro* repair groups, and analysis techniques utilized in this study.**

7.2.3. Experimental Groups and Culture Conditions

Expanded MSCs were seeded at a density of 20 million cells per ml into 1%, 3%, and 5% MeHA and photo-polymerized inside of the previously prepared cartilage rings. Photo-polymerization was carried out within a custom chamber wherein oxygen was purged with $N_2$ gas throughout the 10 minute UV exposure to ensure complete polymerization (365 nm Blak-Ray UV lamp, Model #UVL-56, San Gabriel, CA). These constructs were referred to as *in situ* (IS) repaired constructs.

To investigate the effects of construct maturation on integration, MSCs were encapsulated in 1%, 3%, and 5% MeHA via UV polymerization between glass plates spaced by 2.25 mm as in Chapter 3. Sterile 5 mm diameter biopsy punches were used to create MSC-laden hydrogel cylinders. After 4 weeks of pre-culture, biopsy punches were used to core a 4 mm construct from the 5 mm hydrogels and these cores were press fit

within the additional cartilage defects. This experimental repair group was referred to as pre-culture (PC) repaired constructs.

To serve as a control for the effects of construct maturation within a cartilage defect, additional MSC-seeded MeHA hydrogels were fabricated at the same time (4 mm), but were maintained in free-swelling conditions for the duration of the study. Samples from this control group were referred to as free-swelling (FS) constructs.

MSCs were also encapsulated within agarose (Ag; 2% w/v; Type VII, Sigma, St. Louis, MO) hydrogels (a well established scaffold for cartilage tissue engineering (Mauck *et al*. 2006) to provide a comparison and control for the unique microenvironment of the MeHA hydrogels. Molten MSC-laden Ag was gelled within cartilage defects (to produce IS repair group) and press-fit after 4 weeks of pre-culture (to form a PC group). Lastly, cartilage defects were re-fitted with 4 mm cartilage plugs that were obtained from the initial defect preparation. This cartilage-to-cartilage (C-C) control offered an *in vitro* analog to osteochondral transplantation, an established surgical repair approach.

All FS hydrogel constructs (1 mL/construct) and repaired defects (3 mL/construct) were cultured in TGF-β3 (10 ng/ml, R&D Systems, Minneapolis, MN) supplemented chemically defined medium consisting of high glucose DMEM with 1x PSF, 0.1 μm dexamethasone, 50 μg/mL ascorbate 2-phosphate, 40 μg/mL l-proline, 100 μg/mL sodium pyruvate, ITS+ (6.25 μg/ml insulin, 6.25 μg/ml transferrin, 6.25 ng/ml selenous

acid, 1.25 mg/ml bovine serum albumin, and 5.35 µg/ml linoleic acid) in non-tissue culture treated 6-well plates with feedings thrice weekly.

### 7.2.4. Micro-Computed Tomography (µCT)

Contrast-enhanced micro-computed tomography (µCT) has been used to analyze 3D structure and proteoglycan content of articular cartilage (Palmer *et al*. 2006). 3D µCT imaging was utilized for analysis of cartilage defect filling to visualize the cartilage repair interface and proteoglycan accumulation within the repair material. Samples (n=3) at 4 and 8 weeks were first prepared by staining in Lugol's solution (5% w/w I2 and 10% KI in dH2O) for 24 hours (Palmer *et al*. 2006) and then scanned at an energy level of 70 kV and intensity of 114 µA (vivaCT 40, SCANCO USA, inc, Wayne, PA). 3D reconstructions provided visualization of defect filling and related to proteoglycan content for each hydrogel repair group and the C-C controls.

### 7.2.5. Mechanical Testing

The integration strength of the *in vitro* repaired cartilage was assessed using a push-out test (van de Breevaart Bravenboer *et al*. 2004; Moretti *et al*. 2005). A custom 3.8 mm indenter affixed to an Instron 5848 mechanical testing device pushed the hydrogel repair out of the cartilage annulus (0.2 mm/sec) while recording load. Failure stress (integration strength) was calculated as the quotient of the load at failure and the interface area (height x circumference).

After push out testing, the unconfined equilibrium compressive modulus was derived from a stress relaxation test (10% strain; 1000 sec relaxation) (Mauck *et al*. 2000) as described in Chapter 3. For each group and time point 4-5 samples were analyzed. After equilibration, the dynamic modulus was determined by applying 5 sinusoidal cycles of compression at 1 Hz (1% strain amplitude) (Park *et al*. 2008). Free swelling constructs were similarly assessed.

### 7.2.6. Biochemical Content and Histology

Following the mechanical testing of FS and recently removed repair constructs (PC and IS), each (n = 4-5) was weighed and digested in papain before being analyzed for DNA, sGAG, and collagen content as described in Chapter 4.

Constructs were fixed in 4% paraformaldehyde after μCT scanning, dehydrated, infiltrated with Citrisolv (Fisher), and embedded with paraffin. Sections (8 μm) were stained for collagens (picrosirius red) and imaged at 100 X magnification (Mauck *et al*. 2003).

### 7.2.7. Statistical Analysis

All statistical analyses were performed using SYSTAT (v13, San Jose, CA). Three-way ANOVA was used for biochemical and integration data with hydrogel formulation (Ag, 1%, 3%, and 5% MeHA), culture condition (FS, IS, and PC), and time (4 and 8 weeks) as independent variables. Two-way ANOVA was used for equilibrium modulus with hydrogel formulation (Ag, 1%, 3%, and 5% MeHA) and culture condition (FS, IS, and

PC) as independent variables. Fisher's least significant difference post hoc test was used for each analysis of pair-wise comparisons and a threshold of $p<0.05$ was used to discern significant differences between experimental groups.

## 7.3. Results

### 7.3.1. Repair Construct Morphology and Interface Characteristics

Photo-polymerization of MSC-laden MeHA within cartilage defects resulted in full defect filling with stable integration to the host cartilage at time 0 (i.e. constructs could be easily handled without dislodging the repair material). In some samples, a slight contraction of the IS 1% MeHA hydrogel core was observed with time in culture, but the majority of the repair interface remained intact. No hydrogel contraction was observed for the IS 3%, 5%, or Ag groups with time (data not shown). Constructs maintained in FS conditions for the first 4 weeks increased in opacity, with 1% MeHA and Ag constructs appearing more opaque and palpably stiffer. PC constructs from all groups were stable after being press fit into cartilage defects and remained in place for the final 4 weeks.

Cartilage and constructs were rapidly and effectively infiltrated by the charged contrast agent ($I_2KI$) and based on an inverse relationship of the contrast agent to the content of proteoglycan, the repair interface between native cartilage and the experimental repair constructs was visualized in 3D. These data confirmed that slight hydrogel contractions occur within the 1% MeHA IS repair group. Conversely, PC constructs completely filled the defect space (**Figure 7-2**). Notable gaps were observed at the repair interface in the cartilage to cartilage (C-C) control. No tissue engineered construct presented signal

intensity levels as high as natural cartilage. However, greater signal attenuation was observed for 1% MeHA FS and PC constructs than in the IS repair hydrogels, indicating increased proteoglycan content (**Figure 7-2**). Similarly, increased attenuation in each culture condition (IS, PC, and FS) was observed in both 1% MeHA and 2% Ag compared to either 3% or 5% MeHA.

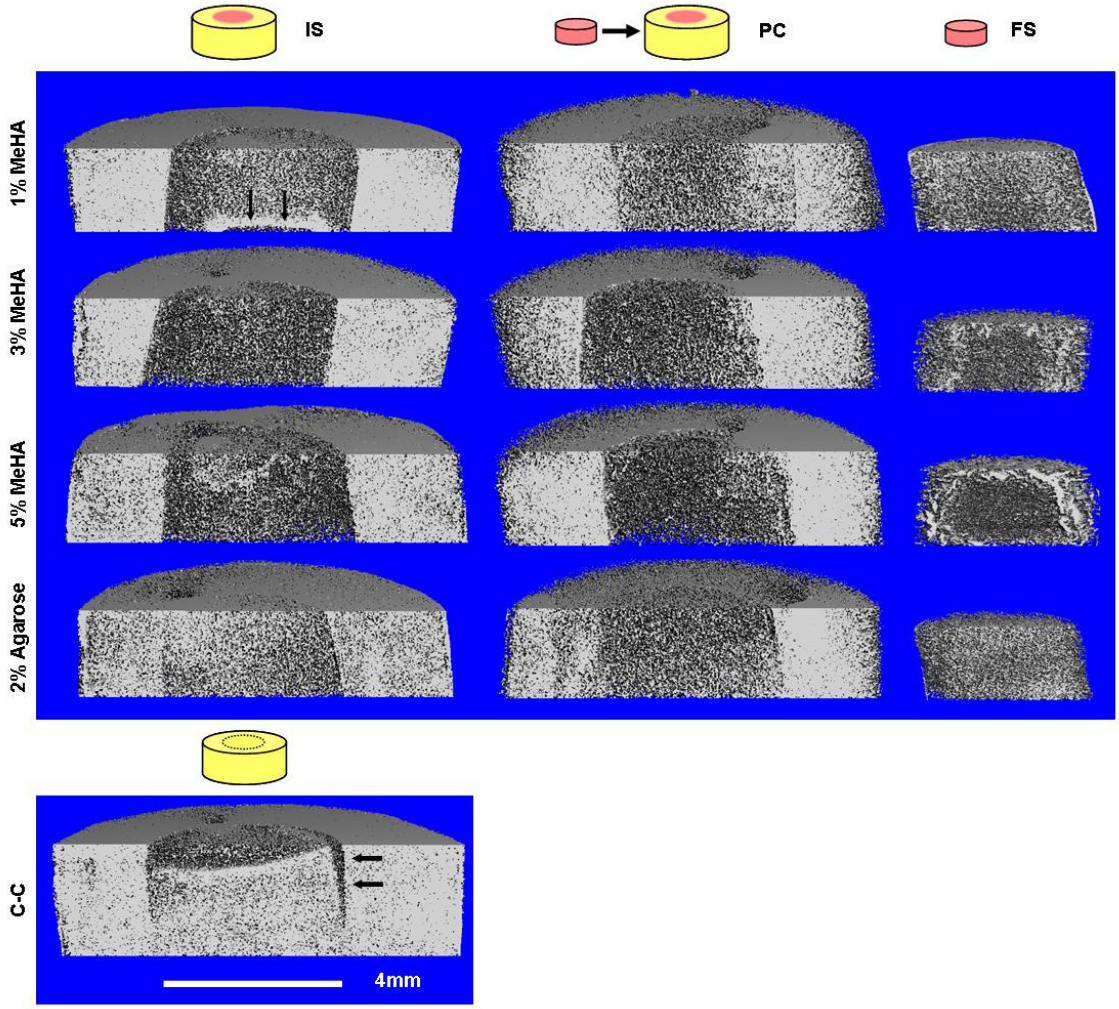


**Figure 7-2: Contrast enhanced μCT imaging of *in vitro* repaired cartilage defects after 8 weeks. Some contraction was observed in the 1% IS repair group (black arrows), while the PC repaired constructs showed no evidence of contraction or gapping. Proteoglycan-associated signal attenuation increased in 1% MeHA and 2% Ag indicating more accumulated proteoglycan than the remaining MeHA groups, yet still less than native cartilage (ring). Signal in FS controls was greater than in IS polymerized samples. C-C controls often contained large gaps between repair cartilage and adjacent host cartilage (black arrows).**

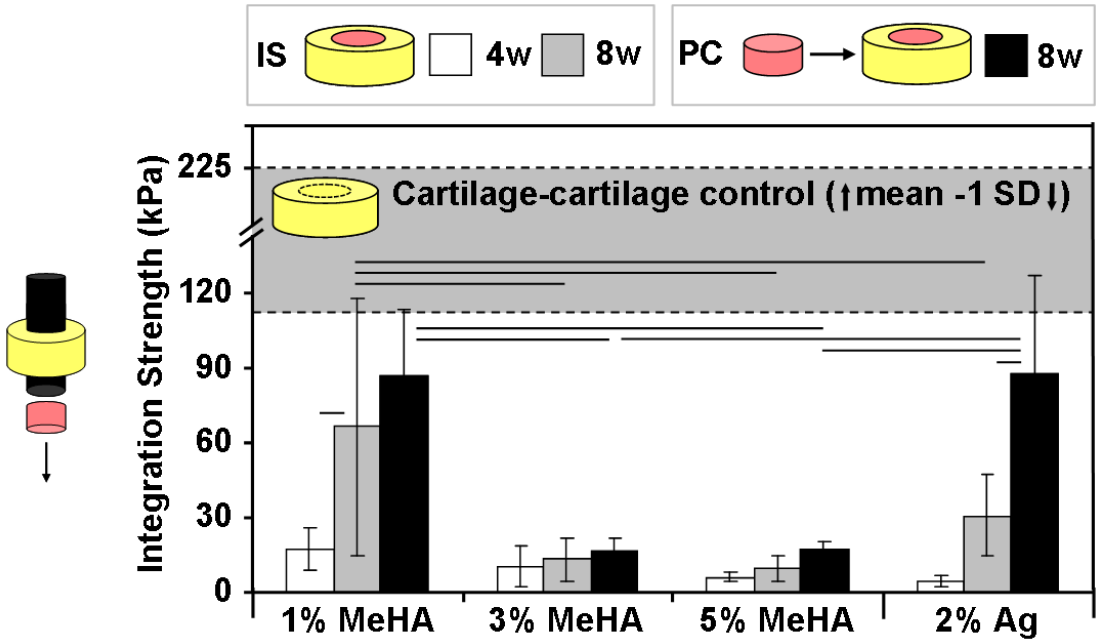


**Figure 7-3: Integration strength of *in vitro* cartilage repair was dependent on both hydrogel formulation and repair technique. The integration of MSC-laden MeHA (1%) and Ag reached nearly half the C-C controls (top grey region), while higher macromer concentration MeHA gels did not support integrative repair. Pre-culture (black bars) improved integration strength in both 1% MeHA and Ag repaired constructs. (n=4-5/group/timepoint; lines indicate p<0.05)**

7.3.2. Mechanical Properties

After 4 weeks of IS repair, the integration strength of each hydrogel group was less than 20 kPa (**Figure 7-3**). The integration strength of IS 1% MeHA constructs at 4 weeks (17 kPa) increased 4 fold (67 kPa) by 8 weeks (p=0.002). Ag IS controls likewise increased from 5 to 31 kPa over this same period (p=0.075). The C-C control constructs reached 93 kPa at 4 weeks and increased to 225 kPa by 8 weeks. The PC technique (at 8 weeks) resulted in a 30% increase (87 kPa) in integration over IS repair for 1% MeHA (p=0.168) and a near 3 fold increase for Ag controls (p<0.001; 88 kPa). The integration strength of 3% and 5% MeHA peaked at 17 kPa for PC, with no significant effects observed for either time (4 or 8 weeks) or repair condition (IS or PC).

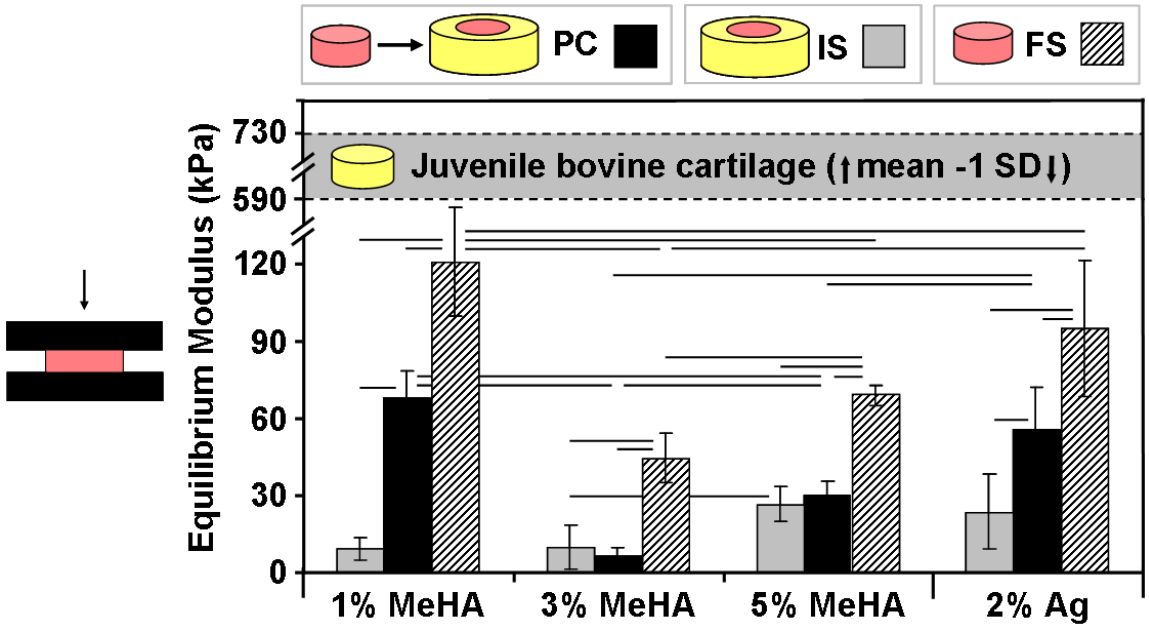


**Figure 7-4: Compressive properties of repair constructs were dependent on both hydrogel formulation and culture condition. IS repair construct properties (grey bars) were severely limited, while FS controls (hatched bars) attained the greatest equilibrium modulus. PC (black bars) improved the compressive properties of the hydrogel repair constructs for 1% MeHA and Ag, but did not match FS controls. (n=4-5/group/timepoint; lines indicate $p<0.05$)**

Compressive properties of the inner core from IS and PC repaired constructs were evaluated after measurement of the integration strength. Strikingly, the equilibrium modulus of FS 1% MeHA reached 120 kPa by 8 weeks, while 8 weeks of IS repair with the same MeHA concentration resulted in a modulus of only 9 kPa (**Figure 7-4**; $p<0.05$). Similarly, IS culture resulted in reductions of equilibrium modulus of at least 50% for each additional hydrogel formulation ($p<0.05$). The modulus of 1% MeHA PC constructs reached 68 kPa , a value that was ~60% of FS controls and more than 7 times greater than IS constructs ($p<0.001$). Likewise, Ag constructs achieved a modulus of 56 kPa for PC compared to 24 kPa for IS at 8 weeks ($p=0.001$). The modulus of both 3% (7 kPa) and 5% (30 kPa) PC MeHA controls was not statistically different than the IS values.

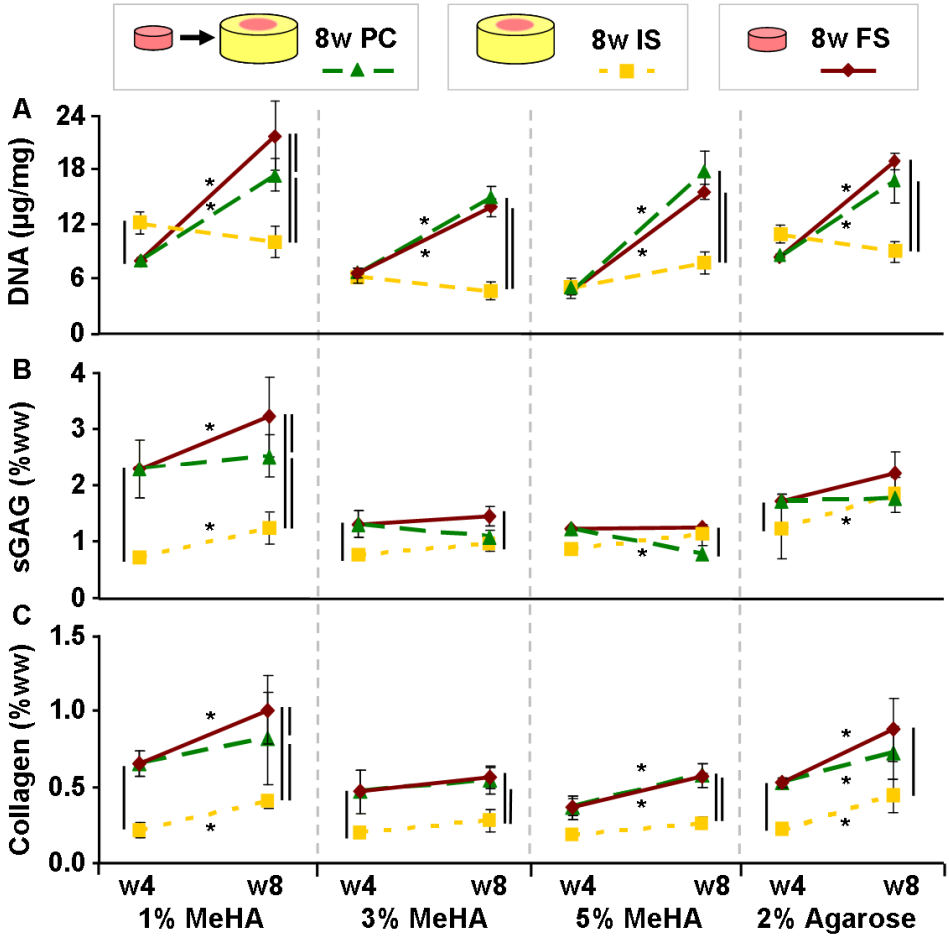


**Figure 7-5: Biochemical content was dependent on hydrogel formulation and culture conditions. sGAG content (A) in 1% MeHA increased significantly in both FS and PC conditions compared to IS repair. IS repair similarly limited collagen accumulation (B) for every MeHA concentration and Ag. DNA content (C) generally increased from week 4 to 8 for PC and FS hydrogels, while DNA content in IS groups did not significantly change. (n=4-5/group/timepoint; lines indicate $p < 0.05$)**

7.3.3. Biochemical Content

Trends in biochemical content followed the measured compressive properties of repair constructs. For example, sGAG content in FS 1% MeHA constructs after 8 weeks (3.2% w/w) was ~25% greater than in PC (2.5%) and ~3 fold greater than in IS (1.2%) constructs ($p<0.05$; **Figure 7-5B**). The sGAG content in 3% and 5% MeHA hydrogels (in all conditions) reached ~1% of wet weight after 4 weeks and did not increase with an additional 4 weeks of culture. sGAG content in Ag FS, PC, and IS constructs reached

~2% of wet weight at 8 weeks, independent of repair condition. The highest level of sGAG in PC constructs was observed in 1% MeHA (2.5%), ~2-3 fold greater than sGAG in the other MeHA-based PC repair groups ($p<0.001$; **Figure 7-5B**).

Collagen content in 1% MeHA constructs mirrored patterns observed for sGAG, with IS constructs containing less than half that of FS or PC constructs (**Figure 7-5C**). While collagen increased through 8 weeks in both 1% MeHA FS ($p<0.001$) and PC ($p=0.062$) constructs, PC constructs contained ~25% less collagen at week 8 ($p=0.029$). While IS collagen levels were equivalent for all MeHA macromer densities, collagen in FS and PC constructs was uniformly greater in 1% MeHA than in either 3% or 5% MeHA ($p<0.05$). Regardless of hydrogel formulation, IS cultured constructs contained less than 50% of the collagen in FS and PC constructs ($p<0.05$). Similarly, collagen in the Ag IS constructs at 8 weeks was 50% of the PC construct levels, while collagen in FS constructs was ~20% higher than in PC constructs ($p=0.144$; **Figure 7-5C**).

DNA content in IS repaired constructs was stable from 4 to 8 weeks of culture ($p>0.05$; **Figure 7-5A**). Conversely, DNA in FS and PC constructs increased ~2 fold ($p<0.005$) during the final 4 week period.

### 7.3.4. Histological Analysis

Histological staining confirmed the quantitative biochemical findings for collagen content (**Figure 7-6**). Picrosirius red staining of collagen was most intense in FS constructs, with slightly less staining in PC constructs, and much less staining in the IS

repaired groups. The interface between the hydrogel and cartilage showed close apposition in all cases with visible collagen deposition at the interface. Collagen in 3% and 5% MeHA constructs was present in isolated accumulations, consistent with the limited matrix distribution previously observed in these higher macromer density gels (see Chapter 4).

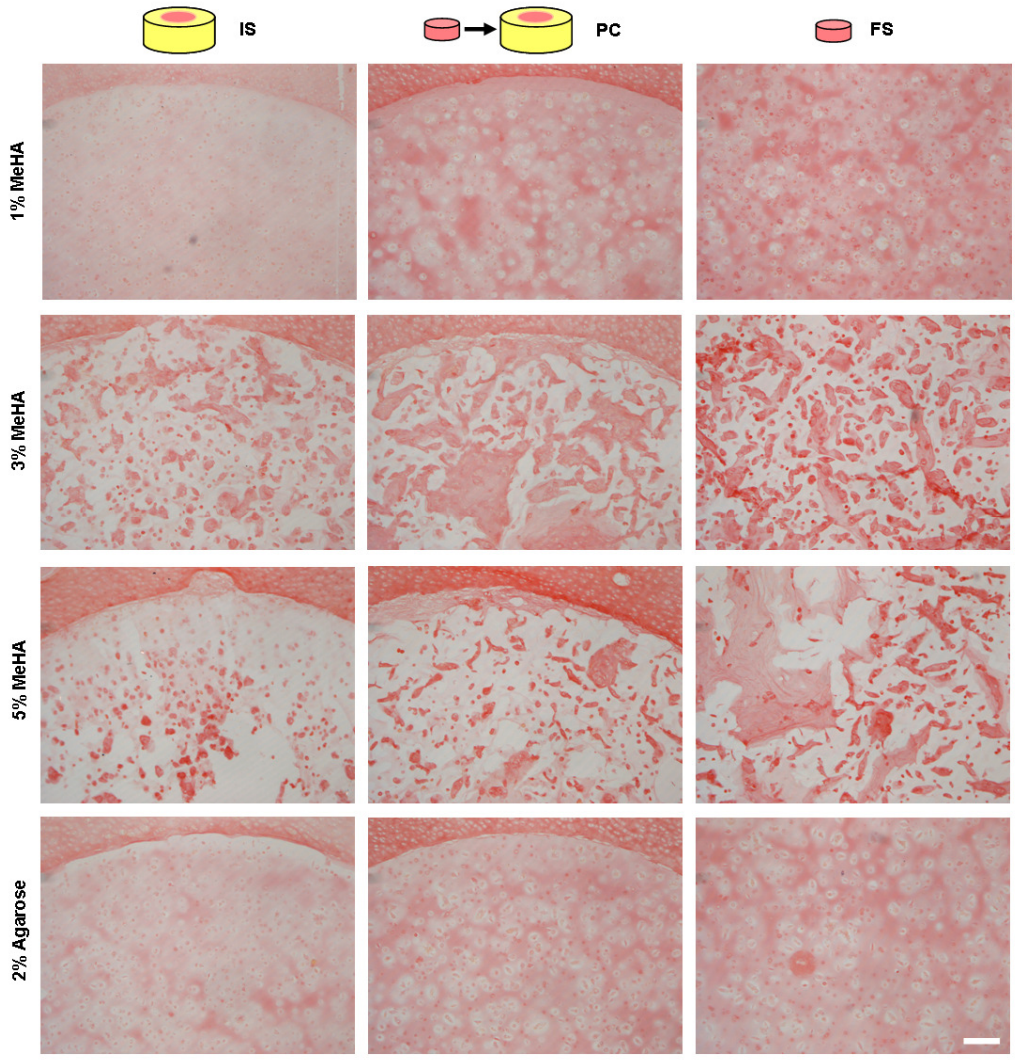


**Figure 7-6: Picrosirius red staining of collagen shows that IS repair limits construct maturation, while increased collagen density was observed in PC and FS constructs. Isolated aggregates of collagen were observed within 3% and 5% MeHA constructs from all experimental groups. (100X original magnification; scale bar = 250 µm)**

## 7.4. Discussion

The functional repair of focal cartilage defects requires the restoration of mechanical function coupled with complete integration between the tissue engineered cartilage and adjacent host cartilage. While tissue engineered cartilage constructs with native compressive properties have been generated, quantitative analysis of the integrative potential of these constructs remains to be demonstrated. We have shown the potential for *in vitro* MSC-based cartilage development with photo-crosslinkable HA hydrogels, but had yet to analyze its capacity for integrative repair. One general concern with constructs that are matured *in vitro* is whether they are capable of integrating to host cartilage. Therefore, the two objectives of the present study were to 1) evaluate the integrative capacity of methacrylated HA hydrogels and 2) to determine the effect of *in vitro* pre-culture (PC) on the integration of tissue engineered cartilage to native cartilage.

The initial selection of HA hydrogels was based on its natural presence in cartilage, capacity for IS polymerization to fill irregularly shaped defects, overall biocompatibility, and *in vivo* degradation. In Chapter 4 it was demonstrated that lower macromer density formulations led to increased compressive properties, however, it was also observed that higher macromer density HA increased dimensional stability (Chung *et al*. 2009), an important factor for the IS formation of hydrogel constructs for cartilage repair. The results from the present study indicate that IS polymerized 1% MeHA remained stable (**Figure 7-2**) and reached integration strengths greater than either of the higher macromer density formulations (**Figure 7-3**). Quantification of matrix accumulation showed that the improved integration in IS 1% MeHA may be a result of the simultaneous increase in

both sGAG and collagen with time, where matrix content in IS 3% and 5% MeHA did not increase (**Figure 7-5B-C**). While integration strength paralleled accumulation of matrix constituents, compressive properties did not develop in either MeHA or Ag hydrogels when used for IS repair.

Given the poor maturation of IS constructs (compared to FS controls), constructs were next allowed a period of PC to mature before being press fit in the cartilage explant repair model. μCT imaging showed a good fit without gapping between tissue engineered and adjacent cartilage (**Figure 7-2**). The integration strength of PC repaired constructs was equal to or better than that of the IS repair groups and the equilibrium modulus of the tissue engineered cartilage from the PC repairs was significantly greater for 1% MeHA and Ag (**Figure 7-3; Figure 7-4**). An initial period of construct maturation resulted in repairs that approached C-C control integration strength while also attaining mechanical properties that were closer to native tissue levels (**Figure 7-7**).

The reduction in equilibrium modulus that was observed in the IS repaired defects may be due to limited nutrient and chondrogenic factor diffusion as compared to those constructs pre-cultured in free-swelling conditions. However, the *in vitro* culture environment of the IS groups more closely mimics the *in vivo* scenario in that the route for diffusion of nutrients and waste is limited to the top of the repair hydrogel. Despite tripling the medium volume with thrice-weekly changes, nutrients may also have been limited by competitive consumption from the adjacent explant cartilage itself. Hunter *et al* suggested that soluble factors from live cartilage explants may limit the IS maturation

of cartilage constructs, concluding that the implantation of mature constructs would result in the best outcomes (Hunter and Levenston 2004). Conversely, Bian *et al* recently showed that a small fraction of chondrocytes co-encapsulated with MSCs could increase differentiation substantially, but had no positive effect when cultured in adjacent gels (Bian *et al*. 2011). These challenges to the undifferentiated MSCs in various hydrogel formulations may help explain lower equilibrium modulus, DNA, sGAG, and collagen content in IS repaired defects compared to PC groups. The constructs used for the PC repairs were maintained for 4 weeks in optimal growth conditions without any conflicting factors released from the adjacent cartilage. This favorable PC period allowed for chondrogenic differentiation and the accumulation of cartilage matrix constituents that persisted (or increased) with 4 additional weeks of culture within the cartilage defect.

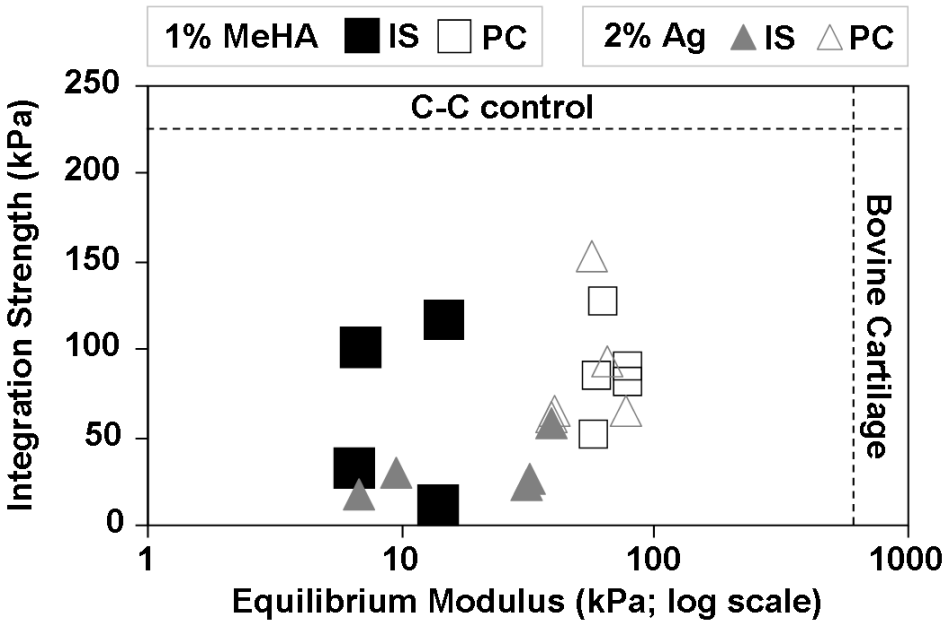


**Figure 7-7: Integration strength vs. equilibrium modulus (log scale) for 1% MeHA and Ag (IS and PC) constructs compared to C-C integration control and equilibrium modulus of juvenile bovine cartilage (see Chapter 9). Functional cartilage repair requires both stable lateral integration and restoration of compressive properties in the defect. The PC repairs for both hydrogels approached C-C repairs for integration compared to IS, though significant progress remains in matching native tissue mechanics.**

In contrast to our findings, Obradovic *et al* reported that repair with immature (5 day PC) chondrocyte seeded polyglycolic acid (PGA) constructs led to greater integration strength when compared to repair with more mature (5 week PC) constructs (Obradovic *et al*. 2001). In addition to using a different scaffold (fibrous PGA mesh) that may promote cell migration into or out of the material, they also utilized a rotating wall bioreactor, which could limit the effects of nutrient diffusion, competitive consumption, and even soluble factors that may have influenced the outcome of the present study. Also, unlike their use of chondrocytes, we used MSCs that undergo differentiation during the PC period. While this study presented a different conclusion on the effects of PC, the increased integration strength of the immature constructs paralleled higher rates of sGAG and collagen accumulation, which was a key finding of the current work. Our observations are supported by Dimicco *et al* who demonstrated that integration is correlated with new collagen deposition (DiMicco and Sah 2001). Recent work by Vinardell *et al* encapsulated MSCs and chondrocytes in agarose to evaluate their potential for *in vitro* integration (Vinardell *et al*. 2009). In that study, sGAG and collagen accumulation was similarly limited with IS maturation, and the reported integration strength for their Ag IS repair group (22.7 kPa) was similar to the Ag IS results in this work (31 kPa).

In order to address our limited understanding of the effects of the IS repair environment on cartilage repair with MSC-laden MeHA, future work will consider repair and co-culture within live and devitalized cartilage as well as co-culture models where chondrocytes and MSCs are in the same gel (Bian *et al*. 2011). Further, while the

observed integration demonstrates the potential for successful repair, the *in vitro* model used here lacks the physical demands of the joint; loading may influence the formation of a stable integrated repair or disrupt a repair interface with insufficient durability. Cyclic deformation of repaired defects *in vitro* could offer new insights into integrative repair durability and the necessary restrictions on post-operative joint motion before the resumption of normal activities. Long-term dynamic compressive loading could also be used to overcome diffusional limitations in IS (and PC) repair by enhancing the diffusion of nutrients and soluble factors (Mauck *et al*. 2003; Albro *et al*. 2008). Continuous loading could further improve the chondrogenic differentiation of MSCs and subsequent maturation of the repair construct (Hunter and Levenston 2002; Mauck *et al*. 2006; Huang *et al*. 2010).

While not addressed here, the use of tissue adhesives and enzymatic degradation of interface surfaces can directly increase integration strength between tissue engineered and adjacent host cartilage (Silverman *et al*. 1999; Peretti *et al*. 2003; Wang *et al*. 2007). The integration strength of the best case in this study (PC 1% MeHA) neared C-C controls and the equilibrium modulus approached native properties (~25%). Future work to improve integration strength may utilize degrading enzymes or tissue adhesives. Additionally, while we have recently demonstrated that increasing the MSC cell density by 3-fold in 1% MeHA resulted in constructs with an equilibrium modulus of over 300 kPa (see Chapter 5), the effect of these higher cell densities on integration has not yet been explored. The increased synthetic activity that markedly increased mechanical properties in this preliminary work may also prove to enhance the integration strength.

Additionally, there may be a temporal component when it comes to pre-culture that is cell density related.

### 7.5. Conclusions

The IS polymerization of MSC-laden hydrogels resulted in a stable integrated repair interface, but addressed only one aspect of functional cartilage repair. Allowing a PC period for the pre-maturation of constructs improved both integration and the compressive properties of the tissue engineered cartilage used for *in vitro* cartilage repair. Future investigations to confirm the mechanism by which the IS environment inhibits construct maturation and the effects of joint motion on integration will lead to further advancements in functional cartilage repair.

# CHAPTER 8: Increasing the Functional Repair Potential of MSC-Seeded Hyaluronic Acid Hydrogel Constructs *In Vitro*

## 8.1. Introduction

The motivation for Chapter 7 was to investigate the repair potential of MSC-seeded MeHA hydrogels by analyzing the integration strength when gels were polymerized *in situ* or were allowed a period of pre-maturation or pre-culture. Two important conclusions come from Chapter 7. First, 1% MeHA is the most supportive formulation for not only the *in vitro* maturation of cartilage-like constructs (Chapters 4-5), but also for the *in vitro* integration of MSC-seeded constructs to adjacent cartilage. Secondly, we noted that allowing hydrogels a pre-culture period before implantation improved integration strength and the compressive properties of the repair construct. While the integration strengths reported in Chapter 7 were higher than previous reports for MSC-based constructs, they were still far below cartilage-to-cartilage controls and chondrocyte-based approaches, indicating there is considerable room to improve the potential for MSC-seeded MeHA for real functional cartilage repair.

Chapter 5 of this thesis determined that 1% MeHA formulations responded to high MSC density and dynamic culture with remarkable increases in functional maturation. Increasing MSC density within this *in vitro* model of repair is a feasible approach to increasing the synthesis of matrix components that are critical in bridging the integration interface, thereby increasing its strength. Furthermore, dynamic culture during the pre-culture phase may lead to accelerated growth, and repaired constructs in dynamic culture

may more closely replicate the dynamic joint environment compared to the static culture conditions previously employed. This study will combine both of these factors pertaining to the maturation of MSC-seeded MeHA constructs to maximize their *in vitro* repair potential.

While considering the compressive properties of a repair material and its integration within a cartilage defect already surpasses the extent to which *in vitro* repair has been studied in this particular model, it remains unclear what level of *in vitro* integration is sufficient to successfully repair articular cartilage *in vivo*. One important consideration is whether the repair interface between the engineered and native cartilage is durable, i.e. whether it will remain stably integrated under normal joint loading conditions. While crack propagation for cartilage-to-cartilage integration has been studied in a single lap test (Fierlbeck *et al*. 2006), no attempts have been made to study the effects of compressive loading on *in vitro* integration within an annular cartilage defect model. The results of such a study could determine the suitability of a repair strategy while offering additional insights into the necessary duration of a prescribed rehabilitation regimens to help protect newly implanted cartilage grafts.

One key tenet of functional cartilage repair is that implanted engineered cartilage perform the required functional role of distributing joint stresses in order to protect cartilage adjacent to a defect from being over loaded which can lead to unwanted degenerative events (Buckwalter and Lane 1997; Wu *et al*. 2002; Wyland *et al*. 2002). Just as the case with the durability of graft integration, this concept has yet to be studied *in vitro*. Some

may argue that graft durability and function are best studied *in vivo*, but orthotopic *in vivo* studies typically show histological images as the only evidence of integration and function without any quantitative analysis. On the other hand, *in vitro* tests are considerably less expensive while allowing for informative biomechanical testing to demonstrate functional repair.

The objective of this study was to enhance functional integration of MeHA constructs within an *in vitro* defect model by seeding them with MSCs at a high density and culturing under dynamic conditions to improve nutrient and growth factor transport. The durability will be assessed by quantifying the integration strength before and after the application of a prolonged period of cyclic compressive deformations. The ability for constructs to participate in load transmission within the *in vitro* defects will be determined by measuring the equilibrium modulus before and after the removal of the engineered, integrated material from the center of the defect.

## 8.2. Methods

### 8.2.1. MSC Isolation and Cartilage Defect Preparation

Juvenile bovine MSCs were isolated and expanded through passage 3 as described in Chapter 3. Cartilage cylinders were removed from juvenile bovine trochlear grooves and maintained in basal medium until 3 days before the implantation of pre-matured constructs when they were formed into annular constructs (see Chapter 7). Briefly, constructs were cut to ~2.25 mm in thickness and a 4 mm core was removed to create the defect (**Figure 8-1**).

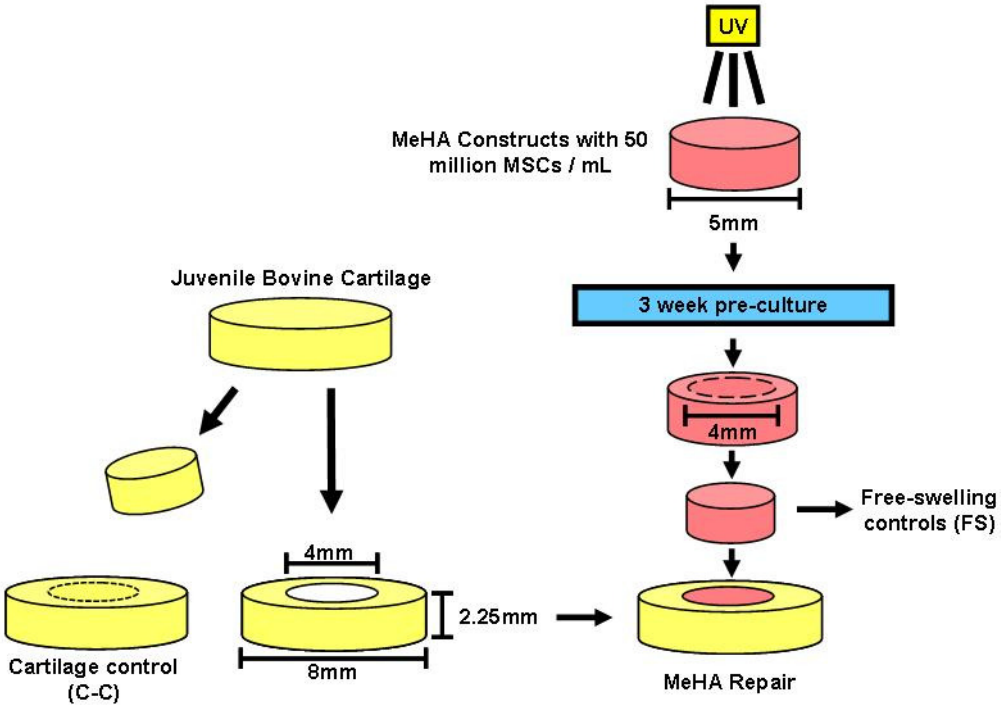


**Figure 8-1: Schematic of the preparation of in vitro cartilage defects, MeHA repaired defects, C-C repair defects, and FS control constructs.**

8.2.2. Defect Repair

Similar to the PC constructs in Chapter 7, MSCs were encapsulated within 1% MeHA at 50 million cells/mL, punched into 5 mm cylinders, and maintained for 3 weeks in chondrogenic medium with TGF-β3 (10 ng/μL) under dynamic culture conditions (orbital shaker; see Chapter 5). At the end of the PC or pre-maturation period, 5 mm constructs were punched to 4 mm, press-fit within the prepared defects (**Figure 8-1**), and the resulting repair composites were cultured dynamically for 6 weeks. Additional constructs underwent mechanical, biochemical, and histological analyses while the remaining gels were maintained in dynamic free-swelling culture for the duration of the 6 week study (FS controls). Cartilage-to-cartilage (C-C) controls were also created by restoring randomized cartilage cores back into cartilage defects (**Figure 8-1**).

8.2.3. Integration Testing and Durability

MeHA repaired and C-C constructs underwent push-out testing after 2 and 6 weeks to determine the integration strength of the repair interface (see Chapter 7). Additional constructs were first subjected to 7200 cycles of 10% deformation at 1 Hz (2 hrs) applied with an Instron material testing device and a custom indenter within a PBS bath.

8.2.4. Load Transmission Testing

To determine the contribution of the MeHA constructs to the distribution of load within a cartilage defect the equilibrium modulus was determined before and after the removal of the MeHA repair construct. Before testing, parallel top and bottom surfaces were created by sectioning with a freezing stage microtome. Stress relaxation tests were conducted consisting of two sequential ramps of 5% and 10% strain (0.05%/sec) that were applied with 20 minutes relaxation after each ramp. Data from the second ramp (5-15% deformation) were extracted and the equilibrium stress and strain values based on the measured construct dimensions. The integration strength was also determined when removing the repair material from the center of the defects. In addition to testing of the C-C controls, fresh cartilage cylinders were tested intact, after punching a 4 mm defect from the center, and after returning the cartilage to the center.

8.2.5. Compression Testing, Biochemistry, and Histology

Compression testing and biochemical analyses of FS controls and the repair material pushed-out of the composite constructs were conducted as described in Chapters 3-4.

Histological staining was performed as in Chapter 3 on FS controls, C-C, and MeHA repaired constructs to visualize the accumulation and distribution of cartilage matrix components in the context of *in vitro* repair.

### 8.2.6. Statistical Analysis

All statistical analyses were performed using SYSTAT (v13, San Jose, CA). Two-way ANOVA was used throughout with repair method (MeHA or C-C) and time as independent variables. A paired one-tailed student's t-test was also utilized to compare the equilibrium modulus of repaired defects to defects after push-out testing. Fisher's least significant difference *post hoc* test was used for each analysis of pair-wise comparisons with a threshold of $p<0.05$ assigned to distinguish significant differences.

## 8.3. Results

### 8.3.1. Integration Strength and Durability of *In Vitro* Repair

Pre-cultured high MSC density MeHA constructs (3 weeks) and cartilage plugs were stably implanted within cartilage rings. Significant integration was observed for the cartilage repaired constructs which reached 419 kPa after only 2 weeks of dynamic culture (**Figure 8-2A**). High MSC density MeHA integrated 22% better than C-C controls reaching 513 kPa after 2 weeks ($p=0.313$), but they did not significantly increase from 2 to 6 weeks (557 kPa; **Figure 8-2A**). C-C integration improved from 2 to 6 weeks ($p=0.01$) reaching 695 kPa, 25% greater than MeHA repaired constructs ($p=0.166$).

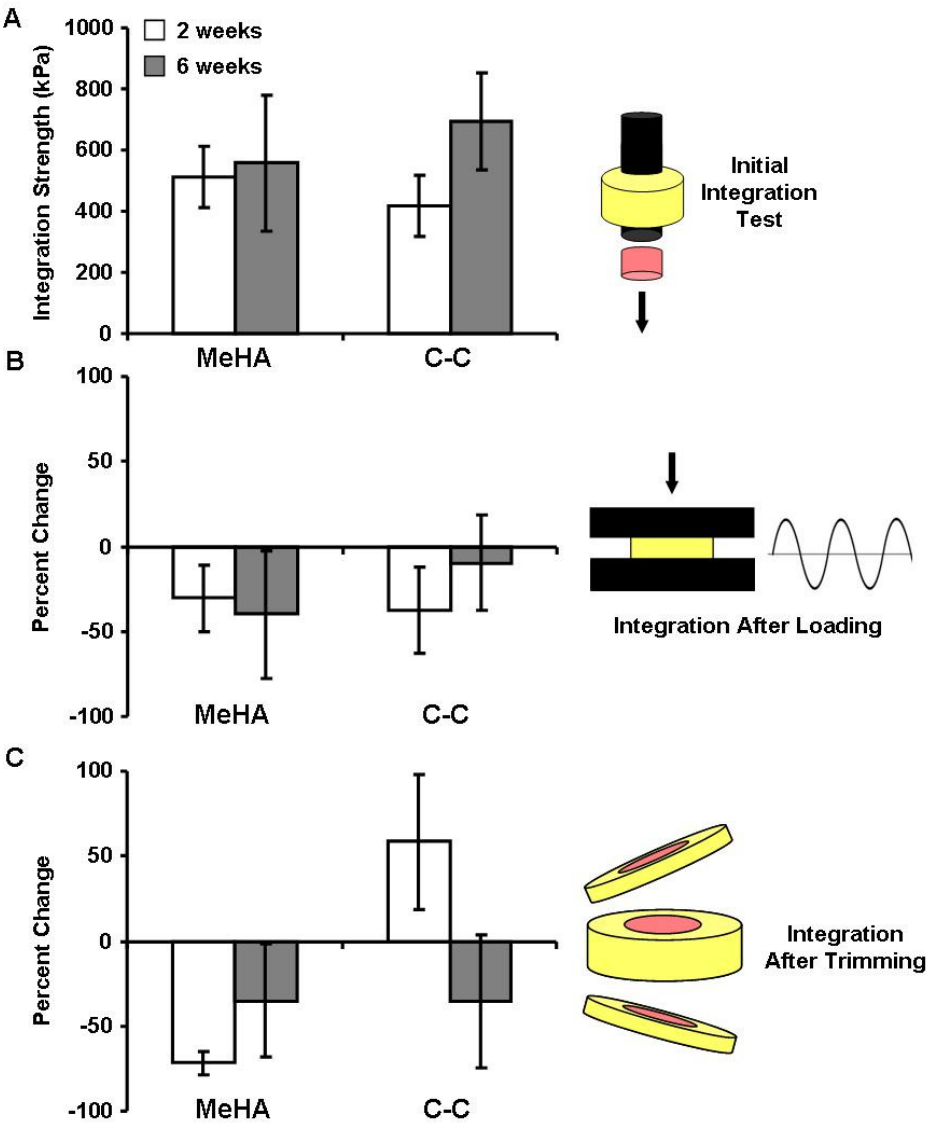


**Figure 8-2: (A) Integration strength of HA and cartilage (C-C) repaired defects after 2 and 6 weeks of chondrogenic culture (n=5-6). (B) The percent change in the integration strength of constructs after the application of 7200 cycles of 10% strain deformations compared to the mean integration strength of unperturbed constructs (n=5-6). (C) The percent change in integration strength was also determined for repaired constructs after removing both the top and bottom layer with a freezing stage microtome (n=4-6). (bars with associated p-values indicate statistically significant comparisons)**

The durability of *in vitro* repair was tested by applying 2 hours of cyclic deformation (10% strain) to MeHA and C-C repair constructs before comparing the integration strength to the untreated control. Overall, the decrease in integration strength resulting

from the prescribed loading scenario for both groups was between 30 and 40%, except for the C-C repair group at 6 weeks which only resulted in a 10% decrease (**Figure 8-2B**).

In order to determine the integration strength independent of any fibrous matrix formed on the outside of the repaired constructs, constructs from the load transmission study which had the top and bottom surfaces removed underwent push-out testing. The resulting comparison at 2 weeks showed a 72% decrease in integration for MeHA while the integration of the C-C group actually increased by 58% (**Figure 8-2C**). However, at 6 weeks the effect of sectioning was similar for both repair groups, where MeHA integration was reduced by 48% and integration of C-C repairs by 36% (**Figure 8-2C**).

### 8.3.2. Compressive Properties of MSC Seeded MeHA Constructs

The FS control constructs increased in equilibrium and dynamic modulus over a total of 9 weeks to attain 793 kPa and 4.7 MPa, respectively (**Figure 8-3A-B**). The *in situ* maturation of MeHA constructs after implantation was significantly reduced, reaching a mean equilibrium modulus of 157 kPa after 9 weeks (3 weeks in pre-culture + 6 weeks *in situ*) and a dynamic modulus of 1.4 MPa ($p<0.001$; **Figure 8-3A-B**).

### 8.3.3. Load Transmission in Repaired Defects

The equilibrium modulus of MeHA repaired defects significantly increased from 770 to 1501 kPa between 2 and 6 weeks ($p=0.001$) while defects repaired with cartilage plugs similarly increased from 518 to 1743 kPa ($p<0.001$; **Figure 8-4A**). The reduction in the

equilibrium modulus for MeHA and cartilage repaired defects after core removal ranged from 32% to 47% after both 2 and 6 weeks ($p<0.05$; **Figure 8-4B**). As an additional control, intact explant cartilage had an equilibrium modulus of 367 kPa that was reduced by ~20% by removing a 4 mm core from its center and a significant effect was still observed when the cartilage was returned to fill the defect ($p<0.05$; **Figure 8-5**).

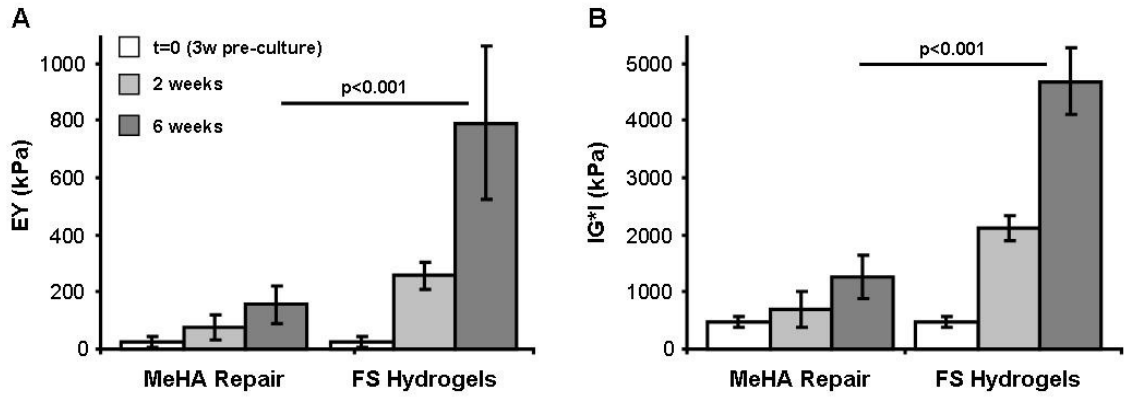


**Figure 8-3: (A) The unconfined equilibrium compressive modulus and (B) dynamic modulus of constructs maintained in free-swelling culture and constructs retrieved from repaired defects after push-out testing. (n=4-11; also included constructs from durability and load transmission tests; bars with associated p-values indicate statistically significant comparisons)**

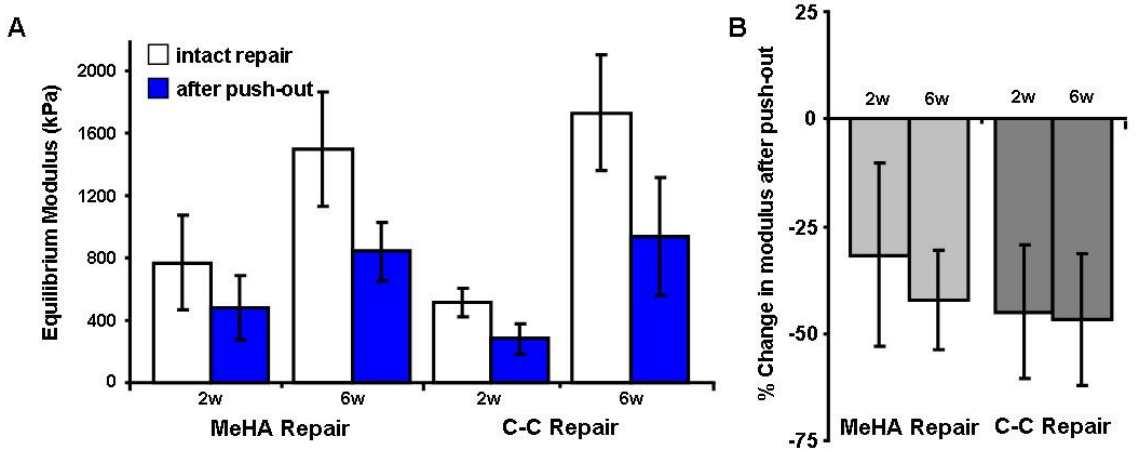


**Figure 8-4: (A) The unconfined equilibrium compressive modulus before and after removal of repair material consisting of either MSC seeded HA hydrogels or cartilage plugs after 2 and 6 weeks of chondrogenic culture (n=5-6). (B) The percent change in equilibrium modulus as a result of removing the center of repaired constructs.**

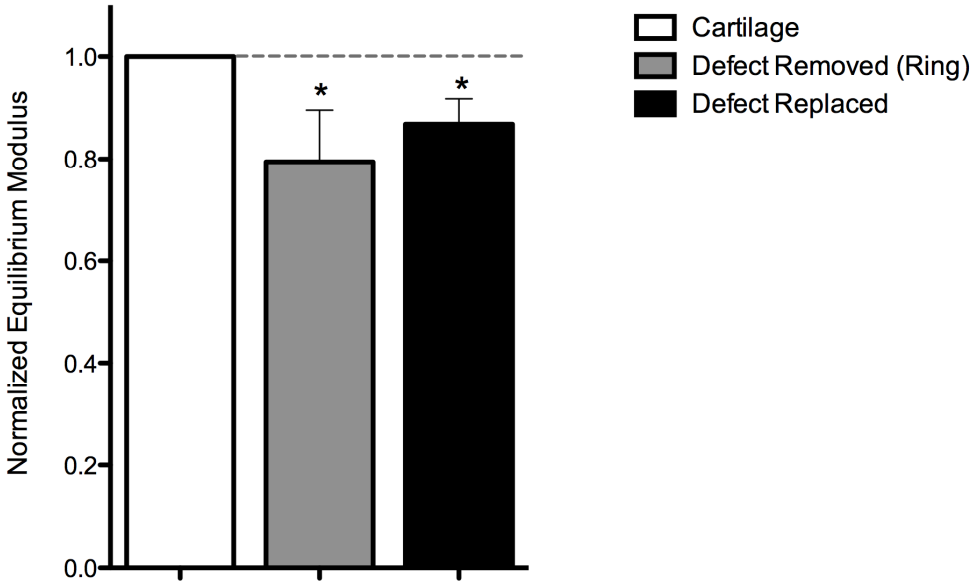


**Figure 8-5: Equilibrium modulus of intact explant cartilage before and after the creation of a 4 mm concentric defect (normalized to intact modulus). To demonstrate the effect of the biopsy incision alone, the removed cartilage was replaced and the cartilage was tested again. (n=4-5; *p<0.05 vs intact cartilage)**

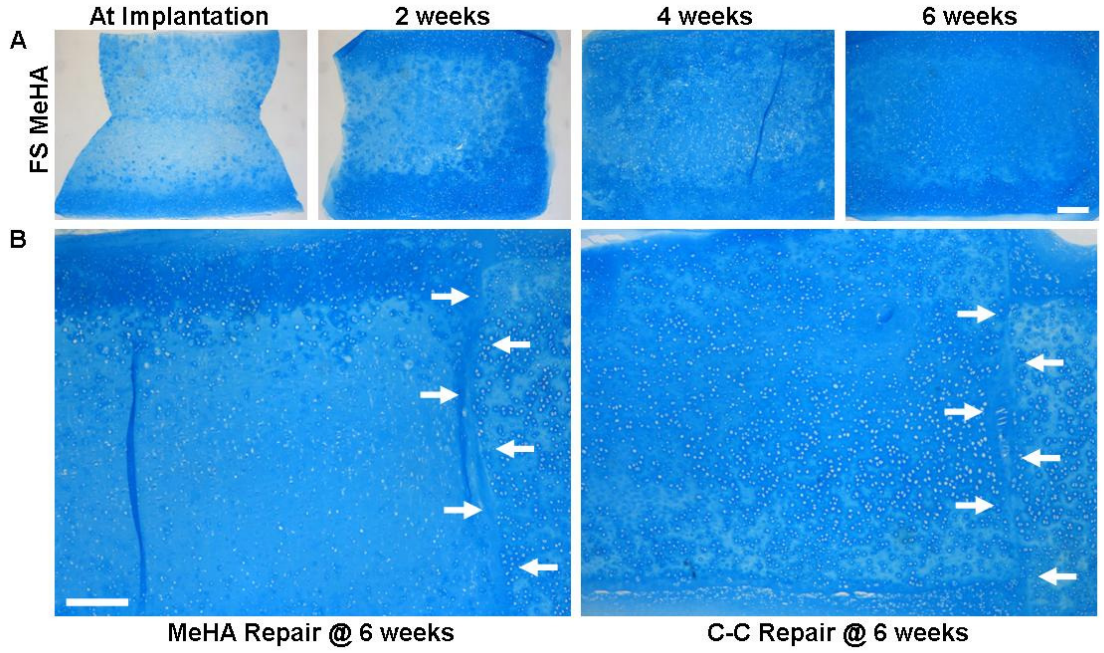


**Figure 8-6: (A) Proteoglycan staining of FS constructs at the time of implantation and after 2, 4, and 6 weeks of FS dynamic culture (25X magnification; scale bar = 0.5 mm). (B) Stained proteoglycan within MeHA and cartilage repaired constructs showing the interface (white arrows) between repair material and defect cartilage (25X magnification; scale bar = 0.5 mm).**

8.3.4. Histology

Proteoglycan staining showed a continual increase in accumulation with maturation, but matrix levels decreased towards the center region of the FS constructs (**Figure 8-6A**). The interface between MeHA and adjacent cartilage appeared continuous with heavy matrix accumulation (white arrows), but a more profound decrease in proteoglycan was observed towards the center of the MeHA constructs (**Figure 8-6B**). A stable interface was also evident in sections of C-C repair control constructs, but slight fissures or gaps were often seen (**Figure 8-6B**).

## 8.4. Discussion

Chapter 7 established the benefit of an initial period of construct maturation before implantation as a means to improve integration strength and the functional properties of engineered cartilage for *in vitro* repair, however, the integration strength only reached 87 kPa (~39% of C-C levels) and the equilibrium modulus only 68 kPa (~20% of native levels). Utilizing high MSC density (50 million/mL) and dynamic culture (orbital shaker) resulted in MeHA-cartilage integration of 513 kPa in just 2 weeks after implantation (**Figure 8-2A**). This level of integration is nearly 6.5 fold greater than what was reported in Chapter 7 and nearly 25 times previously published reports of MSC-based integration (Vinardell *et al*. 2009). Indeed, this result bests all published reports of *in vitro* cartilage integration using chondrocytes, including work by Obradovic *et al* who seeded chondrocytes on polyglycolic acid scaffolds and implanted them within trypsin treated explants to obtain an integration strength of 375 kPa after 8 weeks (Obradovic *et al*.

2001). One published investigation of *in vivo* cartilage-cartilage integration within a subcutaneous mouse model reported values of 840 kPa and 1320 kPa using hyaluronidase and collagenase enzyme treatments, but one criticism of this work was that the fibrous encapsulation was left intact for push-out testing (van de Breevaart Bravenboer *et al*. 2004). Our constructs maintained integration strengths of over 360 kPa even after removal of the top and bottom layers and a stress-relaxation test preceding push-out analysis.

The *in vitro* durability of integrative repair has not previously been examined, therefore no comparisons can be made to the literature. MeHA repaired constructs were subjected to a rather strenuous 2 hour period of cyclic loading which resulted in a 40% reduction in the integration strength, but this reduction was not statistically significant. The integration did not fail catastrophically and remained at 333 kPa, a significant level compared to published reports. Durability testing reduced the integration of the C-C repair group by 36% at week 2, but only 10% at week 6. While this reduction was not statistically significant from the observed reduction in the MeHA repaired defects, it may still suggest that cartilage repaired defects are more suited to resist loading induced fissures at the repair interface.

Moretti *et al* demonstrated that matrix accumulated around the entire defect contributes significantly to the strength of cartilage integration (Moretti *et al*. 2005). To assess this effect in our system, constructs with their top and bottom sections removed were also tested for integration strength. It is important to note that in addition to sectioning of the

construct top and bottom, these constructs were also subjected to two freeze/thaw cycles and a stress relaxation test reaching a peak strain of 15% before integration testing was performed. As a result, 2 week MeHA construct integration was reduced by 72% while C-C integration increased by 58% (**Figure 8-2B**). The histological findings may help interpret this result, where the central regions of implanted MeHA constructs accumulated matrix at a much slower rate than more exterior regions (**Figure 8-6B**). The removal of these exterior regions would mean that the integration strength would solely rely on the interface between the cartilage and the less developed central region. In the case of the C-C repair defects, the middle region is mature cartilage and appeared to contribute more to the integration than the top and bottom regions. This may be in part due to increased congruence or a tighter fit in the center than towards the edges of the interface. Also, synthesized matrix may be more likely to be accumulated in the central rather than exterior regions of the interface. While this early effect may remain a phenomenon, by 6 weeks both MeHA and C-C behaved similarly with a reduction in integration of 48% and 36%, respectively. As the MeHA constructs matured *in situ*, it appeared that the center region began to contribute more to the integration strength than was observed at 2 weeks, while the opposite was true for the C-C repair defect.

Another crucial aspect of functional cartilage repair is the compressive strength of the repair material. Increased seeding density and orbital shaking were applied to help foster construct maturation which did cause MeHA constructs to develop increased equilibrium and dynamic properties *in situ* (**Figure 8-3A-B**). While the properties of FS controls were about 5 fold greater (793 kPa) than the repair constructs ($p<0.001$), they did improve

from 25 kPa upon implantation to 157 kPa after 6 weeks, which is within 50% of the lower limit of native cartilage values. As previously described, construct maturation *in situ* was heterogeneous, resulting in exterior regions of dense matrix with decreased density in the central regions which may have created a fracture zone for some constructs (**Figure 8-7**). Nearly 50% of constructs showed some signs of fracture upon being pushed-out of cartilage defects and a large portion left fragments still fully attached to the wall of the cylindrical defects, indicating that the strength of integration may have exceeded the strength of some constructs. Constructs that were obviously fractured were not tested in compression (**Figure 8-7**), but the possibility remains that visibly intact samples tested in compression contained less visible fractures that would have a significant effect on the determination of equilibrium and dynamic properties. This certainly would not account for the entire difference between the FS and repair constructs, but may offer some explanation as to why the modulus data indicated that development appeared to plateau at 4 weeks.

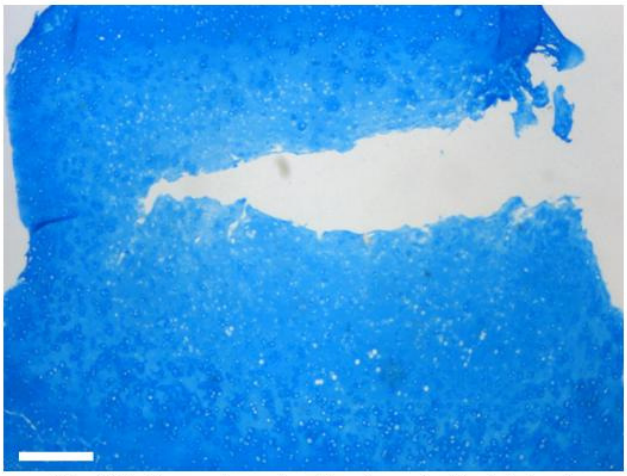


**Figure 8-7: Proteoglycan stained section of MeHA construct retrieved after 6 week push-out testing shows hydrogel fracture through the less developed center region (alcian blue; 25X magnification; scale bar = 0.5 mm).**

To determine the functional consequence of MSC-MeHA repair in the context of the surrounding cartilage, the equilibrium modulus of the repaired defects was determined before and after removal of the repair tissue. The modulus of MSC-MeHA repaired constructs at 6 weeks was similar to the modulus of defects filled with mature cartilage tissue, a technique that represents the clinical procedure of osteochondral grafting. The modulus of the empty rings after MeHA or cartilage plug removal was the same (change in cross-sectional area was accounted for), indicating that the contribution of the cartilage defect itself was comparable for both repair groups. There was a significant reduction in modulus as a result of removing the MeHA or cartilage from the defect center (32-47%; **Figure 8-4B**), which implies that the repair tissue was contributing to the mechanical properties. When intact cylinders were tested before and after creating a 4 mm defect, a smaller but still significant decrease in modulus was also observed (20%; **Figure 8-5**). The larger difference observed in the repair study could be explained by the superphysiologic cartilage growth that occurred, where the observed differences in mechanical properties of the explant cartilage and the repaired defects ($E_Y$ of TGF-β3 cultured defects- 1500 kPA; $E_Y$ of explant cartilage- 350 kPa) may have led to a steeper decline in compressive properties as a result of removing the defect center. Alternatively, the repair material (MeHA or cartilage) and the tissue formed at the repair interface may simply contribute more to the stress response of the entire construct than the center region of intact cartilage. Two key observations from this study arise: 1) it was demonstrated that focal defects diminish the mechanical function of adjacent cartilage and 2) MSC-

MeHA repair restores function within *in vitro* cartilage defects as well as repair with autologous cartilage.

### 8.5. Conclusions

The implementation of higher MSC density and dynamic culture for the repair of *in vitro* cartilage defects with MSC-seeded MeHA hydrogels resulted in greater integration than previous reports of MSC and chondrocyte-based approaches. While the compressive properties of MeHA constructs retrieved after push-out testing improved, they remained lower than native cartilage. Regardless, their functional performance as a composite with the cartilage defect matched that of repaired defects with mature cartilage, ushering this MSC-MeHA system towards pre-clinical testing in a large animal model.

# CHAPTER 9: Cartilage Matrix Formation by Bovine Mesenchymal Stem Cells in Three-Dimensional Culture is Age-Dependent

## 9.1. Introduction

One caveat to the research performed as part of this thesis is the use of healthy juvenile bovine chondrocytes and primarily mesenchymal stem cells (MSCs). It is important to understand the effects of cell age when conducting research on potential clinical applications that involve autologous cell transplantation. Cartilage tissue undergoes remarkable alterations in composition, organization, and mechanical properties with aging (Morrison *et al*. 1996; Williamson *et al*. 2001; Charlebois *et al*. 2004). Aging is implicated in various cartilage pathologies, including osteoarthritis that will affect a major portion of the population (Frankowski and Watkins-Castillo 2002). Short of total joint arthroplasty, current treatments for traumatic cartilage injury and disease include microfracture or osteochondral autografting only offer satisfactory short-term solutions without evidence of long-term function (Steadman *et al*. 2001; Detterline *et al*. 2005; Kleemann 2007). Autologous chondrocyte implantation (ACI) utilizes *in vitro* expanded chondrocytes for implantation into a defect, but this technique also fails to produce functional, integrated repairs (Micheli *et al*. 2001; Knutsen *et al*. 2004; Micheli *et al*. 2006).

One limitation of ACI is the age of available donor chondrocytes. The literature suggests lower proliferation rates, extracellular matrix (ECM) forming potential, and more senescence in aged human chondrocytes (Martin and Buckwalter 2001; Barbero *et al*.

2004; Giannoni *et al*. 2005). Similarly, aged bovine chondrocytes produce less cartilage ECM in 3D culture (Tran-Khanh *et al*. 2005), and adult canine chondrocytes generate functional grafts only when expanded in specialized media (Ng *et al*. 2010). Adkisson and coworkers noted that immature human chondrocytes in a scaffold-free system produced cartilage-like ECM superior to adult chondrocytes (Adkisson *et al*. 2001).

The evidence thus suggests that donor age limits the clinical potential of autologous chondrocytes and has motivated many groups to investigate the use of mesenchymal stem cells (MSCs). MSCs are a multipotent cell type found in bone marrow that can differentiate along osteogenic, chondrogenic, and adipogenic lineages (Baksh *et al*. 2004). Like chondrocytes, however, MSC properties also change with age; MSC density in bone marrow decreases and aged MSCs are slower to proliferate (Stolzing *et al*. 2008). Regardless, aged MSCs can produce functional repair tissue. Rabbit tendon injuries repaired with autologous MSCs from young or aged animals produced repair tissue with equivalent material properties (Dressler *et al*. 2005). Osteogenic and adipogenic MSC differentiation has been reported to be both independent of age (Stenderup *et al*. 2003; Roura *et al*. 2006; Tokalov *et al*. 2007) and dependent on age (Kretlow *et al*. 2008; Coipeau *et al*. 2009). For human MSC chondrogenesis, both age-dependent and age-independent findings have also been noted (Murphy *et al*. 2002; Scharstuhl *et al*. 2007; Payne *et al*. 2010). Recent findings showed a decline of potential in aged human male MSCs, but no decline in female MSCs (Payne *et al*. 2010). Another recent report on fetal and adult human MSCs showed similar adipogenic and osteogenic differentiation, but a small age-related decrease in cartilage ECM formation (Bernardo *et al*. 2007).

Although the literature demonstrates that aging effects MSC and chondrocyte function, no study has compared both cell types with increasing age in the bovine model system. Using the equine model, Kopesky and coworkers reported that adult MSCs in hydrogels form superior engineered tissue compared with juvenile MSCs and adult chondrocytes (Kopesky *et al*. 2010). Conversely, in Chapter 3 we show that juvenile bovine MSCs are inferior to donor-matched chondrocytes in various hydrogels (Mauck *et al*. 2006; Huang *et al*. 2008; Huang *et al*. 2010), but have not considered MSC age in our HA hydrogel system.

The objective of this study was to confirm age-related changes in native cartilage and determine the effects of aging on bovine MSCs and chondrocytes in 3D pellet and hydrogel culture. Specifically, we sought to 1) confirm age-related changes in bovine cartilage, to establish how pellet chondrogenesis changes with age for 2) chondrocytes, and 3) MSCs. 4) Lastly, age-related differences in MSC chondrogenesis within a clinically relevant hydrogel context were investigated.

## 9.2. Methods

### 9.2.1. Aging and Articular Cartilage

To analyze developmental differences in bovine cartilage with age, trochlear groove cartilage from fetal, juvenile, and skeletally mature (adult) stifle joints was analyzed for biochemical content (n=3-5 per donor), biomechanical properties (n=3-5 per donor), and histology (**Figure 9-1A**). This study was repeated three times. Cartilage samples were

harvested and sectioned with a freezing stage microtome to obtain ~1 mm thick x 4 mm diameter samples for mechanical testing. After testing, samples were analyzed for DNA, sulfated glycosaminoglycan (GAG), and collagen content. Histologic staining for proteoglycans and collagens was performed, and split-line directions evaluated across each joint and at each age.

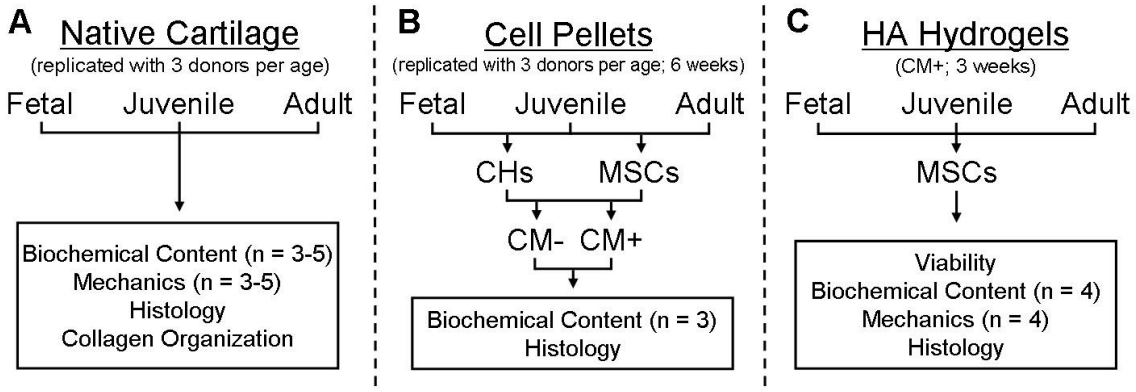


**Figure 9-1: Experimental groups for analysis of fetal, juvenile, and adult native cartilage (A), pellet study of chondrocytes (CHs) and mesenchymal stem cells (MSCs) of fetal, juvenile, and adult origin cultured for 6 weeks in chondrogenic medium with (CM+) and without (CM-) TGF-β3 (B), and the investigation of MSCs within a 3D hyaluronic acid (HA) hydrogel context (C).**

9.2.2. Aged MSCs and Chondrocytes in Pellet Culture

Chondrocytes (primary) and MSCs (expanded) from fetal, juvenile, and adult bovine donors (three donors per age) were isolated, formed into cell-rich pellets (250,000 per pellet), and cultured up to 6 weeks in chondrogenic medium with (CM+) or without (CM-) the chondrogenic induction factor transforming growth factor-β3 (TGF-β3) (Mauck *et al*. 2006) (**Figure 9-1B**). Biochemical assays for DNA, GAG, and collagen content in each pellet were performed (n = 3 per donor), and histological analysis of proteoglycans and collagens as in Chapter 4.

### 9.2.3. Aged MSCs in 3D HA Hydrogels

Bone marrow-derived MSCs from fetal, juvenile, and adult bovine donors (three donors per age) were encapsulated in a photo-crosslinked HA hydrogel (see Chapter 3) and cultured for 3 weeks in chondrogenic medium with TGF-β3 (**Figure 9-1C**). Analyses of cell viability, mechanical testing, and biochemical content were all performed as described in Chapter 4. A histological analysis of proteoglycan and collagen accumulation and distribution was also conducted.

### 9.2.4. Cell and Cartilage Isolation

Fetal (second or third trimester; JBS, Souderton, PA), juvenile (3-6 months; Research 87, Boylston, MA), and adult bovine limbs (2-3 years; Animal Technologies, Tyler, TX) were acquired within 24 hours of slaughter. MSCs from three donors of each age were isolated from tibial or femoral bone marrow extractions by plastic adherence (Mauck *et al*. 2006) and maintained separately in growth medium consisting of DMEM with 10% fetal bovine serum (Invitrogen, Carlsbad, CA) and 1% penicillin-streptomycin-fungizone through Passage 2 or 3. Diced, full-thickness articular cartilage from three donors of each age group was enzymatically digested to release the chondrocytes which were used without passaging (Mauck *et al*. 2006).

### 9.2.5. Split-Line Analysis of Collagen Orientation

Split-line direction was evaluated across fetal and juvenile stifle joints. A round 1.25 mm diameter needle was dipped in India ink and inserted perpendicular to the cartilage surface to the level of the subchondral bone. India ink was drawn into the formed gaps,

creating a clearly visible line. This process was repeated in a grid with 5 mm intervals across the joint surface.

### 9.2.6 Histology

Histologic analysis of cartilage, pellets, and hydrogels was performed. All samples were fixed in 4% paraformaldehyde. Cartilage and hydrogels were embedded in paraffin and sectioned to 8 μm while pellets were cryosectioned to 12 μm. Sections were then stained for proteoglycans with alcian blue (pH 1.0) and for collagen by picrosirius red (see Chapter 3).

### 9.2.7. Statistical Analysis

Cartilage and pellet data are reported as the mean ± SD of results for three donors of each age group (n = 3-4 samples per donor per assay). Hydrogel data is reported as the mean ± SD of four samples from each MSC donor age. We determined differences in biochemical content and mechanical properties between fetal, juvenile, and adult native cartilage using one-way analysis of variance (ANOVA). We determined differences in biochemical content between cell pellets with age (fetal, juvenile, and adult) and media supplementation (with and without TGF-β3) using a two-way ANOVA. We used SYSTAT 13 (Systat Software, Chicago, IL) for all analyses including the Fisher's least significant difference post hoc testing of pair-wise comparisons.

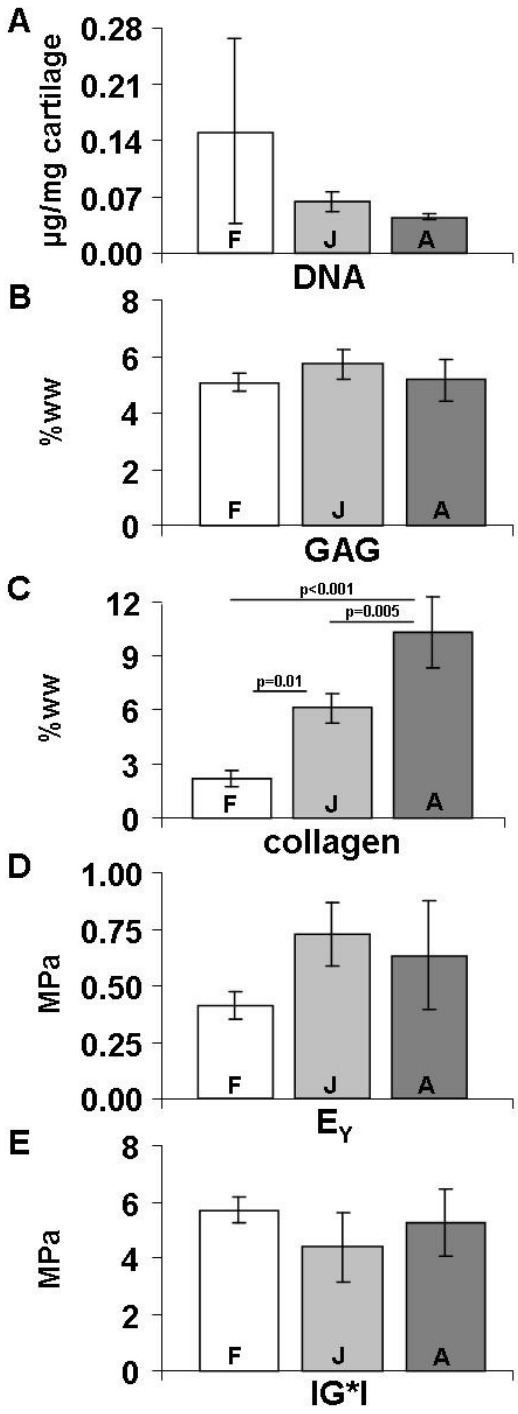


**Figure 9-2: DNA content (A) decreased as the donor age of bovine cartilage increased (F = fetal; J = juvenile; A = adult). Glycosaminoglycan (GAG) content (B) did not change with age, but collagen content (C) increased significantly. Cartilage equilibrium compressive modulus (D) increased slightly with age, whereas the dynamic modulus (E) was independent of age (three donors; n = 3-4 per donor.**

## 9.3. Results

### 9.3.1. Cartilage Composition and Structure Change with Age

Cell density, collagen content, organization, and equilibrium modulus within native cartilage were dependent on donor age. Fetal cartilage DNA content was two and four fold greater than juvenile and adult cartilage, respectively (**Figure 9-2A**). GAG content (per wet weight) ranged between 5% and 6% regardless of cartilage donor age (**Figure 9-2B**). Adult cartilage collagen content (10.3%) was two and four fold greater than juvenile ($p=0.005$) or fetal cartilage ($p<0.001$; **Figure 9-2C**). The compressive modulus of juvenile (0.73 MPa) and adult (0.64 MPa) cartilage was 50% to 75% higher than fetal (0.41 MPa) cartilage (**Figure 9-2D**). Histologic staining confirmed the level of biochemical constituents (**Figure 9-3**) and split-line analysis showed marked differences between fetal and juvenile cartilage with clearly demarcated split-line patterns in juvenile specimens, whereas fetal specimens lacked organization and directionality (**Figure 9-4**).

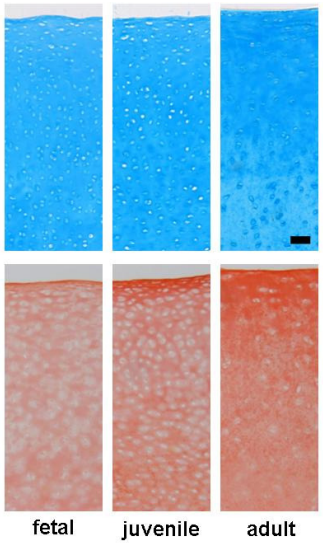


**Figure 9-3: Histologic staining of proteoglycans (top) and collagens (bottom) show age-related changes in proteoglycan and collagen content and localization while providing a visual confirmation of decreasing cellularity with age. Depth-dependent collagen organization increased with donor age (alcian blue and picrosirius red; 100X magnification; scale bar = 50 μm).**

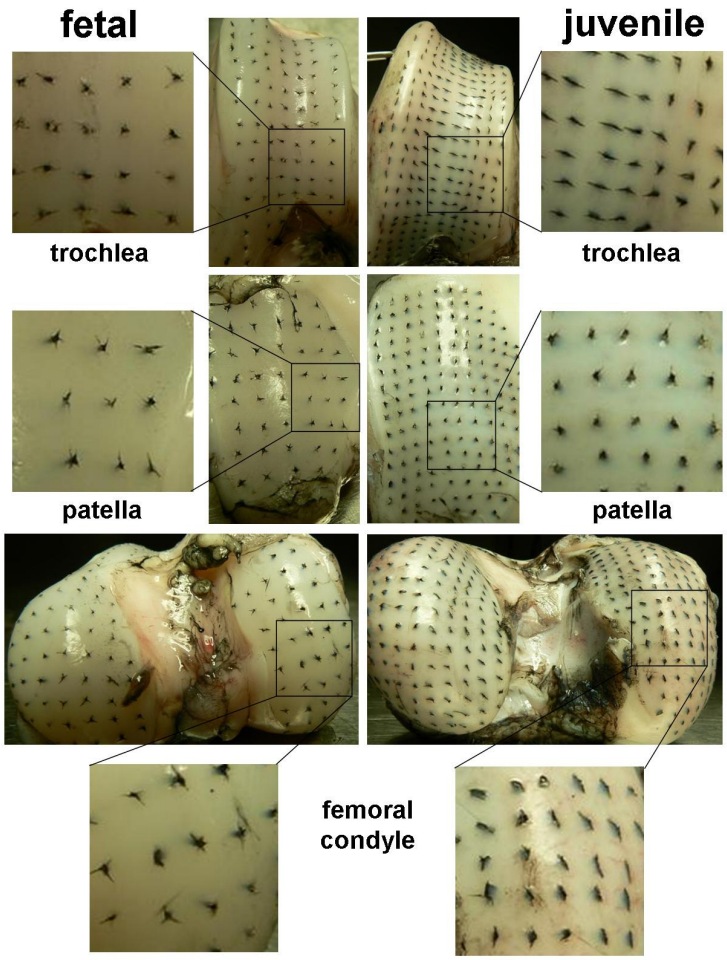


**Figure 9-4: Split-line analysis revealed prominent alignment of collagen fibers in juvenile articular cartilage (right). The star-shaped splitting pattern observed in fetal samples (left) indicated collagen in this immature cartilage is less organized.**

9.3.2. Age Affects MSC and Chondrocyte Matrix Formation in Pellets

The biochemical content in chondrocyte pellets depended on donor age and TGF-β3 supplementation. The DNA content in adult chondrocyte pellets cultured in CM+ for 6 weeks was ~two- and three-fold greater than in juvenile ($p<0.001$) or fetal ($p<0.001$) chondrocyte pellets (**Figure 9-5A**). The GAG levels in fetal chondrocyte pellets in CM+ were at least 50% less than either juvenile ($p=0.001$) or adult ($p=0.210$) pellets (**Figure 9-5B**). The collagen content in fetal chondrocyte pellets was greater than juvenile pellets ($p=0.034$) in CM+ and greater than both juvenile and adult pellets ($p<0.001$) in CM-

(**Figure 9-5C**). Interestingly, CM+ decreased GAG ($p=0.002$) and collagen ($p<0.001$) content of fetal chondrocyte pellets (**Figure 9-5B-C**).

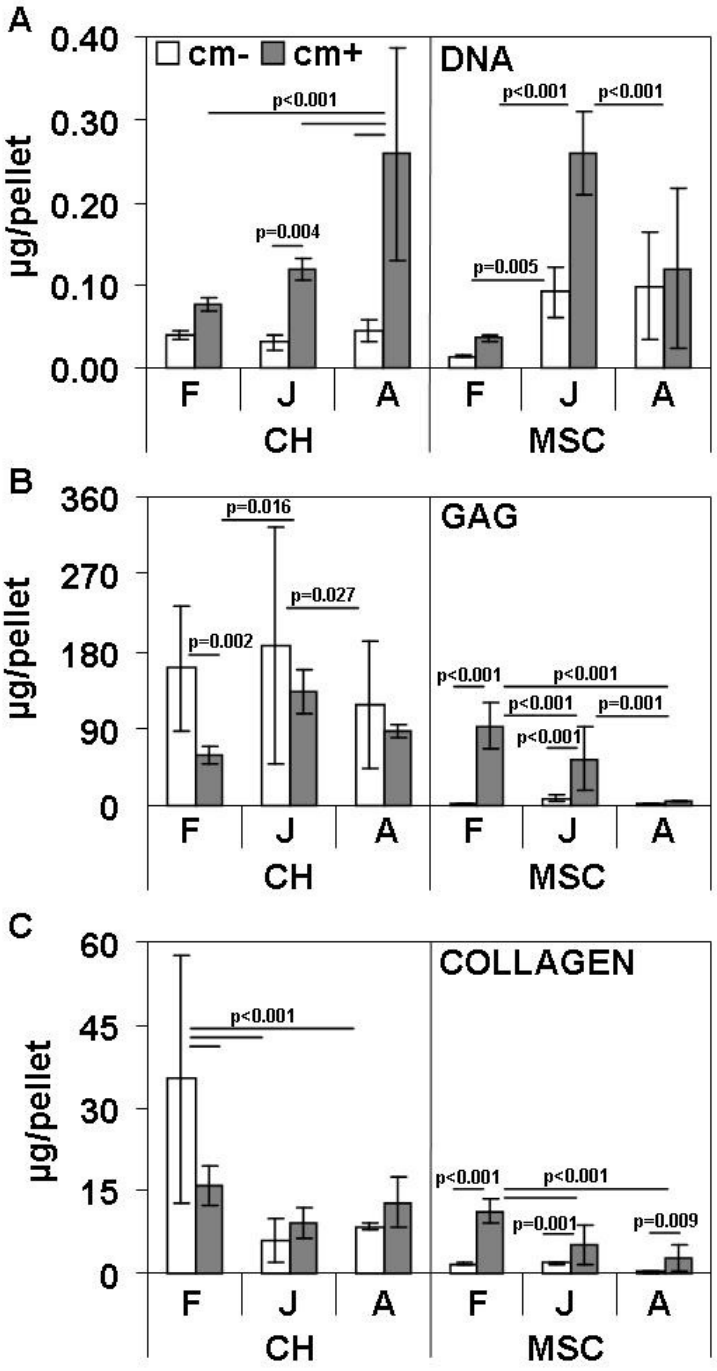


**Figure 9-5: DNA (A), glycosaminoglycan (GAG) (B), and collagen (C) content of mesenchymal stem cell and chondrocyte (CH) pellets from fetal (F), juvenile (J), and adult (A) bovine donors cultured in chondrogenic medium with (CM+) and without TGF-β3 (CM-). Data represent the mean ± SD for three donors per age and three pellet analyses per donor.**

The DNA content of MSC pellets increased with age while ECM levels decreased. The DNA content was generally higher in juvenile and adult pellets than in fetal pellets in CM- or CM+. For adult MSC pellets, CM+ did not alter DNA content ($p=0.485$), whereas CM+ increased fetal ($p=0.465$) and juvenile ($p<0.001$) MSC pellet DNA by ~3-fold. In CM-, MSCs produced very little GAG regardless of age. In CM+, MSCs from all age groups increased in GAG content with fetal MSCs accumulating two- and 15-fold higher levels than juvenile ($p=0.085$) or adult ($p<0.001$) MSCs, respectively. CM+ increased collagen content in MSC pellets for each age group with the greatest collagen accumulation in CM+ fetal pellets (**Figure 9-6**).

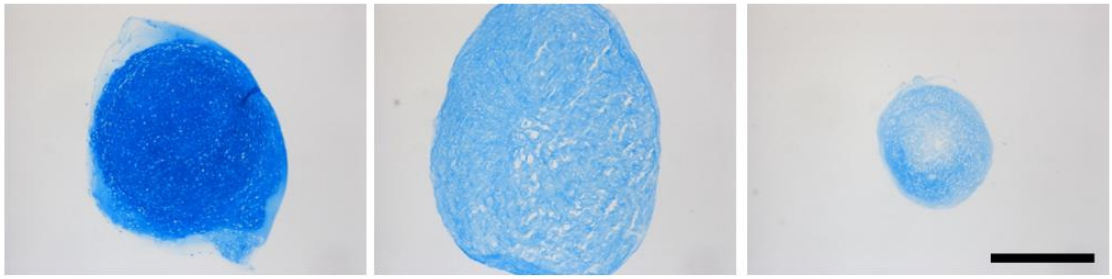


**Figure 9-6: Proteoglycan staining of fetal, juvenile, and adult mesenchymal stem cell (MSC) pellets cultured in chondrogenic medium with TGF-β3 (CM+) for 6 weeks. Fetal MSC pellets accrued more proteoglycan than juvenile pellets; adult MSCs formed the smallest pellets with the least amount of proteoglycan (alcian blue; 50X magnification; scale bar = 500 µm).**

### 9.3.3. Aging Affects MSC Chondrogenesis in HA Hydrogels

MSC chondrogenesis in 3D hydrogels was strongly dependent on donor age. After 3 weeks in CM+, DNA in fetal MSC-seeded gels increased by 48% ($p<0.001$), juvenile DNA changed very little (-15%; $p=0.377$), and adult DNA decreased (-35%; $p<0.001$; **Figure 9-7C**). The GAG content of both fetal and juvenile MSC-seeded constructs

reached approximately 3%, a level ~15-fold higher than adult MSC-laden gels ($p<0.001$; **Figure 9-8A**). Collagen content reached 0.20% in fetal and 0.28% in juvenile MSC-seeded constructs on Day 21, while adult MSC-seeded hydrogels contained ~10 times less collagen (0.03%; $p<0.001$; **Figure 9-8B**). The equilibrium and dynamic moduli of fetal and juvenile MSC hydrogels reached ~90 kPa and ~800 kPa, respectively (**Figure 9-8C-D**). The modulus of HA gels seeded with adult MSCs remained at acellular levels after 3 weeks, 15-fold less than fetal or juvenile MSC gels ($p<0.001$; **Figure 9-8D**).

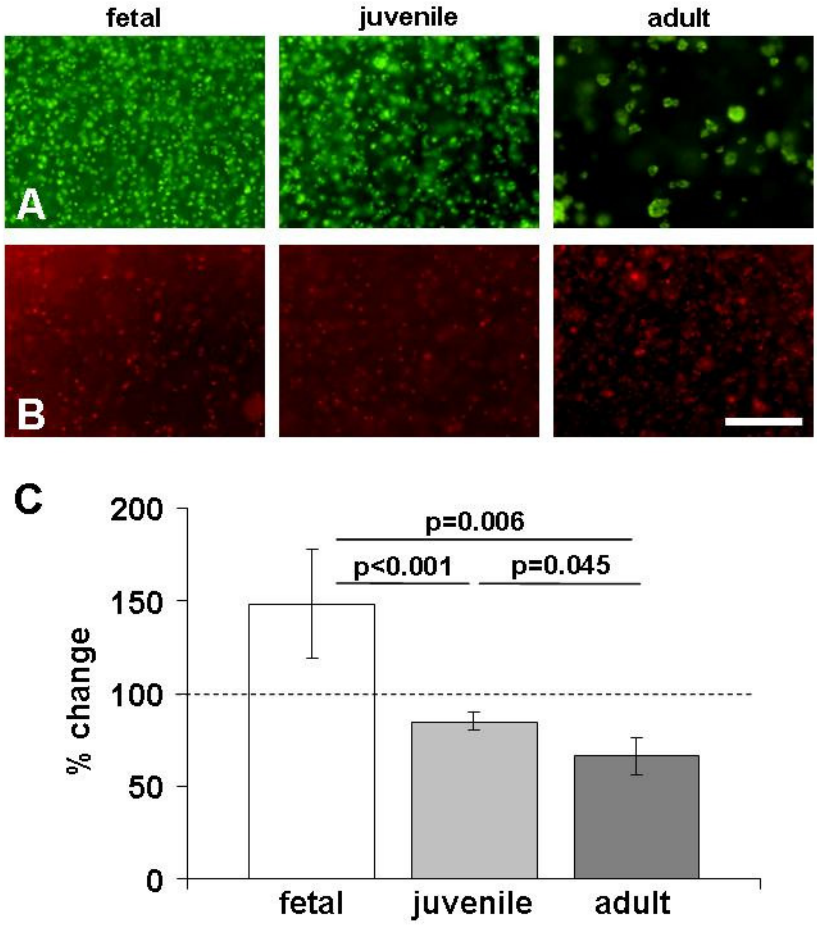


**Figure 9-7: Calcein AM labeling of viable MSCs in HA hydrogels (A) on Day 21 showed more cells in fetal MSC gels and a dramatic decline in viable cells for adult MSCs. Ethidium labeling (B) indicated a greater number of adult MSCs were nonviable compared with gels seeded with fetal or juvenile MSCs (100X magnification; scale bar = 250 μm). DNA content (C) on Day 21, normalized to initial DNA levels, showed fetal MSCs increased in number while adult MSC numbers declined significantly (n = 4; dashed line represents Day 0 levels).**

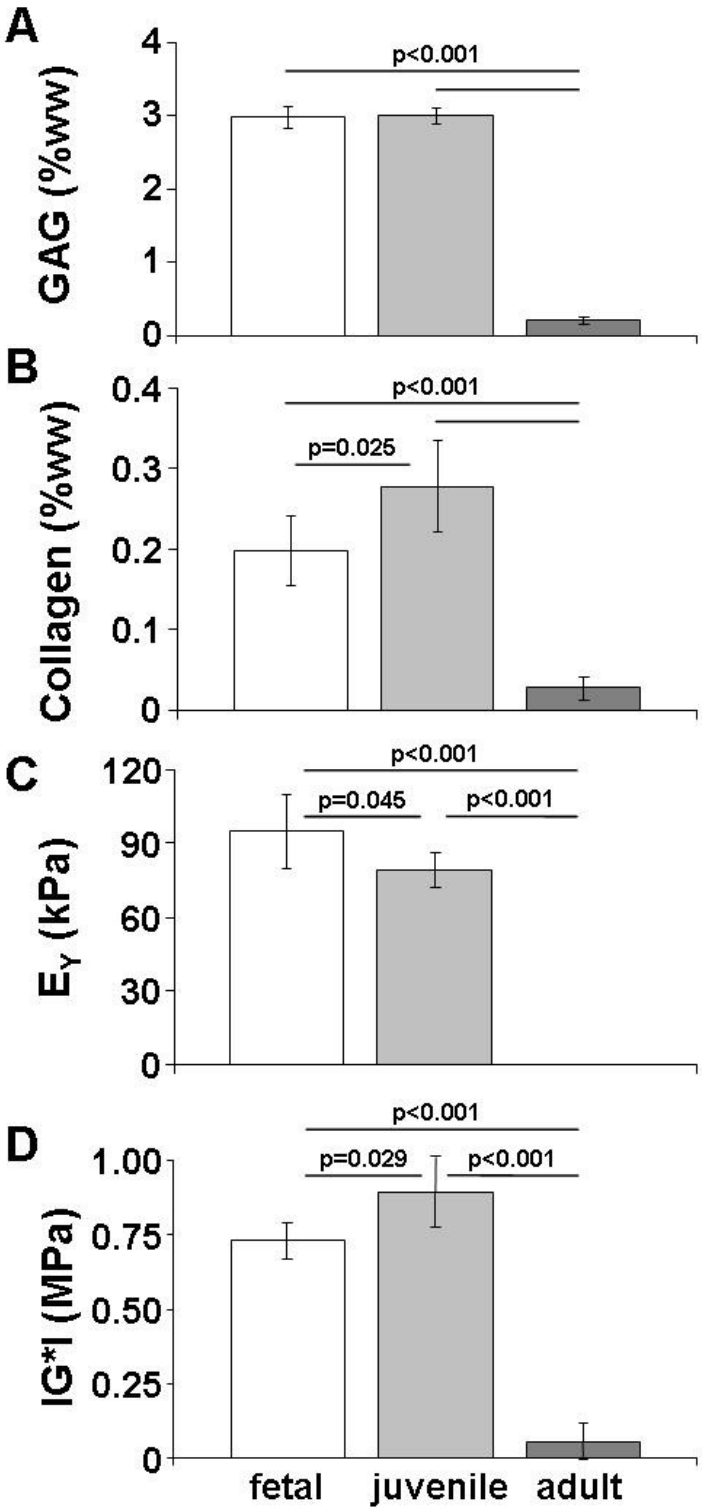


**Figure 9-8: Biochemical content of MSC-seeded HA constructs after 21 days in culture showed an age-dependent accumulation of (A) GAG and (B) collagen. The (C) equilibrium compressive modulus and (D) dynamic compressive modulus of MSC constructs was similarly dependent on MSC age. (n = 4 constructs per age).**

## 9.4. Discussion

Donor cell age may be an important determinant of the success of autologous tissue engineering; however, the current literature presents contradicting evidence in a variety of model systems and culture contexts for MSCs. Our first objective was to confirm age-related changes in bovine articular cartilage. Secondly, we sought to establish how age modulates chondrogenesis of chondrocyte pellets and thirdly, MSC pellets. Lastly, we investigated age-related differences in MSC chondrogenesis in a hydrogel context.

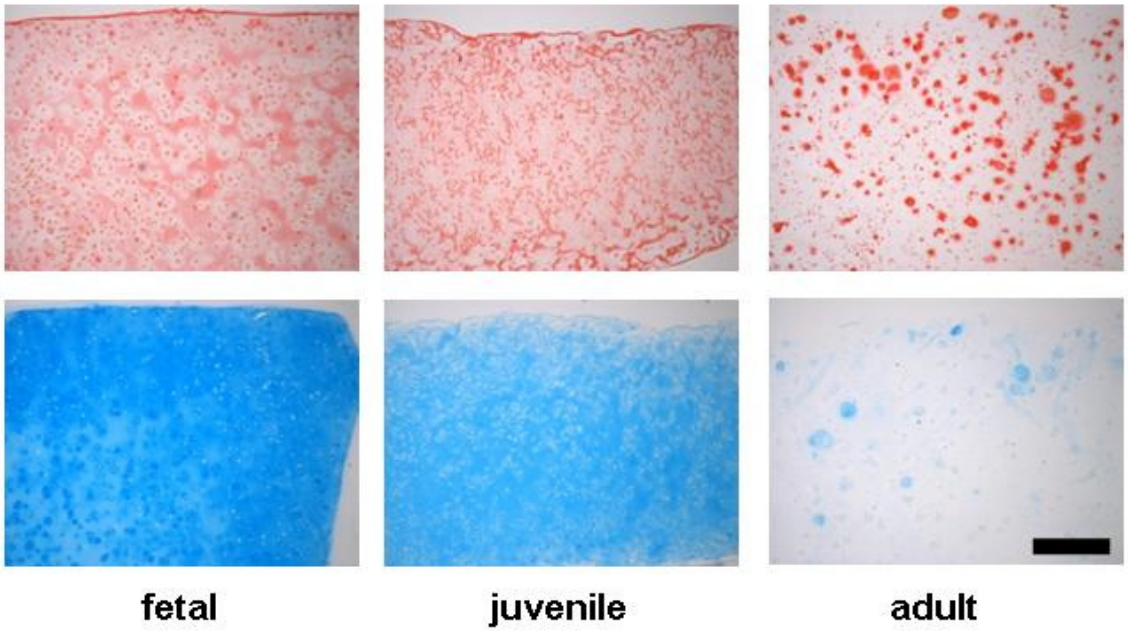


**Figure 9-9: Picrosirius red staining of collagens (top) and alcian blue staining of proteoglycans (bottom) supported the quantitative biochemical measures (50X magnification; scale bar = 250 µm).**

This work was not without limitations. First, the hydrogel study used only MSCs, which was motivated by previous work indicating that chondrocyte function is limited in this HA hydrogel formulation (see Chapter 3), but only TGF-β3 was utilized, where additional growth factors may have elicited different results related to donor age. TGF-β3

is consistently used in tissue engineering to elicit a chondrogenic response, however, it remains possible that our age-related observations are due to changing responsiveness to TGF-β3, which was not studied. Finally, we did not evaluate hypertrophic markers, though, we have previously demonstrated that bovine MSCs in agarose hydrogels do not deposit appreciable amounts of mineral or collagen type X (Huang *et al*. 2009).

Consistent with previous studies (Williamson *et al*. 2001; Williamson *et al*. 2003; Charlebois *et al*. 2004), our findings demonstrate that as bovine cartilage matures, mechanical properties and collagen content increase, GAG content remains stable, and cellularity declines. In human articular cartilage, Temple and colleagues showed no age-related biochemical changes and a decrease in equilibrium modulus for only the 60+ age group, however, the youngest (21-39) age group was already skeletally mature (Temple *et al*. 2007). Studying younger donors, Kempson found increasing tensile properties of human articular cartilage until the third decade and suggested refinement of the collagenous network for 30 years (Kempson 1991). We also observed a marked change in the superficial collagen staining intensity in juvenile and adult bovine samples, consistent with previous studies of fetal to juvenile cartilage (Archer *et al*. 2003). In fully formed and specialized adult cartilage tissue, prevailing collagen orientation in this surface zone defines a "split-line" direction (Bullough and Goodfellow 1968; Clarke 1971) that is remarkably consistent amongst all human subjects (Below *et al*. 2002). In bovine joints, we observed similar split-line patterns in juvenile femoral condyles, trochlear grooves, and patellar cartilage surfaces. Notably, these patterns were entirely absent or poorly defined in fetal cartilage surfaces. This suggests that coincident with load-bearing use,

cartilage undergoes a rapid alteration in not just the amount of biochemical constituents, but also in the structure and functional assembly of these molecules.

Along with changes in cartilage structure and function, chondrocytes extracted from bovine cartilage of differing ages showed differences in biosynthetic activities in a 3D pellet system. TGF-β3 increased DNA content at each age, and most in adult pellets, suggesting a switch from differentiated to proliferative activities. GAG and collagen deposition in fetal and juvenile bovine chondrocyte pellets was generally higher than adult chondrocyte pellets. Interestingly, fetal and juvenile chondrocyte pellets in chemically defined medium with TGF-β3 accumulated less GAG and collagen (fetal only) than those cultured without TGF-β3, a result that has not been previously reported. In contrast, TGF-□β3 improved both GAG content and mechanical properties for immature chondrocytes in the context of 3D agarose hydrogels (Mauck *et al*. 2006). This may indicate a microenvironmental influence (such as cell-to-cell contact) in the interpretation of this soluble factor.

Unlike chondrocytes, pellets formed from bovine MSCs of different ages were strongly age-dependent. TGF-β3 initiated robust chondrogenesis, consistent with the literature (Barry *et al*. 2001). Aged MSC pellets with TGF-β3 accumulated less GAG and collagen than immature MSCs. This decline in MSC potential has been observed in both murine (Kretlow *et al*. 2008) and male (but not female) human (Payne *et al*. 2010) MSCs in pellet format, although donors were skeletally matured. Another study has shown a small decline in matrix production from adult MSCs compared to fetal cells (Barbero *et al*.

2004). However, these reported deficiencies in aged human pellets were not as remarkable as observed in this study with bovine cells.

Bovine MSC chondrogenic capacity in a 3D HA hydrogel environment was also evaluated. Chapter 3 demonstrates that these gels support both human and bovine MSC chondrogenesis (Chung and Burdick 2009). In this study, we used a 1% w/v HA formulation that maximizes matrix formation by juvenile bovine MSCs (see Chapter 4). Similar to pellets, bovine MSCs in this 3D context were highly age dependent, with fetal and juvenile MSCs producing robust samples with compressive properties reaching approximately 20% of native tissue values within 3 weeks. Conversely, adult MSCs produced little ECM, and only minor changes in mechanical properties. Tran-Khanh and coworkers, using bovine chondrocytes, reported a similar age-related decrease in biochemical and biomechanical properties in agarose hydrogels (Tran-Khanh *et al*. 2005). In contrast to these findings, Kopesky and coworkers found that adult equine MSCs in a self-assembling peptide hydrogel generated constructs with greater mechanical properties than either juvenile chondrocytes or MSCs, though only dynamic properties were reported (Kopesky *et al*. 2010).

### 9.5. Conclusions

This work represents a comprehensive investigation of aging in the context of bovine cartilage, 3D cell pellets, and in 3D hydrogels intended for cartilage tissue engineering. We demonstrated that age is an important modulator of cartilage properties and of the MSC and chondrocyte response to TGF-β3 in pellet culture. Most notably, bovine

chondrocytes decrease in matrix-forming capacity in pellet culture with advancing age, but these decreases are smaller than those seen in human chondrocytes (Adkisson *et al.* 2001). Likewise, bovine MSCs show a sharp decrease with age in cartilage matrix-forming capacity that is more severe than reported for human MSCs in this same format (Barbero *et al*. 2004). Overall, at each age, and under ideal conditions (absence of TGF for chondrocytes, presence of TGF for MSCs), bovine chondrocytes in pellet culture produce more GAG and collagen than MSCs, consistent with our previous findings (Mauck *et al*. 2006; Huang *et al*. 2010). Taken together, when considering an autologous cell-based tissue engineering strategy for cartilage repair, age must be an important consideration. Bovine cells are and remain a valuable tool for optimizing new material formulations, but care must be taken to ascertain the similarity in response of cells from this source in comparison to human cells.

**This previously published Chapter was included with kind permission from Springer Science + Business Media: Clinical Orthopaedics and Related Research, "Cartilage Matrix Formation by Bovine Mesenchymal Stem Cells in Three-dimensional Culture Is Age-dependent", PMID 21424832, March 2011, Isaac E. Erickson, Steven C. van Veen, Swarnali Sengupta, Sydney R. Kestle, Robert L. Mauck.**

# CHAPTER 10: Summary and Future Directions

## 10.1. Summary

The function of articular cartilage is to distribute joint loads while providing a nearly frictionless surface for frequent articulations. The unique composition and structural organization of collagens and proteoglycans with this tissue lead to incredible mechanical properties that allow it to perform this function. Like many things found in nature, it has proven rather difficult to engineer a replacement tissue that can either resemble or function as well as native cartilage. This is discouraging for thousands of patients who would benefit from an improved clinical approach for cartilage injuries and disease. The core objective of this thesis was to optimize a tissue engineering system and demonstrate its potential for clinical translation.

It has long been acknowledged that 'materials matter'. In cartilage tissue engineering, a biomaterial serves as the physical environment, often called a scaffold, wherein cells choose to differentiate or remain unchanged, synthesize proteins or remain idle, move or sit still, recruit friends or stay silent, and even live or die. This list of cell decisions is clearly not exhaustive, but demonstrates the key importance of microenvironment on the potential of any material for tissue engineering. In Chapter 3, three fundamentally different hydrogels were considered for their potential to promote mesenchymal stem cell (MSC) differentiation and the subsequent functional maturation of engineered constructs. We demonstrated that the distinctive materials caused different responses by both chondrocytes and MSCs in long term culture. While chondrocytes performed better than

MSCs in agarose hydrogels, the opposite was found for methacrylated hyaluronic acid (MeHA) hydrogels that preferentially supported MSCs for the functional development of cartilage constructs. Analysis of matrix protein content and its correlation to functional properties revealed that hydrogel microenvironments affect the structural organization of synthesized matrix and the subsequent development of functional properties.

The unique preference of MeHA hydrogels for MSCs, together with its convenient ultra-violet light polymerization and natural, biocompatible composition made it a standout for additional study. The work in Chapter 3 used a 2% weight/volume ratio of the modified HA macromer that was established as the most promising formulation for porcine auricular chondrocytes (Chung *et al*. 2006). Using our understanding of the influence of microenvironments on MSC chondrogenesis, Chapter 4 was designed to determine the effect that the MeHA macromer density would have on MSC chondrogenesis and the functional development of engineered constructs. Indeed, it was found that a lower macromer density (1% w/v) doubled the mechanical properties of developing constructs from the 2% formulation. While higher macromer densities did promote chondrogenesis and actually resulted in more accumulated matrix per construct, histological evidence and analyses of diffusion characteristics indicated that these highly crosslinked networks were too restrictive of matrix distribution. The 1% w/v formulation of MeHA resulted in functional properties that matched our previous efforts with MSC-seeded agarose hydrogels.

While it was promising for MeHA to reach agarose levels of mechanical properties, neither gel system seeded with MSCs has been capable of fostering the development of constructs that approach chondrocyte or native tissue levels, a major milestone for the production of a clinically relevant engineered material. Towards this end, Chapter 5 explored the effect of high MSC seeding density and dynamic culture (orbital shaking) as an approach to accelerate construct maturation by improving nutrient and growth factor diffusion to cells throughout the depth of the hydrogels. Increasing the MSC density from 20 to 60 million per mL resulted in a concomitant increase of the equilibrium modulus (121 to 313 kPa). Interestingly, sulfated glycosaminoglycan (sGAG) content increased only slightly and collagen concentrations actually declined in high MSC density 1% MeHA constructs, suggesting a potential role for matrix remodeling in the advanced maturation of these engineered tissues. Adding upon the observed effect of MSC density, we next cultured MeHA constructs on an orbital shaker and observed unprecedented increases in mechanical properties that topped 1 MPa after 9 weeks of culture, more than doubling the results from identical constructs cultured in static conditions. With these findings, we have now accomplished the objective of reaching clinically relevant compressive properties.

Another methodology commonly employed to promote MSC chondrogenesis and construct maturation *in vitro* is the application of dynamic compressive loading using a bioreactor. Physiologic loading is known to be critical in the development of articular cartilage and therefore should not be overlooked as a critical component of any cartilage tissue engineering system for proper conditioning of cells that will eventually be

implanted within a loading environment. In Chapter 6, high MSC density MeHA constructs that were subjected to daily dynamic loading for 9 weeks reached nearly twice the equilibrium modulus of unloaded controls. Constructs that were loaded for only the first 3 weeks also only attained half the modulus of the 9 week loading group, suggesting that initial loading events are not sufficient and that prolonged loading has a continual effect on construct development.

Chapters 3-6 optimized a natural biomaterial, which combined with additional techniques accomplished the key objective of producing constructs with native mechanical properties. While promising, it remains unknown if these MeHA constructs will integrate and function within a cartilage defect. This was tested in Chapter 7 using an *in vitro* model of cartilage integration where cartilage explants are formed into rings, hydrogel constructs are cultured within the ring, and afterwards the force required to dislodge them is measured. Specifically, we tested whether constructs can be formed *in situ* or if they require *in vitro* pre-culture to improve integration and mechanical properties. The results from this study indicated that *in situ* polymerized constructs did have the capacity to integrate, but they did not develop compressive properties, while pre-cultured constructs integrated slightly better with significantly greater mechanical strength. Thinking clinically, this work points toward the necessity of generating more mature constructs before implantation to improve their functional potential *in vivo*.

Chapter 8 was a coalescence of several factors previously found to be beneficial for functional cartilage repair: 1% w/v, high MSC density, dynamic culture, and pre-

maturation before implantation. Using the push-out testing model, the durability of integrated constructs was assessed by testing the integration strength after the application of 2 hours of dynamic compression (1Hz; 10% strain), roughly a half marathon worth of activity. Integration strength was affected by this intense loading regime, but remained on par with the highest published reports of cartilage integration using a chondrocyte-based material. The functionality of the constructs was also assessed by testing the compressive properties of the repaired cartilage defects, which found that MeHA and cartilage repaired defects contributed equally to the composite mechanical properties. However, once removed from the defect, the compressive properties of MeHA constructs were still significantly lower than native cartilage. Regardless, this study reported extraordinary integration strength for MeHA repaired defects coupled with mechanical function equal to repair with mature cartilage.

The last study presented in this thesis was an investigation of the effect that age has on MSC potential for *in vitro* matrix formation. The results clearly indicate that in both pellet and MeHA contexts, younger MSCs have a greater matrix forming potential. This has significant implications for this work and the work of many others who are similarly engaged in tissue engineering research. While young healthy cells can be advantageous in discovering methods and systems to be used for tissue engineering, age should be an important consideration when approaching pre-clinical investigations.

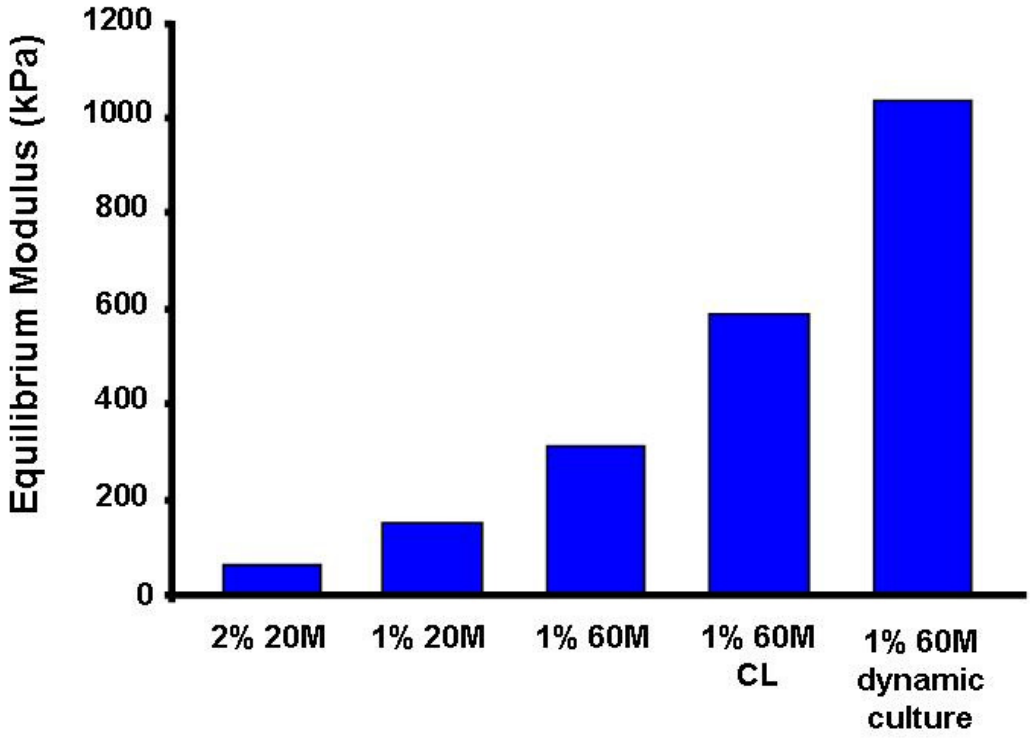


**Figure 10-1: Summary of progress in the development of compressive properties in MSC-seeded MeHA hydrogels starting with 2% w/v formulation the macromer and MSC density were optimized and continuous loading (CL) and dynamic culture were utilized. Each successive step resulted in a doubling of the equilibrium modulus.**

Overall, the work presented in this thesis began with some MSCs, a handful of hydrogels, and the objective of creating a clinically relevant engineered tissue. **Figure 10-1** shows the progression that began with an equilibrium modulus of approximately 50 kPa, and ended with a 20 fold increase to 1 MPa. Along the way, this work also contributed to what we know about the influence of hydrogel microenvironments, density of crosslinked networks, increasing MSC density, dynamic culture systems, and continuous dynamic loading on the *in vitro* maturation of engineered MSC based constructs. Towards understanding the clinical potential of MSC-MeHA constructs, the *in vitro* integration and functionality were assessed, which demonstrated a high level of feasibility.

## 10.2. Limitations and Future Directions

### 10.2.1. Graft Hypertrophy

Chapters 5 and 6 of this thesis reported on MSC-seeded MeHA constructs with mechanical properties that match native tissue and therefore may be suitable for implantation, but evidence suggests that while implanted chondrocyte-based constructs maintain their phenotype, MSC-based constructs become hypertrophic *in vivo* (Pelttari *et al*. 2006; Bian *et al*. 2011). Hypertrophic changes in the MSC-MeHA constructs of this thesis were not examined, but this potential must be explored for this system to progress towards clinical realization. Future *in vitro* studies could investigate the gene expression of collagen type X or assay alkaline phosphotase found in culture medium. Ectopic *in vivo* models could also be utilized, but perhaps the most relevant context would be within an orthotopic large animal model. Regardless, if hypertrophy is found within MSC-MeHA constructs, one method to mitigate this negative effect would be to deliver chemical regulators via microspheres such as parathyroid hormone-related protein which has shown some efficacy in reducing the hypertrophic response of MSC constructs within an ectopic mouse model (Bian *et al*. 2011). Bian *et al* have also demonstrated that co-culture of articular chondrocytes with MSCs helps significantly reduce hypertrophy (Bian *et al*. 2011). While it was determined that this hypertrophy reducing effect was proximity dependent, it remains feasible that neighboring chondrocytes within an *in vivo* or *in vitro* defect could also help maintain the chondrogenic phenotype of MSCs within a repair construct. Lastly, more recent work has shown that dynamic compression may also serve to maintain MSC phenotype (unpublished finding), which strengthens the rationale for a

large animal study to determine if any additional considerations will need to be taken in the engineering of MSC-based cartilage to prevent graft hypertrophy.

### 10.2.2. Dynamic Culture

While the use of an orbital shaker dramatically improved construct mechanical properties and the integration strength of repair, it could be argued that this method of nutrient and growth factor transport does not resemble physiologic processes. Soluble factors reach cells within articular cartilage through synovial fluid and the blood supply of the subchondral bone. The diffusion of soluble factors is enhanced when cartilage undergoes physical deformation through normal joint loading (Mauck *et al*. 2003; Albro *et al*. 2008). While these processes clearly differ from orbital shaking, it therefore remains unclear whether the orbital shaking of *in vitro* constructs offers an aphysiologic advantage or if this process actually more closely resembles the levels of transport found *in vivo*. Future studies could easily reduce the level of dynamic culture by lowering the rpm of the orbital shaker or by applying an intermittent regimen (e.g. 5 min every hour) to establish a lower threshold where positive effects are still observed without what may seem to be supraphysiologic diffusion.

### 10.2.3. Exogenous TGF-β3 Supplementation

Supplementation of chondrogenic medium with cytokines from the transforming growth factor (TGF) superfamily is a key requirement for MSCs to be able to differentiate and form a cartilage like matrix *in vitro* (Johnstone *et al*. 1998) and the TGF-β3 isoform was utilized throughout this thesis at a concentration of 10 ng per mL. This concentration has

been optimized to maximize the chondrogenesis of MSCs *in vitro*, but may exceed physiologic levels where resident cells are less dependent on this cytokine as they have already undergone chondrogenesis. While expensive, this high exogenous supplementation is rationalized, when considering its effectiveness in the development of *in vitro* grown constructs for implantation. However, in the defect model of repair presented in Chapters 7 and 8, it may be difficult to compare results to what may occur *in vivo* where levels of TGF may be significantly reduced. Furthermore, it was shown here and by others that chondrocytes within explant cartilage respond to TGF by significantly increasing biosynthesis which results in growth of mechanical properties. This anabolic response within the defect cartilage likely played a role in the observed integration strength, but the extent of this role could be elucidated in future experiments by utilizing devitalized cartilage as an additional control along with non TGF-supplemented constructs. If the *in vitro* integration response is found to be dependent on TGF-induced chondrocytes within the adjacent cartilage, future work could consider a physiologically relevant dosage of TGF when seeking to understand the applicability of *in vitro* repair. Alternatively, TGF-filled microspheres (Bian *et al*. 2011) could be administered within the interface upon implantation of a engineered graft to enlist the native chondrocyte response for improved healing.

### 10.2.4. MSC Age and Species of Origin

As discussed in Chapter 9, the age and species of progenitor cells are an important consideration when interpreting the results of tissue engineering studies. The age of MSCs in many species has been shown to affect their matrix forming capacity, therefore,

a limitation to this work was the use of juvenile bovine MSCs. Future studies with adult human MSCs will be important to verify the efficacy of this MeHA system in both forming robust constructs and integrating within a cartilage defect. If it proves difficult to show efficacy with aged cells, it may be warranted to investigate the potency of other aged sources of human progenitor cells (e.g. adipose-derived) or perhaps even to consider the implementation of induced pluripotent stem cells which have garnered recent and significant interest (Takahashi *et al*. 2007; Yu *et al*. 2007).

### 10.2.5. Long-Term Durability of Repair

While the work in Chapter 8 offered positive insights into the ability of MeHA repaired defects to withstand loading without failure, the single application regimen was both strenuous and abrupt. A future study that applied daily cyclic compressive loading, but at a lower amplitude, might be more realistic considering the potential immobilization and/or reduction in strenuous activities that would likely follow a procedure where an engineered graft would be implanted. Variables in this study may include the duration of immobilization (time after implantation without loading) and the duration of long-term loading. A properly controlled study of this nature would establish whether continuous loading is detrimental to integration, if dynamic loading enhances integration, and what post-operative activity regimen might be most suitable for future *in vivo* studies.

### 10.2.6. Estimation of Functional Repair

Chapter 8 showed similar function between MeHA and cartilage repaired defect when considering the mechanical properties of the whole repaired construct, but testing in

unconfined compression may have introduced a limitation. The natural loading constraints could be better reproduced and the effects of construct repair could have been better isolated using confined compression testing. As an alternative method to compression testing, a pressure sensing analysis system (e.g. tekscan) could be employed to visualize the distribution of contact stresses on the surface of a repaired defect.

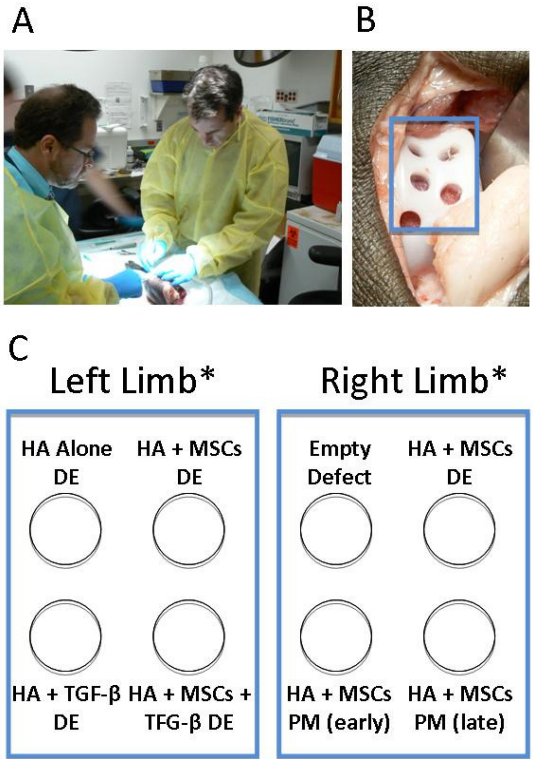


**Figure 10-2: (A) Surgical team executing cadaver simulation in a minipig stifle joint. (B) Close-up of cartilage defects in trochlear groove. (C) Experimental conditions to be tested *in vivo*. (DE=direct encapsulation of MSCs *in situ*; PM=pre-maturation *in vitro*; *Positions within each joint and left/right sides will be randomized)**

### 10.2.7. Large Animal Study

Lastly, the need for a large animal study of cartilage repair is the most critical future direction. It is difficult for *in vitro* studies to account for many aspects of the complex physiology and biomechanics of the joint. Towards this end, a large animal study has been designed to assess the efficacy of MSC-seeded MeHA constructs in repairing

cartilage defects within a pig model (**Figure 10-2**). Several aspects of this thesis will be utilized in this future work including 1% w/v MeHA, high MSC density, pre-culture of constructs before implantation, dynamic culture conditions, μCT imaging, and integration analysis. Biomechanical, biochemical, μCT, and histological findings will offer a comprehensive analysis of the clinical potential of the MSC-MeHA system optimized in this thesis.

### 10.3. Conclusions

While rife with promise, the field of tissue engineering has seen little success over the last two decades. One common difficulty within tissue engineering is the difficulty in recapitulating what nature has already built so perfectly. While this task is likely impossible, we make determinations about what aspects may be most critical for an engineered tissue to perform its necessary function. In cartilage, filling a defect is simple, but replacement cartilage capable of seamless integration and long-term function is the gold standard. With this objective in mind, we have optimized an elegant photo-crosslinked hydrogel system that, when seeded with MSCs, will generate robust tissue with striking similarity to native cartilage. This engineered MSC-based tissue has demonstrated its potential for functional cartilage repair within an *in vitro* cartilage defect model and will be analyzed in a pre-clinical model to ultimately determine its clinical potential. The advances made using this MeHA hydrogel and the concepts and ideas that were evaluated in the various experiments of this thesis represent a significant step towards future success in tissue engineering.

## Appendix 1: Related Publications

**Erickson IE**, Kestle SR, Zellars KH, Farrell MJ, Kim M, Burdick JA, Mauck RL, "High Stem Cell Seeding Densities in Hyaluronic Acid Hydrogels Produce Engineered Cartilage with Native Tissue Properties," manuscript in preparation.

**Erickson IE**, Kestle SR, Kim M, Zellars KH, Dodge GR, Burdick JA, Mauck RL, "Improved Cartilage Repair via *in vitro* Pre-maturation of MSC Seeded Hyaluronic Acid Hydrogels," Biomaterials, in review.

**Erickson IE**, van Veen SC, Sengupta S, Kestle SR, Burdick JA, Mauck RL, "Age-Dependent Cartilage Matrix Formation by Bovine Mesenchymal Stem Cells in 3D Culture," Clinical Orthopaedics & Related Research, 2011, DOI: 10.1007/s11999-011-1869-z.

**Erickson IE**, Huang AH, Sengupta S, Kestle S, Burdick JA, Mauck RL, "Macromer Density Influences Mesenchymal Stem Cell Chondrogenesis and Maturation in Photocrosslinked Hyaluronic Acid Hydrogels," Osteoarthritis & Cartilage, 2009, 17(12):1639-48.

**Erickson IE**, Huang AH, Chung C, Li RT, Burdick JA, Mauck RL, "Differential maturation and structure-function relationships in mesenchymal stem cell- and chondrocyte-seeded hydrogels," Tissue Engineering Part A, 2009, 15(5):1041-52.

Chung C, **Erickson IE**, Mauck RL, Burdick JA, "Differential behavior of auricular and articular chondrocytes in hyaluronic acid hydrogels," Tissue Engineering Part A, 2008, 14(7):1121-31.

Brey DM, **Erickson IE**, Burdick JA, "Influence of macromer molecular weight and chemistry on poly(beta-amino ester) network properties and initial cell interactions," Journal of Biomedical Materials Research A, 2008, Jun 1;85(3):731-41.

## Appendix 2: Related Conference Abstracts

**Erickson IE**, Zellars KH, Kestle SR, Burdick JA, Mauck RL, "Dynamic Compression Promotes Cartilage-like Functional Properties in MSC-seeded Hyaluronic Acid hydrogels," Proceedings of ASME 2011 Summer Bioengineering Conference, Farmington, PA, June 22-25, paper #53661.

Kim M, **Erickson IE**, Burdick JA, Mauck RL, "Transient Exposure to TGF-β3 Improves The Functional Properties of MSC-Seeded Photocrosslinked Hyaluronic Acid Hydrogels," Proceedings of ASME 2011 Summer Bioengineering Conference, Farmington, PA, June 22-25, paper #53906.

**Erickson IE**, Kestle SR, Kim M, Zellars KH, Dodge GR, Burdick JA, Mauck RL, "In Vitro Maturation and Integration of Engineered Chondrogenic Stem Cell-Seeded Hyaluronic Acid Hydrogels," The 57th Annual Meeting of the Orthopaedic Research Society, Long Beach, CA, January 13-16, 2011, volume 36:0255, podium presentation.

**Erickson IE**, Kestle SR, Zellars KH, Burdick JA, Mauck RL, "High Density MSC-Seeded Hyaluronic Acid Constructs Produce Engineered Cartilage with Near-Native Properties," The 57th Annual Meeting of the Orthopaedic Research Society, Long Beach, CA, January 13-16, 2011, volume 36:0314, podium presentation.

**Erickson IE**, Kestle SR, Kim M, Zellars KH, Burdick JA, Dodge GR, Mauck RL, "μCT and Mechanical Analysis of Maturation and Integrative Cartilage Repair in MSC-Seeded HA Hydrogels," Tissue Engineering & Regenerative Medicine International Society-North America Annual Conference and Exposition, Orlando, FL, December 5-8, 2010, paper #1239, podium presentation.

**Erickson IE**, van Veen SC, Sengupta S, Kestle SR, Burdick JA, Mauck RL, " Effects of Aging and TGF-Beta 3 on Chondrocyte and Mesenchymal Stem Cell Matrix Formation," Proceedings of ASME 2010 Summer Bioengineering Conference, Naples, FL, June 15-19, paper #19517, podium presentation.

Kim M, **Erickson IE**, Burdick JA, Dodge GR, Mauck RL, "Differential Chondrogenic Potential of Human and Bovine Mesenchymal Stem Cells in Agarose and Photocrosslinked Hyaluronic Acid Hydrogels," Proceedings of ASME 2010 Summer Bioengineering Conference, Naples, FL, June 15-19, paper #19461.

**Erickson IE**, Kestle SR, Farrell MJ, Burdick JA, Mauck RL, "Macromer Density Mediates Mesenchymal Stem Cell Response to Dynamic Compression in Photo-Crosslinked Hyaluronic Acid Hydrogels," Transactions of the 56th Annual Meeting of the Orthopaedic Research Society, New Orleans, LA, March 6-9, 2010, volume 35:1286.

**Erickson IE**, Kestle SR, Burdick JA, Mauck RL, "*In Vitro* Cartilage Integration of MSC-Seeded Hyaluronic Acid Constructs," Transactions of the 56th Annual Meeting of the Orthopaedic Research Society, New Orleans, LA, March 6-9, 2010, volume 35:1337

Kim M, **Erickson IE**, Yoder J, Mauck RL, Witschey W, Fenty M, Reddy R, Dodge GR, "Evaluation of Integrative Cartilage Repair with Scaffold-Free Constructs," Transactions of the 56th Annual Meeting of the Orthopaedic Research Society, New Orleans, LA, March 6-9, 2010, volume 35:30.

Ionescu LC, Garcia GH, **Erickson IE**, Guevara JL, Shah RP, Sennett BJ, Mauck RL, "*In Vitro* Meniscus Integration is Age Dependent," Transactions of the 56th Annual Meeting of the Orthopaedic Research Society, New Orleans, LA, March 6-9, 2010, volume 35:927.

**Erickson IE**, Sengupta S, Kestle S, Chung C, Burdick JA, Mauck RL, "Macromer Concentration Influences Gel Mechanics, Diffusivity, and Maturation of MSC-Seeded HA Hydrogels," Transactions of the 55th Annual Meeting of the Orthopaedic Research Society, Las Vegas, NV, February 22-25, 2009, volume 34:1723.

**Erickson IE**, Chung C, Burdick JA, Mauck RL, Hyaluronic Acid Macromer Concentration Influences Functional MSC Chondrogenesis in Photocrosslinked MSC-Laden Hydrogels," Proceedings of ASME 2008 Summer Bioengineering Conference, Marco Island, FL, June 25-29, paper #193096.

**Erickson IE**, Huang AH, Chung C, Li RT, Burdick JA, Mauck RL, "Hydrogel Effects on Long-Term Maturation of Chondrocyte and MSC-Laden Hydrogels," Transactions of the 54th Annual Meeting of the Orthopaedic Research Society, San Francisco, CA, March 2-5, 2008, volume 33:0557.

Brey DM, **Erickson IE**, Tan A, Burdick JA, "Controlling Polymer Properties and Cellular Interactions through Poly(alpha-amino ester) Macromer Structure," Society for Biomaterials Annual Meeting, Chicago, IL, April, 2007.

**Erickson IE**, Yang YI, Fitzpatrick K, Kirker KR, Massey MF, Shelby J, "Improved Viability of Adipose-Derived Adult Stem Cells Using Hyaluronan as a Media Supplement," Biointerface 2005: The Annual Surfaces in Biomaterials Foundation Symposium, Minneapolis, MN, October 24-26, 2005.

**Bibliography**

Adkisson, H. D., M. P. Gillis, E. C. Davis, W. Maloney and K. A. Hruska (2001). "In vitro generation of scaffold independent neocartilage." Clinical Orthopaedics and Related Research **October**(391 supplement): S280-294.

Ahsan, T. and R. L. Sah (1999). "Biomechanics of integrative cartilage repair." Osteoarthritis Cartilage **7**(1): 29-40.

Akizuki, S., V. C. Mow, F. Muller, J. C. Pita, D. S. Howell and D. H. Manicourt (1986). "Tensile properties of human knee joint cartilage: I. Influence of ionic conditions, weight bearing, and fibrillation on the tensile modulus." J Orthop Res **4**(4): 379-92.

Albro, M. B., N. O. Chahine, R. Li, K. Yeager, C. T. Hung and G. A. Ateshian (2008). "Dynamic loading of deformable porous media can induce active solute transport." J Biomech **41**(15): 3152-3157.

Archer, C. W., G. P. Dowthwaite and P. H. Francis-West (2003). "Development of synovial joints." Birth Def Res (Part C) **69**: 144-55.

Ateshian, G. A., M. A. Soltz, R. L. Mauck, I. M. Basalo, C. T. Hung and W. M. Lai (2003). "The role of osmotic pressure and tension-compression nonlinearity in the frictional response of articular cartilage." Transport Porous Med **50**: 5-33.

Ateshian, G. A., W. H. Warden, J. J. Kim, R. P. Grelsamer and V. C. Mow (1997). "Finite deformation biphasic material properties of bovine articular cartilage from confined compression experiments." J Biomech **30**(11-12): 1157-64.

Aufderheide, A. C. and K. A. Athanasiou (2007). "Assessment of a Bovine Co-culture, Scaffold-Free Method for Growing Meniscus-Shaped Constructs." Tissue Eng **13**(9): 2195-205.

Awad, H. A., M. Q. Wickham, H. A. Leddy, J. M. Gimble and F. Guilak (2004). "Chondrogenic differentiation of adipose-derived adult stem cells in agarose, alginate, and gelatin scaffolds." Biomaterials **25**(16): 3211-22.

Baksh, D., L. Song and R. S. Tuan (2004). "Adult mesenchymal stem cells: characterization, differentiation, and application in cell and gene therapy." J Cell Mol Med **8**(3): 301-16.

Barbero, A., S. Grogan, D. Schafer, M. Heberer, P. Mainil-Varlet and I. Martin (2004). "Age related changes in human articular chondrocyte yield, proliferation and post-expansion chondrogenic capacity." Osteoarthritis Cartilage **12**(6): 476-84.

Barbero, A., S. Ploegert, M. Heberer and I. Martin (2003). "Plasticity of clonal populations of dedifferentiated adult human articular chondrocytes." Arthritis Rheum **48**(5): 1315-25.

Barry, F., R. E. Boynton, B. Liu and J. M. Murphy (2001). "Chondrogenic differentiation of mesenchymal stem cells from bone marrow: differentiation-dependent gene expression of matrix components." Exp Cell Res **268**(2): 189-200.

Bayliss, M. T., M. Venn, A. Maroudas and S. Y. Ali (1983). "Structure of proteoglycans from different layers of human articular cartilage." Biochem J **209**(2): 387-400.

Below, S., S. P. Arnoczky, J. Dodds, C. Kooima and N. Walter (2002). "The split-line pattern of the distal femur: a consideration in the orientation of autologous cartilage grafts." J Arthros Rel Surg **18**(6): 613-17.

Benya, P. D. and J. D. Shaffer (1982). "Dedifferentiated chondrocytes reexpress the differentiated collagen phenotype when cultured in agarose gels." Cell **30**(1): 215-224.

Bernardo, M. E., J. A. M. Emons, M. Karperien, A. J. Nauta, R. Willemze, H. Roelofs, S. Romeo, A. Marchini, G. A. Rappold, S. Vukicevic, F. Locatelli and W. E. Fibbe (2007). "Human mesenchymal stem cells derived from bone marrow display a better chondrogenic differentiation compared with other sources." Connective Tissue Research **48**(3): 132-140.

Betre, H., S. R. Ong, F. Guilak, A. Chilkoti, B. Fermor and L. A. Setton (2005). "Chondrocytic differentiation of human adipose-derived adult stem cells in elastin-like polypeptide." Biomaterials.

Bian, L., J. V. Fong, E. G. Lima, A. M. Stoker, G. A. Ateshian, J. L. Cook and C. T. Hung (2010). "Dynamic Mechanical Loading Enhances Functional Properties of Tissue-Engineered Cartilage Using Mature Canine Chondrocytes." Tissue Eng Part A **16**(5): 1781-1790.

Bian, L., D. Y. Zhai, R. L. Mauck and J. A. Burdick (2011). "Coculture of Human Mesenchymal Stem Cells and Articular Chondrocytes Reduces Hypertrophy and Enhances Functional Properties of Engineered Cartilage." Tissue Eng Part A **17**(7-8): 1137-1145.

Bian, L., D. Y. Zhai, E. Tous, R. Rai, R. L. Mauck and J. A. Burdick (2011). "Enhanced MSC chondrogenesis following delivery of TGF-[beta]3 from alginate microspheres within hyaluronic acid hydrogels in vitro and in vivo." Biomaterials **In Press, Corrected Proof**.

Bonnet, F., D. G. Dunham and T. E. Hardingham (1985). "Structure and interactions of cartilage proteoglycan binding region and link protein." Biochem J **228**(1): 77-85.

Brittberg, M., A. Lindahl, A. Nilsson, C. Ohlsson, O. Isaksson and L. Peterson (1994). "Treatment of deep cartilage defects in the knee with autologous chondrocyte transplantation." N Engl J Med **331**(14): 889-95.

Broom, N. D. and D. L. Marra (1986). "Ultrastructural evidence for fibril-to-fibril associations in articular cartilage and their functional implication." J Anat **146**: 185-200.

Bryant, S. J. and K. S. Anseth (2003). "Controlling the spatial distribution of ECM components in degradable PEG hydrogels for tissue engineering cartilage." J Biomed Mater Res A **64**(1): 70-9.

Bryant, S. J., C. R. Nuttelman and K. S. Anseth (1999). "The effects of crosslinking density on cartilage formation in photocrosslinkable hydrogels." Biomed Sci Instrum **35**: 309-14.

Buckwalter, J. A. (2002). "Articular cartilage injuries." Clin Orthop(402): 21-37.

Buckwalter, J. A. and N. E. Lane (1997). "Athletics and osteoarthritis." Am J Sports Med **25**(6): 873-81.

Bullough, P. and J. Goodfellow (1968). "The significance of the fine structure of articular cartilage." J Bone Joint Surg Br. **50**(4): 852-857.

Bullough, P. G. (2004). "The role of joint architecture in the etiology of arthritis." Osteoarthritis Cartilage **12**(Supplement 1): 2-9.

Burdick, J. A. and K. S. Anseth (2002). "Photoencapsulation of osteoblasts in injectable RGD-modified PEG hydrogels for bone tissue engineering." Biomaterials **23**(22): 4315-23.

Burdick, J. A., C. Chung, X. Jia, M. A. Randolph and R. Langer (2005). "Controlled degradation and mechanical behavior of photopolymerized hyaluronic acid networks." Biomacromolecules **6**(1): 386-91.

Buschmann, M. D., Y. A. Gluzband, A. J. Grodzinsky, J. H. Kimura and E. B. Hunziker (1992). "Chondrocytes in agarose culture synthesize a mechanically functional extracellular matrix." J Orthop Res **10**(6): 745-58.

Buxton, A. N., J. Zhu, R. Marchant, J. L. West, J. U. Yoo and B. Johnstone (2007). "Design and characterization of poly(ethylene glycol) photopolymerizable semi-interpenetrating networks for chondrogenesis of human mesenchymal stem cells." Tissue Eng **13**(10): 2549-60.

Byers, B. A., R. L. Mauck, I. E. Chiang and R. S. Tuan (2008). "Transient Exposure to Transforming Growth Factor Beta 3 Under Serum-Free Conditions Enhances the

Biomechanical and Biochemical Maturation of Tissue-Engineered Cartilage." Tissue Eng Part A **14**(11): 1821-1834.

Caplan, A. I., M. Elyaderani, Y. Mochizuki, S. Wakitani and V. M. Goldberg (1997). "Principles of cartilage repair and regeneration." Clin Orthop(342): 254-69.

Caterson, E. J., W. J. Li, L. J. Nesti, T. Albert, K. Danielson and R. S. Tuan (2002). "Polymer/alginate amalgam for cartilage-tissue engineering." Ann N Y Acad Sci **961**: 134-8.

Chang, S. C., J. A. Rowley, G. Tobias, N. G. Genes, A. K. Roy, D. J. Mooney, C. A. Vacanti and L. J. Bonassar (2001). "Injection molding of chondrocyte/alginate constructs in the shape of facial implants." J Biomed Mater Res **55**(4): 503-11.

Charlebois, M., M. D. McKee and M. D. Buschmann (2004). "Nonlinear tensile properties of bovine articular cartilage and their variation with age and depth." J Biomech Eng **162**(2): 129-37.

Chen, H. C., H. P. Lee, M. L. Sung, C. J. Liao and Y. C. Hu (2004). "A novel rotating-shaft bioreactor for two-phase cultivation of tissue-engineered cartilage." Biotechnol Prog **20**(6): 1802-9.

Chen, S. S., Y. H. Falcovitz, R. Schneiderman, A. Maroudas and R. L. Sah (2001). "Depth-dependent compressive properties of normal aged human femoral head articular cartilage: relationship to fixed charge density." Osteoarthritis Cartilage **9**(6): 561-9.

Chung, C., M. Beecham, R. L. Mauck and J. A. Burdick (2009). "The influence of degradation characteristics of hyaluronic acid hydrogels on in vitro neocartilage formation by mesenchymal stem cells." Biomaterials **30**(26): 4287-4296.

Chung, C. and J. A. Burdick (2008). "Engineering cartilage tissue." Adv Drug Deliv Rev **60**(2): 243-62.

Chung, C. and J. A. Burdick (2009). "Influence of three-dimensional hyaluronic acid microenvironments on mesenchymal stem cell chondrogenesis." Tissue Eng Part A **15**(2): 243-254.

Chung, C., I. E. Erickson, R. L. Mauck and J. A. Burdick (2008). "Differential behavior of auricular and articular chondrocytes in hyaluronic acid hydrogels." Tissue Eng Part A. **14**(7): 1121-1131.

Chung, C., J. Mesa, G. J. Miller, M. A. Randolph, T. J. Gill and J. A. Burdick (2006). "Effects of auricular chondrocyte expansion on neocartilage formation in photocrosslinked hyaluronic acid networks." Tissue Eng Part A **12**(9): 2665-73.

Chung, C., J. Mesa, M. A. Randolph, M. Yaremchuk and J. A. Burdick (2006). "Influence of gel properties on neocartilage formation by auricular chondrocytes photoencapsulated in hyaluronic acid networks." J Biomed Mater Res A **77A**(3): 518-525.

Clarke, I. C. (1971). "Articular cartilage: a review and scanning electron microscope study. 1. The interterritorial fibrillar architecture." J Bone Joint Surg Br **53**(4): 732-50.

Cohen, N. P., R. J. Foster and V. C. Mow (1998). "Composition and dynamics of articular cartilage: structure, function, and maintaining healthy state." J Orthop Sports Phys Ther **28**(4): 203-15.

Coipeau, P., P. Rosset, A. Langonne, J. Gaillard, B. Delorme, A. Rico, J. Domenech, P. Charbord and L. Sensebe (2009). "Impaired differentiation potential of human trabecular bone mesenchymal stromal cells from elderly patients." Cytotherapy **11**(5): 584-594.

Connelly, J. T., A. J. Garcia and M. E. Levenston (2007). "Inhibition of in vitro chondrogenesis in RGD-modified three-dimensional alginate gels." Biomaterials **28**(6): 1071-83.

Darling, E. M. and K. A. Athanasiou (2005). "Rapid phenotypic changes in passaged articular chondrocyte subpopulations." J Orthop Res **23**(2): 425-32.

Detterline, A. J., S. Goldberg, B. R. Bach, Jr. and B. J. Cole (2005). "Treatment options for articular cartilage defects of the knee." Orthop Nurs **24**(5): 361-6; quiz 367-8.

Diaz-Romero, J., D. Nesic, S. P. Grogan, P. Heini and P. Mainil-Varlet (2007). "Immunophenotypic changes of human articular chondrocytes during monolayer culture reflect bona fide dedifferentiation rather than amplification of progenitor cells." J Cell Physiol.

DiMicco, M. A. and R. L. Sah (2001). "Integrative cartilage repair: adhesive strength is correlated with collagen deposition." J Orthop Res **19**(6): 1105-12.

DiMicco, M. A., S. N. Waters, W. H. Akeson and R. L. Sah (2002). "Integrative articular cartilage repair: dependence on developmental stage and collagen metabolism." Osteoarthritis Cartilage **10**(3): 218-25.

Ding, L., E. Heying, N. Nicholson, N. J. Stroud, G. A. Homandberg, J. A. Buckwalter, D. Guo and J. A. Martin (2005). "Mechanical impact induces cartilage degradation via mitogen activated protein kinases." Osteoarthritis Cartilage **18**(11): 1509-1517.

Domayer, S. E., G. t. H. Welsch, R. Dorotka, T. C. Mamisch, S. Marlovits, P. Szomolanyi and S. Trattnig (2008). "MRI Monitoring of Cartilage Repair in the Knee: A Review." Semin Musculoskelet Radiol **12**(04): 302,317.

Dressler, M. R., D. L. Butler and G. P. Boivin (2005). "Effects of age on the repair ability of mesenchymal stem cells in rabbit tendon." J Orthop Res **23**(2): 287-93.

Dunham, B. P. and R. J. Koch (1998). "Basic Fibroblast Growth Factor and Insulinlike Growth Factor I Support the Growth of Human Septal Chondrocytes in a Serum-Free Environment." Arch Otolaryngol Head Neck Surg **124**(12): 1325-1330.

Emans, P. J., L. W. van Rhijn, T. J. M. Welting, A. Cremers, N. Wijnands, F. Spaapen, J. W. Voncken and V. P. Shastri (2010). "Autologous engineering of cartilage." P Natl Acad Sci USA **107**(8): 3418-3423.

Embry, J. J. and W. Knudson (2003). "G1 domain of aggrecan cointernalizes with hyaluronan via a CD44-mediated mechanism in bovine articular chondrocytes." Arthritis & Rheumatism **48**(12): 3431-3441.

Engler, A. J., S. Sen, H. L. Sweeney and D. E. Discher (2006). "Matrix elasticity directs stem cell lineage specification." Cell **126**(4): 677-89.

Engler, A. J., H. L. Sweeney, D. E. Discher and J. E. Schwarzbauer (2007). "Extracellular matrix elasticity directs stem cell differentiation." J Musculoskelet Neuronal Interact **7**(4): 335.

Erggelet, C., P. Kreuz, E. Mrosek, J. Schagemann, A. Lahm, P. Ducommun and C. Ossendorf (2010). "Autologous chondrocyte implantation versus ACI using 3D-bioresorbable graft for the treatment of large full-thickness cartilage lesions of the knee." Arch Orthop Trauma Surg **130**(8): 957-964.

Erickson, G. R., J. M. Gimble, D. M. Franklin, H. E. Rice, H. Awad and F. Guilak (2002). "Chondrogenic potential of adipose tissue-derived stromal cells in vitro and in vivo." Biochem Biophys Res Commun **290**(2): 763-9.

Erickson, I. E., A. H. Huang, C. Chung, R. T. Li, J. A. Burdick and R. L. Mauck (2009). "Differential maturation and structure-function relationships in mesenchymal stem cell- and chondrocyte-seeded hydrogels." Tissue Eng Part A **15**(5): 1041-1052.

Erickson, I. E., A. H. Huang, S. Sengupta, S. Kestle, J. A. Burdick and R. L. Mauck (2009). "Macromer density influences mesenchymal stem cell chondrogenesis and maturation in photocrosslinked hyaluronic acid hydrogels." Osteoarthritis Cartilage **17**(12): 1639-1648.

Farndale, R. W., D. J. Buttle and A. J. Barrett (1986). "Improved quantitation and discrimination of sulphated glycosaminoglycans by use of dimethylmethylene blue." Biochim Biophys Acta **883**(2): 173-7.

Farrell, M. J., E. S. Comeau and R. L. Mauck (2011). Dynamic Culture Improves Mechanical Functionality of MSC-Laden Tissue Engineered Constructs in a Depth-

Dependent Manner. Proceedings of the ASME 2011 Summer Bioengineering Conference, Farmingtion, Pennsylvania.

Fierlbeck, J., J. Hammer, C. Englert and R. L. Reuben (2006). "Biomechanical properties of articular cartilage as a standard for biologically integrated interfaces." Technology and Health Care **14**(6): 541-547.

Frankowski, J. J. and S. Watkins-Castillo (2002). Primary total knee and hip arthroplasty projections for the U.S. population to the year 2030. Rosemont, IL, American Academy of Orthopaedic Surgeons, Department of Research and Scientific Affairs**:** 1-8.

Giannoni, P., A. Pagano, E. Maggi, R. Arbico, N. Randazzo, M. Grandizio, R. Cancedda and B. Dozin (2005). "Autologous chondrocyte implantation (ACI) for aged patients: development of the proper cell expansion conditions for possible therapeutic applications." Osteoarthritis Cartilage **13**(7): 589-600.

Gratz, K. R., V. W. Wong, A. C. Chen, L. A. Fortier, A. J. Nixon and R. L. Sah (2006). "Biomechanical assessment of tissue retrieved after in vivo cartilage defect repair: tensile modulus of repair tissue and integration with host cartilage." J Biomech **39**(1): 138-146.

Gruber, H. E., J. A. Ingram, K. Leslie, H. J. Norton and E. N. Hanley, Jr. (2003). "Cell shape and gene expression in human intervertebral disc cells: in vitro tissue engineering studies." Biotech Histochem **78**(2): 109-17.

Guettler, J. H., C. K. Demetropoulos, K. H. Yang and K. A. Jurist (2004). "Osteochondral Defects in the Human Knee." Am J Sports Med **32**(6): 1451-1458.

Guilak, F., R. L. Sah and L. A. Setton (1997). Physical regulation of cartilage metabolism. Basic orthopaedic biomechanics. V. C. Mow and W. C. Hayes. Philadelphia, Lippincott-Raven**:** 179-207.

Hannouche, D., H. Terai, J. R. Fuchs, S. Terada, S. Zand, B. A. Nasseri, H. Petite, L. Sedel and J. P. Vacanti (2007). "Engineering of Implantable Cartilaginous Structures from Bone Marrowâ€“Derived Mesenchymal Stem Cells." Tissue Engineering **13**(1): 87-99.

Harris, J. D., R. H. Brophy, R. A. Siston and D. C. Flanigan (2010). "Treatment of Chondral Defects in the Athlete's Knee." Arthroscopy **26**(6): 841-852.

Hauselmann, H. J., R. J. Fernandes, S. S. Mok, T. M. Schmid, J. A. Block, M. B. Aydelotte, K. E. Kuettner and E. J. Thonar (1994). "Phenotypic stability of bovine articular chondrocytes after long-term culture in alginate beads." J Cell Sci **107 ( Pt 1)**: 17-27.

Herberhold, C., S. Faber, T. Stammberger, M. Steinlechner, R. Putz, K. H. Englmeier, M. Reiser and F. Eckstein (1999). "In situ measurement of articular cartilage deformation in intact femoropatellar joints under static loading." J Biomech **32**(12): 1287-95.

Holmes, T. C., S. de Lacalle, X. Su, G. Liu, A. Rich and S. Zhang (2000). "Extensive neurite outgrowth and active synapse formation on self-assembling peptide scaffolds." Proc Natl Acad Sci U S A **97**(12): 6728-33.

Horas, U., D. Pelinkovic, G. Herr, T. Aigner and R. Schnettler (2003). "Autologous chondrocyte implantation and osteochondral cylinder transplantation in cartilage repair of the knee joint. A prospective, comparative trial." J Bone Joint Surg Am **85-A**(2): 185-92.

Huang, A. H., M. J. Farrell, M. Kim and R. L. Mauck (2010). "Long-term dynamic loading improves the mechanical properties of chondrogenic mesenchymal stem cell-laden hydrogel." Eur Cell Mater **19**: 72-85.

Huang, A. H., M. J. Farrell and R. L. Mauck (2010). "Mechanics and mechanobiology of mesenchymal stem cell-based engineered cartilage." Journal of Biomechanics **43**(1): 128-136.

Huang, A. H., A. Stein and R. L. Mauck (2010). "Evaluation of the Complex Transcriptional Topography of Mesenchymal Stem Cell Chondrogenesis for Cartilage Tissue Engineering." Tissue Engineering Part A **16**(9): 2699-2708.

Huang, A. H., A. Stein, R. S. Tuan and R. L. Mauck (2009). "Transient Exposure to Transforming Growth Factor Beta 3 Improves the Mechanical Properties of Mesenchymal Stem Cell-Laden Cartilage Constructs in a Density-Dependent Manner." Tissue Engineering Part A **15**(11): 3461-3472.

Huang, A. H., M. Yeger-McKeever, A. Stein and R. L. Mauck (2008). "Tensile properties of engineered cartilage formed from chondrocyte- and MSC-laden hydrogels." Osteoarthritis and Cartilage **16**(9): 1074-1082.

Huang, A. H., M. Yeger-McKeever, A. Stein and R. L. Mauck (2008 ). "Identification of molecular antecedents limiting functional maturation of MSC-laden hydrogels." Trans of the 54th Annual Meeting of the Orthopaedic Research Society.

Huang, C. Y., K. L. Hagar, L. E. Frost, Y. Sun and H. S. Cheung (2004). "Effects of cyclic compressive loading on chondrogenesis of rabbit bone-marrow derived mesenchymal stem cells." Stem Cells **22**(3): 313-23.

Huang, C. Y., P. M. Reuben, G. D'Ippolito, P. C. Schiller and H. S. Cheung (2004). "Chondrogenesis of human bone marrow-derived mesenchymal stem cells in agarose culture." Anat Rec **278A**(1): 428-436.

Huebsch, N., P. R. Arany, A. S. Mao, D. Shvartsman, O. A. Ali, S. A. Bencherif, J. Rivera-Feliciano and D. J. Mooney (2010). "Harnessing traction-mediated manipulation of the cell/matrix interface to control stem-cell fate." Nat Mater **9**(6): 518-526.

Hung, C. T., R. L. Mauck, C. C. Wang, E. G. Lima and G. A. Ateshian (2004). "A paradigm for functional tissue engineering of articular cartilage via applied physiologic deformational loading." Ann Biomed Eng **32**(1): 35-49.

Hunter, C. J. and M. E. Levenston (2002). "The influence of repair tissue maturation on the response to oscillatory compression in a cartilage defect repair model." Biorheology **39**(1-2): 79-88.

Hunter, C. J. and M. E. Levenston (2004). "Maturation and integration of tissue-engineered cartilages within an in vitro defect repair model." Tissue Eng Part A **10**(5-6): 736-46.

Ionescu, L. C., G. C. Lee, G. H. Garcia, T. L. Zachry, R. P. Shah, B. J. Sennett and R. L. Mauck (2011). "Maturation State-Dependent Alterations in Meniscus Integration: Implications for Scaffold Design and Tissue Engineering." Tissue Eng Part A **17**(1-2): 193-204.

Johnstone, B., T. M. Hering, A. I. Caplan, V. M. Goldberg and J. U. Yoo (1998). "In vitro chondrogenesis of bone marrow-derived mesenchymal progenitor cells." Exp Cell Res **238**: 265-72.

Jones, C. W., C. Willers, A. Keogh, D. Smolinski, D. Fick, P. J. Yates, T. B. Kirk and M. H. Zheng (2008). "Matrix-induced autologous chondrocyte implantation in sheep: objective assessments including confocal arthroscopy." J Orthop Res **26**(3): 292-303.

Kääb, M. J., K. Ito, J. M. Clark and H. P. Nötzli (1998). "Deformation of articular cartilage collagen structure under static and cyclic loading." Journal of Orthopaedic Research **16**(6): 743-751.

Karsenty, G. (2005). "An aggrecanase and osteoarthritis." N Engl J Med **353**(5): 522-3.

Kavalkovich, K. W., R. E. Boynton, J. M. Murphy and F. P. Barry (2002). "Chondrogenic differentiation of human mesenchymal stem cells within an alginate layer culture system." In Vitro Cell Dev Biol Anim **38**(8): 457-466.

Kempson, G. E. (1991). "Age-related changes in the tensile properties of human articular cartilage: a comparative study between the femoral head of the hip joint and the talus of the ankle joint." Biochim Biophys Acta **1075**(3): 223-30.

Kisiday, J., M. Jin, B. Kurz, H. Hung, C. Semino, S. Zhang and A. Grodzinsky (2002). "Self-assembling peptide hydrogel fosters chondrocyte extracellular matrix production

and cell division: Implications for cartilage tissue repair." Proc Natl Acad Sci U S A **99**(15): 9996-10001.

Kisiday, J. D., M. Jin, M. A. DiMicco, B. Kurz and A. J. Grodzinsky (2004). "Effects of dynamic compressive loading on chondrocyte biosynthesis in self-assembling peptide scaffolds." J Biomech **37**(5): 595-604.

Kisiday, J. D., P. W. Kopesky, C. H. Evans, A. J. Grodzinsky, C. W. McIlwraith and D. D. Frisbie (2007). "Evaluation of adult equine bone marrow- and adipose-derived progenitor cell chondrogenesis in hydrogel cultures." J Orthop Res.

Kisiday, J. D., B. Kurz, M. A. DiMicco and A. J. Grodzinsky (2005). "Evaluation of medium supplemented with insulin-transferrin-selenium for culture of primary bovine calf chondrocytes in three-dimensional hydrogel scaffolds." Tissue Eng **11**(1-2): 141-51.

Kleemann, R. U., Schell, Hanna, Thompson, Mark, Epari, Devakara R., Duda, Georg N., Weiler, Andreas (2007). "Mechanical behavior of articular cartilage after osteochondral autograft transfer in an ovine model." The American Journal of Sports Medicine **35**(4): 555-563.

Knudson, C. (1993). "Hyaluronan receptor-directed assembly of chondrocyte pericellular matrix." J. Cell Biol. **120**(3): 825-834.

Knudson, C. B. and W. Knudson (2004). "Hyaluronan and CD44: modulators of chondrocyte metabolism." Clin Orthop Relat Res(427 Suppl): S152-62.

Knutsen, G., L. Engebretsen, T. C. Ludvigsen, J. O. Drogset, T. Grontvedt, E. Solheim, T. Strand, S. Roberts, V. Isaksen and O. Johansen (2004). "Autologous chondrocyte implantation compared with microfracture in the knee. A randomized trial." J Bone Joint Surg Am **86-A**(3): 455-64.

Kopesky, P., C. Lee, R. Miller, J. Kisiday, D. Frisbie and A. Grodzinsky (2007). "Comparable matrix production by adult equine marrow-derived MSCs and primary chondrocytes in a self-assembling peptide hydrogel: effect of age and growth factors." Trans ORS **32**(0255).

Kopesky, P. W., H. Y. Lee, E. J. Vanderploeg, J. D. Kisiday, D. D. Frisbie, A. H. K. Plaas, C. Ortiz and A. J. Grodzinsky (2010). "Adult equine bone marrow stromal cells produce a cartilage-like ECM mechanically superior to animal-matched adult chondrocytes." Matrix Biology In Press, Corrected Proof.

Kretlow, J., Y.-Q. Jin, W. Liu, W. Zhang, T.-H. Hong, G. Zhou, L. S. Baggett, A. Mikos and Y. Cao (2008). "Donor age and cell passage affects differentiation potential of murine bone marrow-derived stem cells." BMC Cell Biology **9**(1): 60.

Kuo, C. K., W. J. Li, R. L. Mauck and R. S. Tuan (2006). "Cartilage tissue engineering: its potential and uses." Curr Opin Rheumatol **18**(1): 64-73.

Lai, W. M. and V. C. Mow (1980). "Drag-induced compression of articular cartilage during a permeation experiment." Biorheology **17**(1-2): 111-123.

Lee, C. R., A. J. Grodzinsky, H. P. Hsu, S. D. Martin and M. Spector (2000). "Effects of harvest and selected cartilage repair procedures on the physical and biochemical properties of articular cartilage in the canine knee." J Orthop Res **18**(5): 790-9.

Lee, H. J., C. Yu, T. Chansakul, N. S. Hwang, S. Varghese, S. M. Yu and J. H. Elisseeff (2008). "Enhanced chondrogenesis of mesenchymal stem cells in collagen mimetic peptide-mediated microenvironment." Tissue Eng Part A **14**(11): 1843-51.

Lee, R. C., E. H. Frank, A. J. Grodzinsky and D. K. Roylance (1981). "Oscillatory compressional behavior of articular cartilage and its associated electromechanical properties." J Biomech Eng **103**(4): 280-92.

Li, W. J., R. Tuli, C. Okafor, A. Derfoul, K. G. Danielson, D. J. Hall and R. S. Tuan (2005). "A three-dimensional nanofibrous scaffold for cartilage tissue engineering using human mesenchymal stem cells." Biomaterials **26**(6): 599-609.

Li, Y., B. P. Toole, C. N. Dealy and R. A. Kosher (2007). "Hyaluronan in limb morphogenesis." Dev Biol **305**(2): 411-20.

Lima, E. G., L. Bian, K. W. Ng, R. L. Mauck, B. A. Byers, R. S. Tuan, G. A. Ateshian and C. T. Hung (2007). "The beneficial effect of delayed compressive loading on tissue-engineered cartilage constructs cultured with TGF-beta3." Osteoarthritis Cartilage **15**(9): 1025-33.

Lutolf, M. P. and J. A. Hubbell (2005). "Synthetic biomaterials as instructive extracellular microenvironments for morphogenesis in tissue engineering." Nat Biotechnol **23**(1): 47-55.

Magnussen, R. A., A. A. Mansour, J. L. Carey and K. P. Spindler (2009). "Meniscus status at anterior cruciate ligament reconstruction associated with radiographic signs of osteoarthritis at 5- to 10-year follow-up: a systematic review." J Knee Surg **22**(4): 347-357.

Maher, S. A., R. L. Mauck, L. Rackwitz and R. S. Tuan (2009). "A nanofibrous cell-seeded hydrogel promotes integration in a cartilage gap model." J Tissue Eng Regen Med **4**(1): 25-29.

Majumdar, M. K., E. Wang and E. A. Morris (2001). "BMP-2 and BMP-9 promotes chondrogenic differentiation of human multipotential mesenchymal cells and overcomes the inhibitory effect of IL-1." J Cell Physiol **189**(3): 275-84.

Mankin, H. J. (1982). "The response of articular cartilage to mechanical injury." J Bone Joint Surg **64-A**(460-66).

Mankin, H. J., V. C. Mow, J. A. Buckwalter, J. P. Iannotti and A. Ratcliffe (1994). Form and Function of Articular Cartilage. Orthopaedic Basic Science. S. R. Simon. Rosemont, Il, AAOS**:** 1-44.

Maroudas, A. (1968). "Physicochemical Properties of Cartilage in the Light of Ion Exchange Theory." Biophysical Journal **8**(5): 575-595.

Maroudas, A. (1979). Physicochemical properties of articular cartilage. Adult Articular Cartilage. M. A. R. Freeman. Kent, UK, Pitman Med.**:** 215-323.

Martin, J. A. and J. A. Buckwalter (2001). "Telomere erosion and senescence in human articular cartilage chondrocytes." J Gerontol A Biol Sci Med Sci **56**(4): B172-9.

Masuda, K., R. L. Sah, M. J. Hejna and E. J. Thonar (2003). "A novel two-step method for the formation of tissue-engineered cartilage by mature bovine chondrocytes: the alginate-recovered-chondrocyte (ARC) method." J Orthop Res **21**(1): 139-48.

Mauck, R. L., B. A. Byers, X. Yuan and R. S. Tuan (2007). "Regulation of Cartilaginous ECM Gene Transcription by Chondrocytes and MSCs in 3D Culture in Response to Dynamic Loading." Biomech Model Mechanobiol **6**(1-2): 113-125.

Mauck, R. L., J. M. Helm and R. S. Tuan (2006). "Chondrogenesis of human MSCs in a 3D self-assembling peptide hydrogel: functional properties and divergent expression profiles compared to pellet cultures." Trans ORS **31**: 775.

Mauck, R. L., C. T. Hung and G. A. Ateshian (2003). "Modeling of neutral solute transport in a dynamically loaded porous permeable gel: implications for articular cartilage biosynthesis and tissue engineering." J Biomech Eng **125**(5): 602-14.

Mauck, R. L., S. B. Nicoll, S. L. Seyhan, G. A. Ateshian and C. T. Hung (2003). "Synergistic action of growth factors and dynamic loading for articular cartilage tissue engineering." Tissue Eng **9**(4): 597-611.

Mauck, R. L., S. L. Seyhan, G. A. Ateshian and C. T. Hung (2002). "Influence of seeding density and dynamic deformational loading on the developing structure/function relationships of chondrocyte-seeded agarose hydrogels." Ann Biomed Eng **30**(8): 1046-56.

Mauck, R. L., M. A. Soltz, C. C. Wang, D. D. Wong, P. H. Chao, W. B. Valhmu, C. T. Hung and G. A. Ateshian (2000). "Functional tissue engineering of articular cartilage through dynamic loading of chondrocyte-seeded agarose gels." J Biomech Eng **122**(3): 252-60.

Mauck, R. L., C. C. Wang, F. H. Chen, H. Lu, G. A. Ateshian and C. T. Hung (2003). "Dynamic deformational loading of chondrocyte-seeded agarose hydrogels modulates deposition and structural organization of matrix constituents." Proc. ASME 2003 Summer Bioengineering Conference: 531.

Mauck, R. L., C. C. Wang, E. S. Oswald, G. A. Ateshian and C. T. Hung (2003). "The role of cell seeding density and nutrient supply for articular cartilage tissue engineering with deformational loading." Osteoarthritis Cartilage **11**(12): 879-90.

Mauck, R. L., X. Yuan and R. S. Tuan (2006). "Chondrogenic differentiation and functional maturation of bovine mesenchymal stem cells in long-term agarose culture." Osteoarthritis Cartilage **14**(2): 179-89.

Mayer-Wagner, S., T. S. Schiergens, B. Sievers, D. Docheva, M. Schieker, O. B. Betz, V. Jansson and P. E. Muller (2010). "Membrane-Based Cultures Generate Scaffold-Free Neocartilage In Vitro: Influence of Growth Factors." Tissue Engineering Part A **16**(2): 513-521.

Meachim, G. and C. Roberts (1971). "Repair of the joint surface from subarticular tissue in the rabbit knee." J. Anat. **109**(2): 317-327.

Meinel, L., S. Hofmann, V. Karageorgiou, L. Zichner, R. Langer, D. Kaplan and G. Vunjak-Novakovic (2004). "Engineering cartilage-like tissue using human mesenchymal stem cells and silk protein scaffolds." Biotechnol Bioeng **88**(3): 379-91.

Micheli, L., C. Curtis and N. Shervin (2006). "Articular cartilage repair in the adolescent athlete: is autologous chondrocyte implantation the answer?" Clin J Sport Med **16**(6): 465-70.

Micheli, L. J., J. E. Browne, C. Erggelet, F. Fu, B. Mandelbaum, J. B. Moseley and D. Zurakowski (2001). "Autologous chondrocyte implantation of the knee: multicenter experience and minimum 3-year follow-up." Clin J Sport Med **11**(4): 223-8.

Morales, T. I. and V. C. Hascall (1988). "Correlated metabolism of proteoglycans and hyaluronic acid in bovine cartilage organ cultures." J Biol Chem **263**(8): 3632-8.

Moretti, M., D. Wendt, D. Schaefer, M. Jakob, E. B. Hunziker, M. Heberer and I. Martin (2005). "Structural characterization and reliable biomechanical assessment of integrative cartilage repair." J Biomech **38**(9): 1846-54.

Morrison, E. H., M. W. Ferguson, M. T. Bayliss and C. W. Archer (1996). "The development of articular cartilage: I. The spatial and temporal patterns of collagen types." J Anat **189**(Pt 1): 9-22.

Mow, V. C., M. C. Gibbs, W. M. Lai, W. B. Zhu and K. A. Athanasiou (1989). "Biphasic indentation of articular cartilage--II. A numerical algorithm and an experimental study." Journal of Biomechanics **22**(8-9): 853-861.

Mow, V. C., S. C. Kuei, W. M. Lai and C. G. Armstrong (1980). "Biphasic creep and stress relaxation of articular cartilage in compression." J Biomech Eng **102**(1): 73-84.

Muir, H. (1970). "The intracellular matrix in the environment of connective tissue cells." Clin Sci **38**(2): 8P.

Muir, H. (1980). The chemistry of the ground substance of joint cartilage. The Joints and Synovial Fluid. S. L. New York, Academic Press**:** 27-94.

Muir, H. (1983). "Proteoglycans as organizers of the intercellular matrix." Biochem Soc Trans **11**(6): 613-22.

Muir, H., P. Bullough and A. Maroudas (1970). "The distribution of collagen in human articular cartilage with some of its physiological implications." J Bone Joint Surg Br **52**(3): 554-63.

Murdoch, A. D., L. M. Grady, M. P. Ablett, T. Katopodi, R. S. Meadows and T. E. Hardingham (2007). "Chondrogenic Differentiation of Human Bone Marrow Stem Cells in Transwell Cultures: Generation of Scaffold-Free Cartilage." Stem Cells **25**(11): 2786-2796.

Murphy, J. M., K. Dixon, S. Beck, D. Fabian, A. Feldman and F. Barry (2002). "Reduced chondrogenic and adipogenic activity of mesenchymal stem cells from patients with advanced osteoarthritis." Arthritis Rheum **46**(3): 704-13.

Nagase, H. and H. Kashiwagi (2003). "Aggrecanases and cartilage matrix degradation." Arthritis Res Ther. **5**(2): 94-103.

Nettles, D. L., T. P. Vail, M. T. Morgan, M. W. Grinstaff and L. A. Setton (2004). "Photocrosslinkable Hyaluronan as a Scaffold for Articular Cartilage Repair." Ann Biomed Eng **32**(3): 391-397.

Neuman, R. E. and M. A. Logan (1950). "The Determination of Hydroxyproline." Journal of Biological Chemistry **184**(1): 299-306.

Ng, K. W., E. G. Lima, L. Bian, C. J. O'Conor, P. S. Jayabalan, A. M. Stoker, K. Kuroki, C. R. Cook, G. A. Ateshian, J. L. Cook and C. T. Hung (2010). "Passaged adult chondrocytes can form engineered cartilage with functional mechanical properties: a canine model." Tissue Eng Part A **16**(3): 1041-1051.

Ng, K. W., R. L. Mauck, L. Y. Statman, E. Y. Lin, G. A. Ateshian and C. T. Hung (2006). "Dynamic deformational loading results in selective application of mechanical

stimulation in a layered, tissue-engineered cartilage construct." Biorheology **43**(3-4): 497-507.

Ng, K. W., C. C. Wang, R. L. Mauck, T. A. Kelly, N. O. Chahine, K. D. Costa, G. A. Ateshian and C. T. Hung (2005). "A layered agarose approach to fabricate depth-dependent inhomogeneity in chondrocyte-seeded constructs." J Orthop Res **23**(1): 134-41.

Niemeyer, P., J. M. Pestka, P. C. Kreuz, C. Erggelet, H. Schmal, N. P. Suedkamp and M. Steinwachs (2008). "Characteristic Complications After Autologous Chondrocyte Implantation for Cartilage Defects of the Knee Joint." Am J Sports Med **36**(11): 2091-2099.

Nixon, A. J., J. T. Lillich, N. Burton-Wurster, G. Lust and H. O. Mohammed (1998). "Differentiated cellular function in fetal chondrocytes cultured with insulin-like growth factor-I and transforming growth factor-beta." J Orthop Res **16**(5): 531-41.

Novotny, J. E., C. M. Turka, C. Jeong, A. J. Wheaton, C. Li, A. Presedo, D. W. Richardson, R. Reddy and G. R. Dodge (2006). "Biomechanical and Magnetic Resonance Characteristics of a Cartilage-like Equivalent Generated in a Suspension Culture." Tissue Engineering **12**(10): 2755-2764.

Nuttelman, C. R., M. C. Tripodi and K. S. Anseth (2005). "Synthetic hydrogel niches that promote hMSC viability." Matrix Biol **24**(3): 208-18.

Obradovic, B., I. Martin, R. F. Padera, S. Treppo, L. E. Freed and G. Vunjak-Novakovic (2001). "Integration of engineered cartilage." J Orthop Res **19**(6): 1089-97.

Oliveira, J. T., L. S. Gardel, T. Rada, L. Martins, M. E. Gomes and R. L. Reis (2010). "Injectable gellan gum hydrogels with autologous cells for the treatment of rabbit articular cartilage defects." J Orthop Res **28**(9): 1193-1199.

Palmer, A. W., R. E. Guldberg and M. E. Levenston (2006). "Analysis of cartilage matrix fixed charge density and three-dimensional morphology via contrast-enhanced microcomputed tomography." P Natl Acad Sci USA **103**(51): 19255-19260.

Park, S., C. T. Hung and G. A. Ateshian (2004). "Mechanical response of bovine articular cartilage under dynamic unconfined compression loading at physiological stress levels." Osteoarthritis Cartilage **12**(1): 65-73.

Park, S., S. Nicoll, R. Mauck and G. Ateshian (2008). "Cartilage mechanical response under dynamic compression at physiological stress levels following collagenase digestion." Ann Biomed Eng **36**(3): 425-434.

Park, S. Y., C. T. Hung and G. A. Ateshian (2003). "Mechanical response of bovine articular cartilage under dynamic unconfined compression loading at physiological stress levels." J Biomech **12**(1): 391-400.

Park, Y., M. P. Lutolf, J. A. Hubbell, E. B. Hunziker and M. Wong (2004). "Bovine primary chondrocyte culture in synthetic matrix metalloproteinase-sensitive poly(ethylene glycol)-based hydrogels as a scaffold for cartilage repair." Tissue Eng **10**(3-4): 515-22.

Pattappa, G., H. K. Heywood, J. D. de Bruijn and D. A. Lee (2010). "The metabolism of human mesenchymal stem cells during proliferation and differentiation." Journal of Cellular Physiology: n/a-n/a.

Payne, K. A., D. M. Didiano and C. R. Chu (2010). "Donor sex and age influence the chondrogenic potential of human femoral bone marrow stem cells." Osteoarthritis and Cartilage **In Press, Corrected Proof**.

Pelttari, K., A. Winter, E. Steck, K. Goetzke, T. Hennig, B. G. Ochs, T. Aigner and W. Richter (2006). "Premature induction of hypertrophy during in vitro chondrogenesis of human mesenchymal stem cells correlates with calcification and vascular invasion after ectopic transplantation in SCID mice." Arthritis & Rheumatism **54**(10): 3254-3266.

Peretti, G. M., V. Zaporojan, K. M. Spangenberg, M. A. Randolph, J. Fellers and L. J. Bonassar (2003). "Cell-based bonding of articular cartilage: An extended study." J Biomed Mater Res A **64**(3): 517-24.

Pittenger, M. F., A. M. Mackay, S. C. Beck, R. K. Jaiswal, R. Douglas, J. D. Mosca, M. A. Moorman, D. W. Simonetti, S. Craig and D. R. Marshak (1999). "Multilineage potential of adult human mesenchymal stem cells." Science **284**: 143-147.

Ponticiello, M. S., R. M. Schinagl, S. Kadiyala and F. P. Barry (2000). "Gelatin-based resorbable sponge as a carrier matrix for human mesenchymal stem cells in cartilage regeneration therapy." Journal of Biomedical Materials Research **52**(2): 246-255.

Prockop, D. J. (1997). "Marrow stromal cells as stem cells for nonhematopoietic tissues." Science **276**(5309): 71-4.

Quinn, T. M., P. Kocian and J. J. Meister (2000). "Static compression is associated with decreased diffusivity of dextrans in cartilage explants." Arch Biochem Biophys **384**(2): 327-34.

Redler, I., V. C. Mow, M. L. Zimny and J. Mansell (1975). "The ultrastructure and biomechanical significance of the tidemark of articular cartilage." Clin Orthop(112): 357-62.

Rice, M. A., P. M. Homier, K. R. Waters and K. S. Anseth (2008). "Effects of directed gel degradation and collagenase digestion on the integration of neocartilage produced by chondrocytes encapsulated in hydrogel carriers." J Tissue Eng Regen Med **2**(7): 418-429.

Roth, V. and V. C. Mow (1980). "The intrinsic tensile behavior of the matrix of bovine articular cartilage and its variation with age." J Bone Joint Surg Am **62**(7): 1102-17.

Roura, S., J. Farre, C. Soler-Botija, A. Llach, L. Hove-Madsen, J. J. Cairo, F. Godia, J. Cinca and A. Bayes-Genis (2006). "Effect of aging on the pluripotential capacity of human CD105(+) mesenchymal stem cells." Eur J Heart Fail: 555-563.

Ruckstuhl, H., E. de Bruin, E. Stussi and B. Vanwanseele (2008). "Post-traumatic glenohumeral cartilage lesions: a systematic review." BMC Musculoskeletal Disorders **9**(1): 107.

Sahoo, S., C. Chung, S. Khetan and J. A. Burdick (2008). "Hydrolytically degradable hyaluronic acid hydrogels with controlled temporal structures." Biomacromolecules **9**(4): 1088-1092.

Salinas, C. N., B. B. Cole, A. M. Kasko and K. S. Anseth (2007). "Chondrogenic differentiation potential of human mesenchymal stem cells photoencapsulated within poly(ethylene glycol)-arginine-glycine-aspartic acid-serine thiol-methacrylate mixed-mode networks." Tissue Eng **13**(5): 1025-34.

Scharstuhl, A., B. Schewe, K. Benz, C. Gaissmaier, H.-J. Bühring and R. Stoop (2007). "Chondrogenic potential of human adult mesenchymal stem cells is independent of age or osteoarthritis etiology." Stem Cells **25**(12): 3244-3251.

Schnabel, M., S. Marlovits, G. Eckhoff, I. Fichtel, L. Gotzen, V. Vecsei and J. Schlegel (2002). "Dedifferentiation-associated changes in morphology and gene expression in primary human articular chondrocytes in cell culture." Osteoarthritis Cartilage **10**(1): 62-70.

Sethe, S., A. Scutt and A. Stolzing (2006). "Aging of mesenchymal stem cells." Ageing Res Rev **5**(1): 91-116.

Setton, L. A., W. Zhu and V. C. Mow (1993). "The biphasic poroviscoelastic behavior of articular cartilage: role of the surface zone in governing the compressive behavior." J Biomech **26**(4-5): 581-92.

Sheehy, E. J., C. T. Buckley and D. J. Kelly (2011). "Chondrocytes and bone marrow-derived mesenchymal stem cells undergoing chondrogenesis in agarose hydrogels of solid and channelled architectures respond differentially to dynamic culture conditions." J Tissue Eng Regen Med.

Silverman, R. P., D. Passaretti, W. Huang, M. A. Randolph and M. J. Yaremchuk (1999). "Injectable Tissue-Engineered Cartilage Using a Fibrin Glue Polymer." Plast Reconstr Surg **103**(7): 1809-1818.

Sittinger, M., J. Bujia, W. W. Minuth, C. Hammer and G. R. Burmester (1994). "Engineering of cartilage tissue using bioresorbable polymer carriers in perfusion culture." Biomaterials **15**(6): 451-6.

Smeds, K. A., A. Pfister-Serres, D. Miki, K. Dastgheib, M. Inoue, D. L. Hatchell and M. W. Grinstaff (2001). "Photocrosslinkable polysaccharides for in situ hydrogel formation." J Biomed Mater Res **54**(1): 115-21.

Soltz, M. A. and G. A. Ateshian (1998). "Experimental verification and theoretical prediction of cartilage interstitial fluid pressurization at an impermeable contact interface in confined compression." Journal of Biomechanics **31**(10): 927-934.

Soltz, M. A. and G. A. Ateshian (2000). "Interstitial Fluid Pressurization During Confined Compression Cyclical Loading of Articular Cartilage." Annals of Biomedical Engineering **28**(2): 150-159.

Song, L. and R. S. Tuan (2004). "Transdifferentiation potential of human mesenchymal stem cells derived from bone marrow." Faseb J **18**(9): 980-2.

Steadman, J. R., W. G. Rodkey and J. J. Rodrigo (2001). "Microfracture: surgical technique and rehabilitation to treat chondral defects." Clin Orthop Relat Res(391 Suppl): S362-9.

Stegemann, H. and K. Stalder (1967). "Determination of hydroxyproline." Clin Chim Acta **18**(2): 267-73.

Stenderup, K., J. Justesen, C. Clausen and M. Kassem (2003). "Aging is associated with decreased maximal life span and accelerated senescence of bone marrow stromal cells." Bone **33**(6): 919-26.

Stern, R. (2003). "Devising a pathway for hyaluronan catabolism: are we there yet?" Glycobiology **13**(12): 105R-115R.

Stockwell, R. A. (1979). Biology of Cartilage Cells. New York, Cambridge University Press.

Stokes, D. G., G. Liu, I. B. Coimbra, S. Piera-Velazquez, R. M. Crowl and S. A. Jimenez (2002). "Assessment of the gene expression profile of differentiated and dedifferentiated human fetal chondrocytes by microarray analysis." Arthritis Rheum **46**(2): 404-19.

Stolzing, A., E. Jones, D. McGonagle and A. Scutt (2008). "Age-related changes in human bone marrow-derived mesenchymal stem cells: Consequences for cell therapies." Mechanisms of Ageing and Development **129**(3): 163-173.

Takahashi, K., K. Tanabe, M. Ohnuki, M. Narita, T. Ichisaka, K. Tomoda and S. Yamanaka (2007). "Induction of Pluripotent Stem Cells from Adult Human Fibroblasts by Defined Factors." Cell **131**(5): 861-872.

Tallheden, T., C. Bengtsson, C. Brantsing, E. Sjogren-Jansson, L. Carlsson, L. Peterson, M. Brittberg and A. Lindahl (2005). "Proliferation and differentiation potential of chondrocytes from osteoarthritic patients." Arthritis Res Ther **7**(3): R560-8.

Tam, H. K., A. Srivastava, C. W. Colwell and D. D. D'Lima (2007). "In vitro model of full-thickness cartilage defect healing." J Orthop Res **25**(9): 1136-1144.

Temple, M. M., W. C. Bae, M. Q. Chen, M. Lotz, D. Amiel, R. D. Coutts and R. L. Sah (2007). "Age- and site-associated biomechanical weakening of human articular cartilage of the femoral condyle." Osteoarthritis and Cartilage **15**(9): 1042-1052.

Terraciano, V., N. Hwang, L. Moroni, H. B. Park, Z. Zhang, J. Mizrahi, D. Seliktar and J. Elisseeff (2007). "Differential Response of Adult and Embryonic Mesenchymal Progenitor Cells to Mechanical Compression in Hydrogels." Stem Cells.

Toh, W. S., E. H. Lee, X.-M. Guo, J. K. Y. Chan, C. H. Yeow, A. B. Choo and T. Cao (2010). "Cartilage repair using hyaluronan hydrogel-encapsulated human embryonic stem cell-derived chondrogenic cells." Biomaterials **31**(27): 6968-6980.

Tokalov, S. V., S. Gruner, S. Schindler, G. Wolf, M. Baumann and N. Abolmaali (2007). "Age-related changes in the frequency of mesenchymal stem cells in the bone marrow of rats." Stem Cells and Development **16**(3): 439-446.

Toole, B. P. (2004). "Hyaluronan: from extracellular glue to pericellular cue." Nat Rev Cancer **4**(7): 528-39.

Tran-Khanh, N., C. D. Hoemann, M. D. McKee, J. E. Henderson and M. D. Buschmann (2005). "Aged bovine chondrocytes display a diminished capacity to produce a collagen-rich, mechanically functional cartilage extracellular matrix." J Orthop Res **23**(6): 1354-62.

van de Breevaart Bravenboer, J., C. D. In der Maur, P. K. Koen Bos, L. Feenstra, J. A. N. Verhaar, H. Weinans and G. J. V. M. Osch (2004). "Improved cartilage integration and interfacial strength after enzymatic treatment in a cartilage transplantation model." Arthritis Res Ther. **6**(5): 469-476.

Vinardell, T., S. Thorpe, C. Buckley and D. Kelly (2009). "Chondrogenesis and Integration of Mesenchymal Stem Cells Within an In Vitro Cartilage Defect Repair Model." Ann Biomed Eng **37**(12): 2556-2565.

Volpin, G., G. Dowd, H. Stein and G. Bentley (1990). "Degenerative arthritis after intra-articular fractures of the knee. Long-term results." J Bone Joint Surg Br **72-B**(4): 634-638.

Vunjak-Novakovic, G., I. Martin, B. Obradovic, S. Treppo, A. J. Grodzinsky, R. Langer and L. E. Freed (1999). "Bioreactor cultivation conditions modulate the composition and mechanical properties of tissue-engineered cartilage." J Orthop Res **17**(1): 130-8.

Walter, H., A. Kawashima, W. Nebelung, W. Neumann and A. Roessner (1998). "Immunohistochemical analysis of several proteolytic enzymes as parameters of cartilage degradation." Pathol Res Pract **194**(2): 73-81.

Wang, D.-A., S. Varghese, B. Sharma, I. Strehin, S. Fermanian, J. Gorham, D. H. Fairbrother, B. Cascio and J. H. Elisseeff (2007). "Multifunctional chondroitin sulphate for cartilage tissue-biomaterial integration." Nat Mater **6**(5): 385-392.

Wang, H. and G. A. Ateshian (1997). "The normal stress effect and equilibrium friction coefficient of articular cartilage under steady frictional shear." J Biomech **30**(8): 771-6.

Wang, L., K. Seshareddy, M. L. Weiss and M. S. Detamore (2009). "Effect of Initial Seeding Density on Human Umbilical Cord Mesenchymal Stromal Cells for Fibrocartilage Tissue Engineering." Tissue Engineering Part A **15**(5): 1009-1017.

Wang, Y., C. Ding, A. E. Wluka, S. Davis, P. R. Ebeling, G. Jones and F. M. Cicuttini (2006). "Factors affecting progression of knee cartilage defects in normal subjects over 2 years." Rheumatology **45**(1): 79-84.

Weisser, J., B. Rahfoth, A. Timmermann, T. Aigner, R. Brauer and K. von der Mark (2001). "Role of growth factors in rabbit articular cartilage repair by chondrocytes in agarose." Osteoarthritis Cartilage **9 Suppl A**: S48-54.

Williams, C. G., T. K. Kim, A. Taboas, A. Malik, P. Manson and J. Elisseeff (2003). "In vitro chondrogenesis of bone marrow-derived mesenchymal stem cells in a photopolymerizing hydrogel." Tissue Eng **9**(4): 679-88.

Williamson, A. K., A. C. Chen, K. Masuda, E. J. Thonar and R. L. Sah (2003). "Tensile mechanical properties of bovine articular cartilage: variations with growth and relationships to collagen network components." J Orthop Res **21**(5): 872-80.

Williamson, A. K., A. C. Chen and R. L. Sah (2001). "Compressive properties and function-composition relationships of developing bovine articular cartilage." J Orthop Res **19**(6): 1113-21.

Wooley, P. H., M. J. Grimm and E. L. Radin (2005). The Structure and Function of Joints. Arthritis and Allied Conditions. W. J. Koopman and L. W. Moreland, Lippincott Williams & Wilkins.

Wu, J. Z., W. Herzog and E. M. Hasler (2002). "Inadequate placement of osteochondral plugs may induce abnormal stress-strain distributions in articular cartilage --finite element simulations." Med Eng Phys **24**(2): 85-97.

Wyland, D. J., F. Guilak, D. M. Elliott, L. A. Setton and T. P. Vail (2002). "Chondropathy after meniscal tear or partial meniscectomy in a canine model." J Orthop Res **20**(5): 996-1002.

Yaeger, P. C., T. L. Masi, J. L. de Ortiz, F. Binette, R. Tubo and J. M. McPherson (1997). "Synergistic action of transforming growth factor-beta and insulin-like growth factor-I induces expression of type II collagen and aggrecan genes in adult human articular chondrocytes." Exp Cell Res **237**(2): 318-25.

Yu, J., M. A. Vodyanik, K. Smuga-Otto, J. Antosiewicz-Bourget, J. L. Frane, S. Tian, J. Nie, G. A. Jonsdottir, V. Ruotti, R. Stewart, I. I. Slukvin and J. A. Thomson (2007). "Induced Pluripotent Stem Cell Lines Derived from Human Somatic Cells." Science **318**(5858): 1917-1920.

Zhou, S., K. Eid and J. Glowacki (2004). "Cooperation between TGF-beta and Wnt pathways during chondrocyte and adipocyte differentiation of human marrow stromal cells." J Bone Miner Res **19**(3): 463-70.